Event Triggered Cubature Kalman Filter

by

Marzieh Kooshkbaghi

A thesis submitted in partial fulfillment of the requirements for the degree of

Doctor of Philosophy
in
Control Systems

Department of Electrical and Computer Engineering

University of Alberta

Abstract

The Event-triggered state estimation problem has been at the forefront of systems research for several decades and has seen multiple successful applications in diverse areas such as signal processing, target tracking, and navigation systems. Event-triggered state estimation offers a promising solution to data traffic congestion, in which information between sensors and estimators, takes place aperiodically in an event-based manner. In this research we tackle some practical problems encountered in this field and endeavour to improve the state of the art.

In the first part, we develop the necessary theory to develop a discrete-time event-triggered cubature Kalman filter for nonlinear systems with noisy measurements. We show that the proposed filter offers excellent performance in the state estimation of the high dimensional nonlinear systems compared to the other previously proposed nonlinear filters which typically suffer from possible divergence, or curse of dimensionality. In addition, the proposed filter has bounded state estimation error while reducing the communication burden.

In the next part of this research, we study the effect of the packet dropout in the transmission of information on the state estimator performance. Packet dropouts are caused by imperfect communication channels, and are therefore unavoidable when information is received by the filter via a communication network. We first develop the nonlinear filter to reduce the estimation error. Then we show that if the packet arrival rate is lower bounded, then the error covariance matrix is bounded. In addition, by properly tuning the value of the event-triggered threshold, one can guarantee the boundedness of the estimation error.

Then, we consider the effect of transmission delay in the triggered measurement from the sensors to the remote nonlinear estimator. We first discuss the difficulties involved in dealing with time-delays in the context of state estimation and formulate the need for a new algorithm. Then we develop a proper nonlinear filter and show that by using the proposed event-triggered cubature Kalman filter, accurate estimates of the states can be achieved despite time delays, while reducing transmission of information between system and the

filter. To show the advantages of the proposed filters, we evaluate the performance of the proposed filters applied to a synchronous machine.

In the next part, we turn our attention to the developing of a nonlinear filter for more realistic scenario. We develop a nonlinear event-triggered adaptive filter for high dimensional nonlinear systems. The adaptive mechanism is important whenever there are sudden changes in the system states. We show that although the upper bound of the error covariance matrix and the estimation error could be affected, one can guarantee the convergence and the boundedness of the state estimation error by properly designing the nonlinear filter and tuning the event-triggered threshold value and the rate of the packet arrival.

Finally, the effect of the transmission delay and the sudden changes of the states are considered and we develop a nonlinear filter for high dimensional nonlinear systems which could tackle these issues while reducing the amount of data transferring between the sensors and the remote state estimator.

Preface

This thesis is an original work by Marzieh Kooshkbaghi. As detailed in the following, some chapters of this thesis have been published or submitted for publication as scholarly articles in which Professor Horacio J. Marquez was the supervisory author and has contributed to concepts formation and the manuscript composition.

- The results of Chapter 3 has been published in the article: M. Kooshkbaghi, H. J. Marquez, "Event-Triggered State Estimation of High Dimensional Nonlinear Systems with Highly Nonlinear State Space Model Using Cubature Kalman Filter," *CCECE 2019*, May 2019, Canada.

- The results of Chapter 4 has been accepted for publication in the article: M. Kooshkbaghi, H. J. Marquez, "Event-Triggered Discrete-Time Cubature Kalman Filter for Nonlinear Dynamical Systems with Packet Dropout," *IEEE Transactions on Automatic Control* September 2019.

- The results of Chapter 6 has been published in the article: M. Kooshkbaghi, H. J. Marquez, and W. Xu, "Event-Triggered Approach to Dynamic State Estimation of a Synchronous Machine Using Cubature Kalman Filter," *IEEE Transactions on Control Systems Technology,*, July 2019, DOI: 10.1109/TCST.2019.2923374.

- The results of Chapter 7 has been submitted for publication in the article: M. Kooshkbaghi, H. J. Marquez,"Strong Tracking Discrete-Time Event-Triggered Cubature Kalman Filter for Nonlinear Dynamical Systems with Packet Dropout," *Internationa Journal of Robust and Nonlinear Control, September 2019.*

- *The results of Chapter 5 and Chapter 8 are currently under preparation to be submitted to related journals.*

To my beloved parents, and my brother Mahdi
for their endless love and support

Acknowledgements

Firstly, I would like to express my sincere appreciation to Prof. Horacio J.Marquez for his great support and supervision during this research project. This research and dissertation would not have been possible without his continuous guidance. To my committee, Dr. Tongwen Chen, and Dr. Mahdi Tavakoli. I am extremely grateful for your assistance and suggestions throughout this study.

I would kindly appreciate all nice friends whom I met during my Ph.D. program. Specifically, I would like to thank Kiko and his mother Esma, Zahra, Behnaz, Hafez, Shahed, Masoud and Faezeh for their friendly encouragement and support.

Specifically, I would like to thank my friends, Mohsen and Seyed Hossein, who helped me with some problems which I encountered during the last four years. I also thank to my old friends Hamed, Kasra, Mehran, Naeimeh, and my friends in Mehrnami High school for all memorable moments I had with them. Last but not the least, my deepest gratitude goes to my parents and brother for their unconditional support and patience.

Marzieh Kooshkbaghi
Edmonton, Alberta
Canada

Contents

List of Tables

List of Figures

Notation

$\mathbb{R}$	The sets of real number
$\mathbb{R}^n$	The set of real n-dimensional vector
$\mathbb{R}^{n\times m}$	The set of real $n \times m$ matrices
$\forall$	Universal quantifier
$x \in X$	x is an element of set X
$X \subset Y$	X is a subset of Y
A^T	Transpose of matrix or vector A
A^{-1}	Inverse of matrix A
$\|\cdot\|$ or $\|\cdot\|$	Euclidean norm of a vector or matrix
$\|\cdot\|_\infty$ or $\|\cdot\|_\infty$	∞-norm of a vector

Abbreviations

CKF	Cubature Kalman Filter
EKF	Extended Kalman Filter
UKF	Unscented Kalman Filter
LTI	Linear Time-Invariant
TC	Triggering Condition
LMI	Linear Matrix Inequality
ETM	Event-Triggered Mechanism
SMIB	Single Machine Infinite Bus
DECKF	Discrete-Time Event-Triggered Cubature Kalman Filter

Chapter 1

Introduction

1.0.1 Background

Cyber-Physical System (CPS) is a term used to describe "a ubiquitous and smart integration of sensing devices, computing processors and communication networks that reliably interacts with the physical world (with the probable involvement of humans in the loop) in real time" [1]. CPSs play an important role in many diverse areas such as smart ecosystems. Typical example of CPSs are energy systems, medical systems, smart grids, transportation networks, process control and automation and wearable devices.

Cyber physical systems usually exchange information among physical components and cyber components through wired or wireless communication channels. The use of wireless communication channels brings multiple benefits such as low wiring cost but introduces the need to carefully manage the communication resources. For instance, wireless sensors and processors may have constrained energy provided by batteries, so the energy management is of a great importance. On the other hand, band-limited networks are used as a means of communication between sensors, state estimators, controllers, and the actuators which can introduce several challenges such as transmission delay and packet dropouts.

In the traditional approach, signals are transmitted in a periodic or time-triggered manner which means that activities take place at predefined points in time. Time triggered approach is easy to implement but it occupies excessive bandwidth. In general, communication should only occur when relevant information needs to be transmitted between system components. Event-triggered data transferring is a promising solution.

The event-triggered approach is an alternative to classical periodic sampling, in which information between system components is exchanged only when a specified triggering condition (TC) is violated, as opposed to periodically. The TC can be defined in different forms and varies depending on the nature of the system.The primary benefit of event-triggered

sampling is a, possibly significant, reduction in data transmission between different components of the networked system while maintaining comparable performance. The price paid for this reduction is additional complexity in the analysis and design, originated in the non-periodic nature of the sampling.

Parallel to the event-triggered transmission problem which has been thoroughly investigated in the recent years, state estimation for complex networks has gained significant attention [24–26]. State estimators can be used to estimate the target state of a dynamical system from a noisy signal received from the remote sensors through the communication channel. The estimated states can be used for monitoring CPSs, or energy management in power networks. For example, in power systems, voltages, frequencies and the angles of the generators can be estimated by using PMU data.

It is important to note that both observers and state estimators can be used to estimate system states, but there are some differences between them. Dynamic observers are commonly used for deterministic systems to generate unmeasured internal states in real-time, given a set of output measurements (and sometimes inputs). Sliding mode observers, unknown input observers, nonlinear observers are examples of observers designed using different techniques and applicable to systems with certain characteristics. State estimators, on the other hand, are designed to deal with random process disturbances, measurement noises, and uncertainty in the system models. Examples of well established state estimators include Kalman filters, Extended Kalman filters (EKF), Unscented Kalman filters (UKF) and Cubature Kalman filters (CKF). State estimators are used in multiple applications ranging from aerospace systems to medical devices.

Event-based state estimation has been a challenging problem over the last decade. The primary characteristic of the event-based state estimation systems is that they can provide performance very similar to classical state estimation approaches while reducing the transmission of information between plant and state estimators. The main problem is then to design the triggering mechanism/state estimator in a way that the desired stability and/or performance for the event-triggered system is achieved which is more difficult compared with the periodic counterparts . This is also more challenging when the model of the system mismatches to the practical one and the packet dropouts and delays happen during the data transferring through the communication channel.

1.0.2 Literature Survey

Research on the event-based systems done in late 1990's [27], has attracted much attention due to its capacity to reduce the communication and computational costs while maintaining system performance.

In [27], Astrom focused on "Lebesgue sampling" which is performed along vertical axis and provides sampled values of the signal when a certain event-triggered condition is violated. In this reference, the authors consider a first order stochastic system and showed that the event-based sampling can improve the performance compared to periodic sampling in terms of smaller output variance at the same average sampling rate. The results of this work were extended to the second-order case in [64].

[65] is one of the first work in which an event-triggered PID controller is defined and the stability of the system is studied. In this work, the time-triggered and event-triggered controller performance for a double-tank process is compared and it is shown that by using an event-based mechanism, the control execution is reduced while the controller performance is satisfactory.

Encouraged by this early work, much research has been reported on the event-based control, including closed loop stability and performance. In [28], a Lyapunov method was used to analyze the asymptotic behaviour of the event-triggered nonlinear system for a given state feedback controller, and a lower bound on the inter-sample period was proposed. Periodic event based control is proposed in [29], which indicates that events can only be activated at some sampling instants of the periodic sampled data system. In [29, 66–68], the authors studied the effect of the event-triggered mechanism on the performance of the controller, and a trade-off between the system performance and the control law complexity was derived.

Event-triggered state estimation has also received attention. In [69], the performance of the periodic and the event-based sampling state estimation for the first and second order systems are studied.

Event-triggering scheme designing is one of the important issues in event-triggered state estimation. Normally, it is difficult to design a triggering mechanism to gain all state estimation goals. In [35, 70–72], the authors propose to design the event-triggering schemes by using constrained optimization problem. In these literature, they consider to design the triggering condition by optimizing certain performance under the constraints on sensor transmissions.

The main goal of this thesis is to design an event-triggered state estimator based on the predefined event-triggered mechanism. Event-triggering condition determines the measurement information available to the estimator. Different conditions have been proposed. The description of different event-triggered conditions are given in [32, 73].

In [20, 74], an event-triggered filter with "send-on-delta" mechanism, which is the most practical event-triggering condition, is defined. In "send-on-delta" mechanism, new measurement is sent to the estimator when the distance between the current measurement and the last sent measurement exceeds a predefined threshold. "Innovation-level-based" event-triggered mechanism is applied to state estimator in [30, 53, 75, 77]. In this mechanism, the predicted measurement is sent to the scheduler from the estimator. Based on the current measurement and the predicted measurement, the event-triggered mechanism decides whether to send the current measurement to the estimator. The drawback of this type of triggering condition, however, is that extra feedback communication from the estimator (local filters or remote filters) to the sensor is needed to obtain the predicted measurement. So it increases the hardware and energy requirements in the implementation of the event-triggering scheme. "Variance-Based" condition is studied in [76], in which the estimation error covariance is compared to the minimum achievable estimation error covariance obtained based on the periodic measurements and if the difference exceeds the predefine threshold, the new measurement would be sent to the remote state estimator.

Besides to the triggering mechanism designing problems, estimator design is the most important problem of the event-based state estimation. At each time instant, the estimator receives point valued/set valued information from the sensors. When the event-triggering condition is satisfied, the outputs of the sensors (point valued information) are exactly known to the estimators. On the other hand, the estimator might have knowledge of the information in event-triggering set (set valued information) when the event-triggering condition is not satisfied. Different estimators have been proposed.

In [20], a minimum mean square error estimator was derived for linear systems with stochastic disturbances based on hybrid information from multiple sensors, which provide their measurement updates according to separate event-triggering conditions. The approximate Gaussian approach is introduced and the conditional densities are assumed to be Gaussian to handle the non-Gaussian distribution caused by the exploitation of the event-triggered measurement information. It is shown that the optimal estimator depends on the conditional mean and covariance of the measurement innovations. The trade-off between performance and communication rate is also studied. In [32], an event-based estimator with

hybrid measurement updates is proposed. This reference uses the sum-of-Gaussian approach to approximate the uniform distribution with a sum of a finite number of Gaussian distributions to reduce the computational complexity. In this approach, parameters need to be tuned carefully to guarantee the asymptotic boundedness of the estimation error covariance matrix. In [30], an event-based state estimation problem for linear time invariant systems in the framework of Maximum Likelihood (ML) was studied and the computation of upper and lower bounds for the communication rate was discussed. In [31], the state estimation problem for a class of stochastic event-triggering conditions is considered and MMSE estimates were obtained without introducing additional approximations. In [33], the authors consider the noises and the event-triggering conditions as stochastic and non-stochastic uncertainties and an event-based estimate was obtained by minimizing the worst-case mean square error. In [78], the application of the set-valued filters with set-valued measurements to the event-triggered state estimators are discussed and the properties of the proposed filter is studied. Reference [34] considers the event-based finite-horizon state-estimation for scalar systems. Reference [35] extended their work to vector systems.

All of the above mentioned references focus on linear systems. Dynamic systems used in many applications are often nonlinear. Bayesian filtering is applied to an important class of state estimation problems, which are describable by a discrete-time nonlinear state-space model with additive Gaussian noise. A major difficulty in this problem is that when the system equations are nonlinear, the posterior density cannot be described by a finite number of statistics, and an approximation must be made.

Well established sub-optimal popular solutions include the Extended Kalman Filter (EKF) [2], based on the first order linearization, and the Unscented Kalman Filter (UKF) [3], based on the so-called "unscented" transformation.

Both filters, EKF and UKF, have been applied extensively for online dynamic state estimation of nonlinear systems, however, they both have limitations: EKF uses a linear approximation of the system model which introduces error in state estimates and and can cause the solutions to diverge from the true state [4, 16]. In general, UKF performs better than EKF in terms of robustness and speed of convergence, but it suffers from computational complexity, sometimes referred to as the curse of dimensionality, [5–7].

Cubature Kalman filters, recently proposed in [8], offer an attractive and numerically stable solution with low computational effort to the nonlinear state estimation problem. The CKF assumes that the predictive density of the joint state-measurement random variable is Gaussian. In this way, the optimal Bayesian filter reduces to the problem of how to

compute various multi-dimensional Gaussian weighted moment integrals which can be done efficiently using a cubature rule. CKFs, have been used in several applications including navigation, maneuvering and tracking of robots [9–11]. A number of implementations have been reported to show that the CKF has superior performance over UKF [21,22]. Stochastic stability and convergence of CKFs was reported in [12, 13].

Despite the interest in the event-based linear state estimation, event-based nonlinear estimations have received comparatively less attention. In [14], an event-based CKF for Smart grid is presented using an"Innovation-Level-Based" event-triggered condition based on the difference between the current and predicted measurement. As mentioned earlier, the drawback of this type of triggering condition, however, is that the feedback communication from the estimator (local filters or remote filters) to the sensor is needed to obtain the predicted measurement. In comparison to this recent result, we consider "Send-on-Delta" event-trigger condition in which the feedback communication from the estimator is not needed which reduces the hardware and energy requirements for implementing the event-triggering scheme [15].

The nonlinear filters mentioned above work poorly in the presence of sudden changes in the states. In many practical applications, sudden changes in the states leads to the bias in the estimation process [45]. Examples include important applications, such as maneuvering aircraft tracking, underwater target tracking, and eye tracking for vision-based human computer interaction applications, and most control applications requiring state estimation as part of the control law.

Adaptive filters provide a solution that can cope with sudden changes in the system states. Among all adaptive nonlinear filtering methods, strong tracking filter (STF) has attracted considerable attention [36]. STF introduces a suboptimal fading factor to the error covariance matrix that reduces the effect of old measurements while enhancing the effect of new measurements to modify the error covariance matrix and the filter gain in real-time, thus enhancing estimation quality [37]. It is shown theoretically in [45] that the process noise covariance in the state model is corrected by introducing the dynamic fading factor to error covariance matrix, which results in an improvement of the state estimation. STF can be applied along with most nonlinear state estimators such as EKF, UKF, and CKF. References [41–44] propose strong tracking extended and unscented Kalman filters. In [38–40] a strong tracking cubature Kalman filter for maneuvering target tracking is studied.

Nonlinear state estimators mentioned above assume that the communication channel is

reliable. In CPSs, perfect communication is impossible because of network effects, such as packet dropouts, and network delay in the communication channels. Thus, the problem of designing nonlinear filter with packet dropout in the communication channels has attracted significant attention. Reference [16] studies EKF with packet dropout while [23] focuses on stochastic stability of extended Kalman filters with packet dropout. Reference [17] shows that in the existence of a lower bound for the communication rate, the estimation error is bounded. In [18] stochastic stability of UKFs in the presence of packet dropout is studied. Reference [5], studies the stochastic stability of unscented Kalman filter in the presence of event-triggered mechanism and packet dropout. In [46], a strong tracking filter for a system with delayed measurements is proposed.

EKF and UKF, with one sampling time randomly delayed measurements have been proposed in [48]. In [47], a generic framework of a Gaussian approximation (GA) filter was proposed.

1.1 Summary of Contributions

In the previous section we discussed that, recently, the event based state estimation has found wide application in cyber physical systems, control systems, system monitoring, and signal processing. However, so far, there have been very few results reported about event-triggered nonlinear state estimation, and there are some important open problems which remain unsolved. In this thesis we aim at providing solutions to the nonlinear event-triggered state estimation problem. In this section we provide a brief summary of the main contributions. More detailed explanation of the results can be found in the related chapters.

In *Chapter 3*[1], an event-triggered discrete time Cubature Kalman filter for high dimensional nonlinear system with highly nonlinear state space model with noisy measurements over a wireless network is developed. We show that our proposed nonlinear filter with a well designed event-triggered mechanism can significantly reduce the communication data between the system sensors and the filter while the estimation error is kept bounded, thus reducing potential network-related congestion issues. Our solution makes use of a so-called "Send-on-Delta" type event-triggering condition in which a new sample is triggered if the measured signal deviates by "delta" from the most recent sample. Thus, the sensor node does not broadcast a new message while the sampled signal remains within a certain interval

[1]The results of this chapter has been published in the article: M. Kooshkbaghi, H. J. Marquez, "Event-Triggered State Estimation of High Dimensional Nonlinear Systems with Highly Nonlinear State Space Model Using Cubature Kalman Filter," *CCECE 2019*, May 2019, Canada

of confidence. We also show the advantages of employing cubature Kalman filters over the more established and more explored extended Kalman filters and unscented Kalman filters, frequently used in the literature, to estimate the nonlinear systems. We argue that better estimates can be obtained using the CKF and justify our claims in our simulations, both using periodic and event-triggered sampling. We show that the event-triggered approach allows us to obtain excellent estimates, while reducing the flow of information with respect to classical periodic systems.

In *Chapter 4*[2], we study the effect of the packet dropout during data transmission from the system to the remote state estimator in the communication channels, on the design of the event-triggered CKF. All CPSs require transferring data from the measurement sensors to the state estimator through an imperfect wired or wireless sensor network with typical practical issues which may result in undesirable effects such as data packet drop out. A binary random variable is introduced to model the arrival of a measurement and we define an upper bound for the rate of the packet dropout to guarantee the convergence of the proposed filter. Then we study the boundedness of the estimation error and we derive a relation between the estimation error upper bound and the event-triggered threshold value.

In *Chapter 5*, we consider delay in the communication channels. As we mentioned before, the communication channels are not perfect and reliable. In practice, the presence of time delays and packet dropouts are inevitable in applications with wired/wireless communications channels caused by aging and network congestion. Unfortunately, the designed event based state estimators can not be extended to the case with time delay in the communication channels. In the presence of the delay in communication channels, the real time measurements may not be received by the estimator, and the state estimation will not be updated properly. In addition, the posterior PDF of the measurement noise needs to be updated. CKF algorithm with one-step randomly delayed measurements is proposed in [47]. To the best of the author's knowledge, CKF algorithm with the event-triggered mechanism and randomly delayed measurements have not been reported which is the contribution of this chapter.

In *Chapter 6*[3] , we evaluate the performance of the proposed CKF under different communication conditions, namely in the presence of different triggering threshold and

[2]The results of this chapter has been accepted for publication in the article: M. Kooshkbaghi, H. J. Marquez, "Event-Triggered Discrete-Time Cubature Kalman Filter for Nonlinear Dynamical Systems with Packet Dropout," *IEEE Transactions on Automatic Control* Sep. 2019.

[3]The results of this chapter has been published in the article: M. Kooshkbaghi, H. J. Marquez, and W. Xu, "Event-Triggered Approach to Dynamic State Estimation of a Synchronous Machine Using Cubature Kalman Filter," *IEEE Transactions on Control Systems Technology, DOI: 10.1109/TCST.2019.2923374.*

different delay probabilities when applied to a synchronous machine. We show the advantage of employing the proposed cubature Kalman filters over the more established and more explored filters such as extended Kalman filters and unscented Kalman filters, frequently used in the literatures to estimate the states of synchronous machines.

In *Chapter 7*[4], We consider another topic of interest in the theory of the event-triggered state estimator when there are sudden changes in the states. The previously proposed nonlinear filters such as Cubature Kalman filter have poor performance in the presence of the sudden changes in the states which leads to the bias in the estimation process. The concept of strong fading factor in the state error covariance matrix based on the residual sequence is a promising solution for these kinds of problems [49, 51, 62]. So, we will develop a new filtering algorithm, a strong tracking discrete-time event-triggered cubature Kalman filter (STDECKF), to reduce the amount of data transmission between the measuring sensors and the remote state estimator and to reduce the low accuracy of the filtering under sudden changes in the states condition. We compare the performance of the newly designed event-triggered state estimator in the different condition. In addition, we show that under some condition, the proposed filter estimation error and the estimation error covariance are bounded.

Finally, in *Chapter 8*, we develop a new event-triggered filtering algorithm, based on the orthogonality principle, considering delay in the communication channels and the sudden changes in the states. In this situation, we need to reduces the effect of old/delay measurements on the filtering process and to enhance the effect of new measurements to modify the error covariance matrix. A fading factor is used to enhance the performance of the filter while the data transmission between the sensors and the remote filter is reduced. To the best of the author's knowledge, strong tracking CKF algorithm with the event-triggered mechanism and randomly delayed measurements have not been reported which is the contribution of this chapter.

[4]The results of this chapter has been submitted for publication in the article: M. Kooshkbaghi, H. J. Marquez,"Strong Tracking Discrete-Time Event-Triggered Cubature Kalman Filter for Nonlinear Dynamical Systems with Packet Dropout," *Internationa Journal of Robust and Nonlinear Control, September 2019.*

Chapter 2

Discrete-Time Cubature Kalman Filter

Over the past decades, the state estimation of nonlinear systems has attracted significant attention from the research community. There are many efficient nonlinear filtering algorithms which have been proposed. Among those, extended Kalman filters and unscented Kalman filters are widely used for nonlinear systems. The EKF and UKF algorithm are described briefly in the Appendix. EKF is based on the first order linearization, and therefore its performance deteriorates when dealing with systems with high nonlinearities. On the other hand, unscented Kalman filter typically offers better performance than extended Kalman filters, but suffer from the so-called curse of dimensionality [52] and its application is limited to low order systems. Recently, Cubature Kalman filter (CKF) were proposed in [8], based on a Bayesian filter under Gaussian approximation. CKF has less computational complexity and offers numerical stability compared to the other widely used nonlinear filters. These properties make CKF a proper choice for high dimensional nonlinear systems with high nonlinearities.

In this chapter, we summarize the discrete-time cubature Kalman filter proposed in [8] that will be used in later chapters.

Notation: $\mathbb{R}$ represents the field of real numbers, $\mathbb{R}^n$ and $\mathbb{R}^{n\times m}$ are the set of n-dimensional real vectors and and $n \times m$ real matrices, respectively. A^T represents the transpose of $A \in \mathbb{R}^{n\times m}$, and B^{-1} is the inverse of $B \in \mathbb{R}^{n\times n}$. $E\{x\}$ is the expectation of the random variable x and $p\{x|y\}$ the probability distribution of x with respect to y, respectively. $\|.\|$ denotes the Euclidean norm of the vector $x \in \mathbb{R}^n$.

2.0.1 Problem Statement

Consider the nonlinear discrete-time system and the nonlinear measurement model given in (2.1) and (2.2), respectively.

$$x_{k+1} = f(x_k, u_k) + \omega_k, \tag{2.1}$$

$$y_{k+1} = h(x_{k+1}) + \nu_{k+1}, \tag{2.2}$$

where $x_k \in \mathbb{R}^{n_x}$ is the state vector, $u_k \in \mathbb{R}^{n_u}$ is the control input vector, $y_k \in \mathbb{R}^{n_y}$ is the measurement vector, $k \in N$ is a discrete time factor. ω and ν are the process noise and the measurement noise respectively, which are assumed to be uncorrelated zero-mean Gaussian white noise sequences with covariance $Q \in \mathbb{R}^{n_x \times n_x}$ and $R \in \mathbb{R}^{n_y \times n_y}$, respectively. $f(.)$ and $h(.)$ are the continuously differentiable nonlinear state function and the measurement function with respect to the system state x_k.

The objective of this chapter is to summarize the design of the optimal state estimator for the nonlinear system with the state space model stated in (2.1) and (2.2). A detailed design of the filtering algorithm is given in the following subsection.

2.0.2 Baysian Filter In The Gaussian Domain

In this subsection, we present the discrete-time optimal Bayesian filter. Under the Gaussian assumption of the density functions, the recursive Bayesian filter can be derived in two Time and Measurement update steps as follows,

- ***Time update:*** The mean of the Gaussian predictive density is as follows,

$$\hat{x}_{k+1|k} = E[x_{k+1}|D_k], \tag{2.3}$$

  where $D_k = \{u_i, y_i\}$, $i = 1...k$, shows the history of input measurement pairs up to time k. Substituting (2.1) in (2.3) we have,

$$\begin{aligned} \hat{x}_{k+1|k} =& E[f(x_k, u_k) + \nu_k|D_k] = \int_{\mathbb{R}^{n_x}} f(x_k, u_k) p(x_k|D_k) dx_k \\ &= \int_{\mathbb{R}^{n_x}} f(x_k, u_k) N(x_k; \hat{x}_k, \hat{P}_k) dx_k. \end{aligned} \tag{2.4}$$

  Note that ν_k is assumed to be zero-mean and uncorrelated with the past measurements, and the $N(x_k; \hat{x}_k, P_k)$ is conventional symbol for a Gaussian density. The error covariance is as follows,

$$\begin{aligned} \hat{P}_{k+1|k} =& E[(x_{k+1} - \hat{x}_{k+1|k})(x_{k+1} - \hat{x}_{k+1|k})^T|y_{1:k}] \\ &= \int_{\mathbb{R}^{n_x}} f(x_k, u_k) f(x_k, u_k)^T N(x_k; \hat{x}_k, \hat{P}_k) dx_k \\ &- \hat{x}_{k+1|k} \hat{x}_{k+1|k}^T + Q_k. \end{aligned} \tag{2.5}$$

- ***Measurement update:*** The predicted measurement and the associated covariance are as follows,

$$\hat{y}_{k+1|k} = \int_{\mathbb{R}^{n_x}} f(x_k, u_k) N(x_{k+1}; \hat{x}_{k+1|k}, \hat{P}_{k+1|k}) dx_{k+1}, \tag{2.6}$$

$$\begin{aligned} \hat{P}_{yy,k+1|k} = &\int_{\mathbb{R}^{n_x}} h(x_{k+1}) h(x_{k+1},)^T N(x_{k+1}; \hat{x}_{k+1|k}, \hat{P}_{k+1|k}) dx_{k+1} \\ &- \hat{y}_{k+1|k} \hat{y}^T_{k+1|k} + R_{k+1}. \end{aligned} \tag{2.7}$$

The cross-covariance is,

$$\hat{P}_{xy,k+1|k} = \int_{\mathbb{R}^{n_x}} x_{k+1} h(x_{k+1})^T N(x_{k+1}; \hat{x}_{k+1|k}, \hat{P}_{k+1|k}) dx_{k+1} - \hat{x}_{k+1|k} \hat{y}^T_{k+1|k}, \tag{2.8}$$

and the conditional Gaussian density of the joint state and the measurement can be written as follow,

$$p([x^T_{k+1} \quad y^T_{k+1}]^T | D_k) = N(\begin{pmatrix} \hat{x}_{k+1|k} \\ \hat{y}_{k+1|k} \end{pmatrix}, \begin{pmatrix} \hat{P}_{k+1|k} & \hat{P}_{xy,k+1|k} \\ \hat{P}^T_{xy,k+1|k} & \hat{P}_{yy,k+1|k} \end{pmatrix}). \tag{2.9}$$

The Bayesian filter computes the posterior density when it receives a new measurement. The posterior density is as follows,

$$p(x_{k+1}|D_{k+1}) = N(x_{k+1}; \hat{x}_{k+1}, \hat{P}_{k+1}) \tag{2.10}$$

where,

$$\begin{aligned} \hat{x}_{k+1} &= \hat{x}_{k+1|k} + K_{k+1}(y_{k+1} - \hat{y}_{k+1|k}) \\ \hat{P}_{k+1} &= \hat{P}_{k+1|k} - K_{k+1} \hat{P}_{yy,k+1|k} K^T_{k+1} \\ K_{k+1} &= \hat{P}_{xy,k+1|k} \hat{P}^{-1}_{yy,k+1|k} \end{aligned} \tag{2.11}$$

The optimal Bayesian filter includes various multi-dimensional Gaussian weighted moment integrals which are all of the form *"nonlinear function Gaussian density"* that are present in (2.4)-(2.8) which can be approximately computed by using a "Cubature" rule.

2.0.3 Cubature Kalman Filter

We now summarize the fundamentals of the cubature Kalman filter proposed in [8]. As it is shown in Subsection 2.0.2, the Bayesian paradigm relies on the fact that the conditional density of the state at each measurement, or the *posteriori* density of the state, contains a complete description of the state at that time. In addition, the filtering algorithm consists of two steps: (i) (time update) propagates the posteriori density between measurement instants, and (ii) (measurement update) uses the Bayes' rule to update the propagated

posteriori measurements at each measurement instant. The time and measurement update procedures, however, require solving multidimensional integrals of the form:

$$I(f) = \int_{\mathbb{R}^{n_x}} f(\mathbf{x}) N(\mathbf{x}; \hat{\mathbf{x}}, \hat{P}) d\mathbf{x}, \tag{2.12}$$

where n_x is the dimension of the state, the covariance $\hat{P}$ satisfies $\hat{P} = SS^T$. When the system is nonlinear, solving this integral is either very difficult or impossible and an approximation must be made.

The CKF uses a third-degree spherical-radial cubature rule to select $2n_x$ cubature points to approximate the integral as follows:

$$I(f) \approx \sum_{i=1}^{2n_x} \frac{1}{2n} f(\hat{x} + S\xi_i). \tag{2.13}$$

The $2n_x$ cubature points are selected as follows

$$\xi_i = \begin{cases} \sqrt{n} e_i & i = 1, 2, \cdots, n_x \\ -\sqrt{n} e_{i-n} & i = n+1, n+2, \cdots, 2n_x, \end{cases} \tag{2.14}$$

where $e_i \in \mathbb{R}^{n_x \times 1}$, is the i^{th} elementary column vector. The CKF algorithm consists of a time update step and a measurement update step in which the approximation described is used to estimate the new covariance matrices and states. In the time update step, we calculate the cubature points as follows,

$$X_{i,k} = S_k \xi_i + \hat{x}_k \qquad i = 1, 2, ..., 2n_x. \tag{2.15}$$

where $\hat{x}_k$ is the posteriori state estimate and $\hat{P}_k = S_k S_k^T$. Then the propagated cubature points and the predicted state and associated covariance can be calculated using (2.16), (2.17) and (2.18), respectively.

$$X^*_{i,k+1|k} = f(X_{i,k}, u_k) \qquad i = 1, 2, ..., 2n_x, \tag{2.16}$$

$$\hat{x}_{k+1|k} = \frac{1}{2n_x} \sum_{i=1}^{2n_x} X^*_{i,k+1|k}, \tag{2.17}$$

$$\hat{P}_{k+1|k} = \frac{1}{2n_x} \sum_{i=1}^{2n_x} X^*_{i,k+1|k} X^{*T}_{i,k+1|k} - \hat{x}_{k+1|k} \hat{x}^T_{k+1|k} + Q_k. \tag{2.18}$$

In the measurement update step we compute new cubature points, and propagated cubature points using (2.19) and (2.20):

$$X_{i,k+1|k} = S_{k+1|k} \xi_i + \hat{x}_{k+1|k} \qquad i = 1, 2, ..., 2n_x, \tag{2.19}$$

$$Y_{i,k+1|k} = h(X_{i,k+1|k}, u_{k+1}) \qquad i = 1, 2, ..., 2n_x. \tag{2.20}$$

The predicted measurement as well as the innovation covariance and the cross-covariance can be calculated as follows:

$$\hat{y}_{k+1|k} = \frac{1}{2n_x} \sum_{i=1}^{2n_x} Y_{i,k+1|k}, \tag{2.21}$$

$$\hat{P}_{yy,k+1} = \frac{1}{2n_x} \sum_{i=1}^{2n_x} Y_{i,k+1|k} Y_{i,k+1|k}^T - \hat{y}_{k+1|k} \hat{y}_{k+1|k}^T + R_{k+1}, \tag{2.22}$$

$$\hat{P}_{xy,k+1} = \frac{1}{2n_x} \sum_{i=1}^{2n_x} X_{i,k+1|k} Y_{i,k+1|k}^T - \hat{x}_{k+1|k} \hat{y}_{k+1|k}^T. \tag{2.23}$$

Finally, the Kalman gain, and the state estimation and the corresponding error covariance are given by:

$$K_{k+1} = \hat{P}_{xy,k+1} \hat{P}_{yy,k+1}^{-1}, \tag{2.24}$$

$$\hat{x}_{k+1} = \hat{x}_{k+1|k} + K_{k+1}(y_{k+1} - \hat{y}_{k+1|k}), \tag{2.25}$$

$$\hat{P}_{k+1} = \hat{P}_{k+1|k} - K_{k+1} \hat{P}_{yy,k+1} K_{k+1}^T. \tag{2.26}$$

Chapter 3

Event-Triggered Discrete-Time Cubature Kalman Filter

In this chapter [1] , we present a complete theory of the discrete-time event-triggered Cubature Kalman filter (DECKF) applicable to high dimensional nonlinear systems with noisy measurements. A scenario is considered in which local measurements are transmitted to a remote state estimator when an event-triggered condition is satisfied. The presence of the triggering rule thus reduces data transmission between local sensors and the remote estimator, resulting in a more efficient use of energy and communication resources. In the proposed filter, first "Send-on-delta event-triggered" mechanism is used, which reduces the feedback communication between the sensors and the remote state estimators compared to the other event-triggered schemes such as "innovation-level-based" mechanism, to determines whether or not information is to be sent through the communication channel to the remote filter.

We then propose a cubature Kalman filter to estimate the system states based on the received measurements. We show that by choosing a proper triggering threshold, the estimation error and the prediction error covariance of the state estimator remain bounded while reducing the data communication between the sensors, compared to traditional state estimator without event-triggered mechanism.

The rest of this chapter is organized as follows. In Section 3.1 the nonlinear system model, and the event-triggered rule are defined. In Section 3.2, the complete theory of the discrete-time event-triggered CKF for nonlinear systems is studied. Simulation results are presented in Section 3.3 to show the efficiency of the proposed filter and finally Section 3.4 summarizes the results of this chapter.

[1] The results of this chapter has been published in the article: M. Kooshkbaghi, H. J. Marquez, "Event-Triggered State Estimation of High Dimensional Nonlinear Systems with Highly Nonlinear State Space Model Using Cubature Kalman Filter," *CCECE 2019*, May 2019, Canada

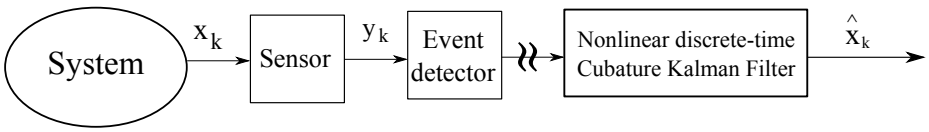

Figure 3.1: A System with Event-Triggered Mechanism

3.1 Problem formulation

3.1.1 System model

Recalling from *Chapter 2*, we consider the nonlinear discrete-time system model as follows,

$$x_{k+1} = f(x_k, u_k) + \omega_k, \tag{3.1}$$

$$y_{k+1} = h(x_{k+1}) + \nu_{k+1}. \tag{3.2}$$

$x_k \in \mathbb{R}^{n_x}$ and $y_k \in \mathbb{R}^{n_y}$ are the state vector, and output measurement vector, respectively. $u_k \in \mathbb{R}^{n_u}$ is the control input. The process noise ω and the measurement noise ν are uncorrelated zero-mean Gaussian white noise sequences with Covariance $Q \in \mathbb{R}^{n_x \times n_x}$ and $R \in \mathbb{R}^{n_y \times n_y}$, respectively.

3.1.2 Event-triggered data transferring mechanism

The block diagram of the networked system with the event-triggered CKF is shown in *Figure 3.1.* Here the sensor measures the system's output y_k in a periodic manner. Sensor outputs are sent to the event detector which determines whether or not information is to be sent through the communication channel to the remote CKF. The event detector works as follows: let y_k represent the current sensor measurement and $\overline{y}$ denotes the last measurement transmitted through the channel. Define now the binary decision variable γ_k as follows:

$$\gamma_k = \begin{cases} 1 & if \quad (y_k - \bar{y})^T (y_k - \bar{y}) > \delta \\ 0 & \text{otherwise.} \end{cases} \tag{3.3}$$

The parameter $\delta > 0$ is the threshold of the event-triggered mechanism. The event detector updates the output value and sends new information through the communication channel if and only if $\gamma_k = 1$. Thus, defining

$$\bar{y}_k = y_k + (1 - \gamma_k)(\overline{y} - y_k), \tag{3.4}$$

we see that

$$\bar{y}_k = \begin{cases} y_k & if \quad \gamma_k = 1 \\ y_k - e_k & \text{otherwise,} \end{cases} \tag{3.5}$$

where $\bar{y}_k$ is the measurement transmitted at time k, and $e_k = (y_k - \bar{y})$.

As mentioned before, in this chapter, we develop a design framework for CKFs for nonlinear discrete-time systems with the event-triggered data transmission defined in (3.3).

Note 3.1: *With the event-triggering mechanism, the conditional densities are no longer Gaussian, and the numerical integration of the multi-dimensional integrals used in computing the mean and the covariance of nonlinear filter become computationally too expensive. There are some proposed approaches which directly tackle the non-Gaussian issues caused by the event-triggering conditions. For instance, in [32] the sums of Gaussians approach, is introduced to approximate the non-Gaussian density function. In [31], a class of stochastic event-triggering conditions were proposed to obtain the estimation without additional approximation. In this work, we assume that all conditional densities remain approximately Gaussian after event-triggered sampling [53]. This assumption has been widely used in many references [77], [5, 6].*

3.2 Discrete-Time Event-Triggered Cubature Kalman Filter

In this section, we consider the nonlinear system in the presence of the event-triggered mechanism and we derive CKF estimation error covariance and CKF gain. Note that in order to derive the nonlinear filtering problem with the event-triggered mechanism, the linearization with first order approximation is implemented to facilitate the following discussion.

Theorem 3.1: *Consider the system* (3.1)-(3.2) *with the event-triggered mechanism* (3.3)-(3.4)*. The cubature Kalman filter estimation error covariance and the filter gain are as follows,*

$$\begin{aligned}\hat{P}_{k+1} =&(I-K_{k+1}B_{k+1})\hat{P}_{k+1|k}(I-K_{k+1}B_{k+1})^T + K_{k+1}(1-\gamma_{k+1})E\{e_{k+1}e_{k+1}^T\}\\ &\times(1-\gamma_{k+1})^T K_{k+1}^T + (1-\gamma_{k+1})E\Big\{(I-K_{k+1}B_{k+1})\widetilde{x}_{k+1|k}e_{k+1}^T K_{k+1}^T\\ &-K_{k+1}\nu_{k+1}e_{k+1}^T K_{k+1}^T - K_{k+1}e_{k+1}\nu_{k+1}^T K_{k+1}^T + K_{k+1}e_{k+1}\tilde{x}_{k+1|k}^T\\ &\times(I-K_{k+1}B_{k+1})^T\Big\} + K_{k+1}RK_{k+1}^T,\end{aligned} \tag{3.6}$$

$$\begin{aligned}K_{k+1} =&\Big(1+a_1(1-\gamma_{k+1})\Big)\hat{P}_{k+1|k}B_{k+1}^T\Big[\Big(1+a_1(1-\gamma_{k+1})\Big)B_{k+1}\hat{P}_{k+1|k}B_{k+1}^T+\\ &\Big(1+a_2(1-\gamma_{k+1})\Big)R_{k+1}+(1+a_1^{-1}+a_2^{-1})(1-\gamma_{k+1})\delta I\Big]^{-1}.\end{aligned} \tag{3.7}$$

In this expression, $B_{k+1}=\beta_{k+1}H_{k+1}$*, where* $H_{k+1}=\frac{\partial h(x)}{\partial x}|_{x=\hat{x}_{k+1|k}}$ *is the Jacobian matrix and* $\beta_{k+1}=diag(\beta_{1,k+1},\beta_{2,k+1},...,\beta_{n_y k+1})$ *is an unknown diagonal matrix representing the error incurred in neglecting the higher order terms of the series.* $\widetilde{x}_{k+1|k}$ *and* $\hat{P}_{k+1|k}$ *are the prediction error and the prediction error covariance, respectively.* $a_1>0$ *and* $a_2>0$ *are two positive arbitrary parameters.*

Proof. The event-triggered system estimation error (difference between the real state x_{k+1} and the posterior state $\hat{x}_{k+1}$) and the event-triggered system prediction error (difference between the real state x_{k+1} and the predicted state $\hat{x}_{k+1|k}$), are as follows:

$$\widetilde{x}_{k+1} = x_{k+1} - \hat{x}_{k+1}, \tag{3.8}$$

$$\widetilde{x}_{k+1|k} = x_{k+1} - \hat{x}_{k+1|k}. \tag{3.9}$$

Substituting (3.1) and (2.17) into (3.9) and expanding $f(x_k, u_k)$ in Taylor series, we obtain:

$$\widetilde{x}_{k+1|k} = \nabla f(\hat{x}_k, u_k)\widetilde{x}_k + \sum_{j=1}^{\infty} \frac{1}{(2j+1)!} \nabla^{(2j+1)} f(\hat{x}_{k-1}, u_k)\tilde{x}_k^{(2j+1)} + \omega_k, \tag{3.10}$$

where $\nabla = \frac{\partial}{\partial x}|_{x=\hat{x}_k}$. (3.10) can be written as follows,

$$\widetilde{x}_{k+1|k} = A_k\widetilde{x}_k + \omega_k. \tag{3.11}$$

$A_k = \frac{\partial f(x)}{\partial x}|_{x=\hat{x}_k}$ is the Jacobian matrix. Similarly, for the measurement prediction error (difference between the real system measurement y_{k+1} and the predicted measurement $\hat{y}_{k+1|k}$), we have,

$$\widetilde{y}_{k+1|k} = B_{k+1}\widetilde{x}_{k+1|k} + \nu_{k+1}. \tag{3.12}$$

Substituting (3.4) in (2.25), we have,

$$\hat{x}_{k+1} = \hat{x}_{k+1|k} + K_{k+1}\Big(\widetilde{y}_{k+1|k} - (1-\gamma_{k+1})e_{k+1}\Big), \tag{3.13}$$

replacing (3.13) into (3.8), and taking (3.12) into account, the estimation error is as follows,

$$\widetilde{x}_{k+1} = (I - K_{k+1}B_{k+1})\widetilde{x}_{k+1|k} - K_{k+1}\nu_{k+1} + K_{k+1}(1-\gamma_{k+1})e_{k+1}, \tag{3.14}$$

substituting (3.14) in (3.11), we obtain the following,

$$\widetilde{x}_{k+1|k} = A_k(I - K_kB_k)\widetilde{x}_{k|k-1} - A_kK_k\nu_k + A_kK_k(1-\gamma_k)e_k + \omega_k. \tag{3.15}$$

Substituting (3.14) into $\hat{P}_{k+1} = E\{\widetilde{x}_{k+1}\tilde{x}_{k+1}^T\}$, the estimation error covariance matrix, (3.6) can be obtained.

To derive the filter gain we use the following *Lemma 3.1*,

Lemma 3.1: *For any two vectors $x, y \in R^n$, the following inequality holds: $xy^T + yx^T \leq \varepsilon xx^T + \varepsilon^{-1}yy^T$, where $\varepsilon > 0$ is a scalar [5].*

The following inequalities follow immediately by application of *Lemma 3.1* with $a_1 > 0$ and $a_2 > 0$.

$$\begin{aligned}&(I - K_{k+1}B_{k+1})\widetilde{x}_{k+1|k}e_{k+1}^TK_{k+1}^T + K_{k+1}e_{k+1}\tilde{x}_{k+1|k}^T(I - K_{k+1}B_{k+1})^T \leq \\ &a_1(I - K_{k+1}B_{k+1})\widetilde{x}_{k+1|k}\tilde{x}_{k+1|k}^T(I - K_{k+1}B_{k+1})^T + a_1^{-1}K_{k+1}e_{k+1}e_{k+1}^TK_{k+1},\end{aligned} \tag{3.16}$$

$$
\begin{aligned}
&- K_{k+1}\nu_{k+1}e_{k+1}^{T}K_{k+1}^{T} - K_{k+1}e_{k+1}\nu_{k+1}^{T}K_{k+1}^{T} \leq \\
&a_2 K_{k+1}\lambda_{k+1}\nu_{k+1}\nu_{k+1}^{T}K_{k+1}^{T} + a_2^{-1}K_{k+1}e_{k+1}e_{k+1}^{T}K_{k+1}.
\end{aligned} \tag{3.17}
$$

Substituting (3.16) and (3.17) in (3.6) we have,

$$
\begin{aligned}
&\hat{P}_{k+1} \leq (I - K_{k+1}B_{k+1})\hat{P}_{k+1|k}(I - K_{k+1}B_{k+1})^{T} + K_{k+1}R_{k+1}K_{k+1}^{T} \\
&+ K_{k+1}(1-\gamma_{k+1})E\{e_{k+1}e_{k+1}^{T}\}(1-\gamma_{k+1})^{T}K_{k+1}^{T} + (1-\gamma_{k+1})E\Big\{a_1(I- \\
&K_{k+1}B_{k+1})\widetilde{x}_{k+1|k}\tilde{x}_{k+1|k}^{T}(I - K_{k+1}B_{k+1})^{T} + a_1^{-1}K_{k+1}e_{k+1}e_{k+1}^{T}K_{k+1}^{T} \\
&+ a_2 K_{k+1}\nu_{k+1}\nu_{k+1}^{T}K_{k+1}^{T} + a_2^{-1}K_{k+1}e_{k+1}e_{k+1}^{T}K_{k+1}^{T}\Big\}.
\end{aligned} \tag{3.18}
$$

The upper bound of the error covariance matrix is as follows,

$$
\begin{aligned}
\overline{P}_{k+1} =&\Big(1 + a_1(1-\gamma_{k+1})\Big)(I - K_{k+1}B_{k+1})\hat{P}_{k+1|k}(I - K_{k+1}B_{k+1})^{T} + (1 + a_2 \\
&\times (1-\gamma_{k+1}))K_{k+1}R_{k+1}K_{k+1}^{T} + (1-\gamma_{k+1})(1 + a_1^{-1} + a_2^{-1})K_{k+1}\delta I K_{k+1}^{T}.
\end{aligned} \tag{3.19}
$$

The filtering gain K_{k+1} will be designed by minimizing the upper bound of the error covariance matrix. Taking the partial derivative of the $\overline{P}_{k+1}$, the event-triggered CKF gain, (3.7) can be obtained.

$$
\frac{\partial tr\overline{P}_{k+1}}{\partial K_{k+1}} = 0. \tag{3.20}
$$

This completes the proof. ■

Note that the uses of *Lemma 3.1* bring in conservatism for the filter design. Even so, the parameters a_1 and a_2 can be chosen appropriately to reduce such conservatism. In the next chapter, we briefly explain this isssue. Table 3.1, provides the algorithm of the proposed event-triggered discrete-time cubature Kalman filter. Note that the proposed DECKF is a derivative-free filter, which does not require computation of the Jacobian matrix. Suppose that $\hat{P}_{k+1|k}$ is the predicted state error covariance matrix, then based on $\hat{P}_{k+1|k}^{xy} = \hat{P}_{k+1|k}B_{k+1}^{T}$, one can derive the following $B_{k+1} = (\hat{P}_{xy,k+1|k})^{T}(\hat{P}_{k+1|k})^{-1}$ [39], where $\hat{P}_{xy,k+1|k}$ is the cross-covariance matrix. CKF algorithm consists of prediction steps and update steps. In the prediction steps, the CKF propagates the estimate from the last time step to the current time step before the arrival of fresh measurement data. In the update steps, the filter updates the estimate using collected measurements.

3.3 Simulation Results

In this section the effectiveness of the proposed method is illustrated by a tracking scenario where the objective is to track the trajectory of the two link robot arm in Figure 3.2. We compare the trade-off between the communication rate and the estimation quality under different conditions such as different triggering threshold values.

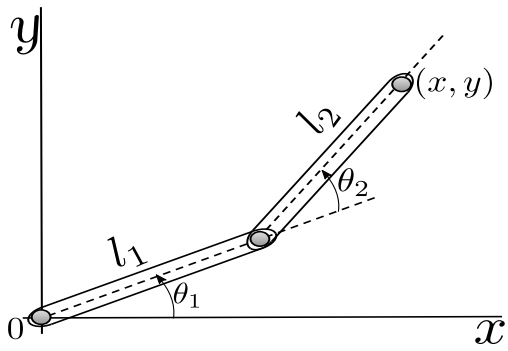

Figure 3.2: Two link robot arm illustrating how the Cartesian coordinates (x; y) of the end effector is mapped to the given angles.

The state space model of the system is as follows.

$$\theta_{k+1} = \theta_k + \omega_k, \tag{3.21}$$

$$Y_k = \begin{pmatrix} cos(\theta_{1,k}) & cos(\theta_{1,k} + \theta_{2,k}) \\ sin(\theta_{1,k}) & sin(\theta_{1,k} + \theta_{2,k}) \end{pmatrix} \begin{pmatrix} l_1 \\ l_2 \end{pmatrix} + \nu_k, \tag{3.22}$$

where states, $\theta = [\theta_1 \quad \theta_2]^T$, show the joint angles of the arm and $Y = [x \quad y]^T$, shows the position of the end effector of the robot arm. The length of the links are considered as $l_1 = 1$, and $l_2 = 2$, respectively. Noises which perturb the state and the measurement equations are $\omega \sim \ N(0, diag[0.01, 0.1])$, and $\nu \sim N(0, 0.005I)$.

Figure 3.3 and *Figure 3.4* show the comparison between the tracking results of a system with the event-triggered threshold of $\delta = 0.01$, and $\delta = 0.05$, respectively. The number of data transmission for the system without event-triggered mechanism, $\delta = 0$, is 6300 which reduces significantly to 3900 and 1190 for $\delta = 0.01$ and $\delta = 0.05$, respectively. *Figure 3.5* shows the result for the time that $\delta > 0.1$, which the filter diverges. In *Figure 3.6*, we compare the RMSE results of the filter with different event-triggered threshold. From the results, it can be concluded that by increasing the triggering threshold the estimation quality would be degraded. Also, from the tracking and RMSE results, we select $\delta = 0.05$ as the threshold of event triggered mechanism as it has a good tracking result while it reduces the communication rate.

3.4 Summary

In this chapter, we present a complete theory of a nonlinear filter for high dimensional nonlinear systems under the event-triggered mechanism. As mentioned in the introduction, the event-triggered formulation is an alternative to conventional periodic discrete-time sampling which can render similar performance while reducing communication between sensors

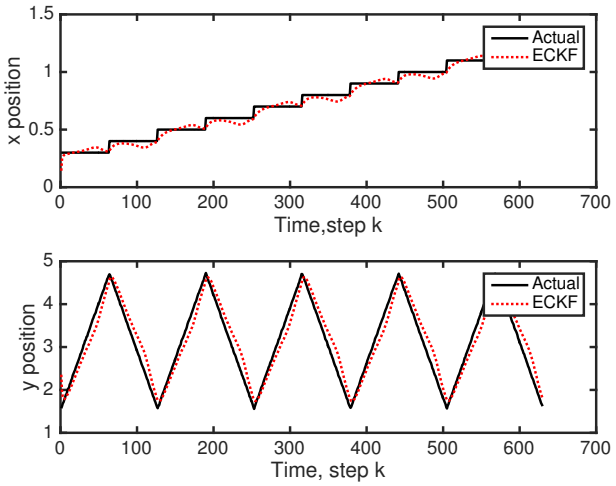

Figure 3.3: Tracking results with triggering threshold $\delta = 0.01$

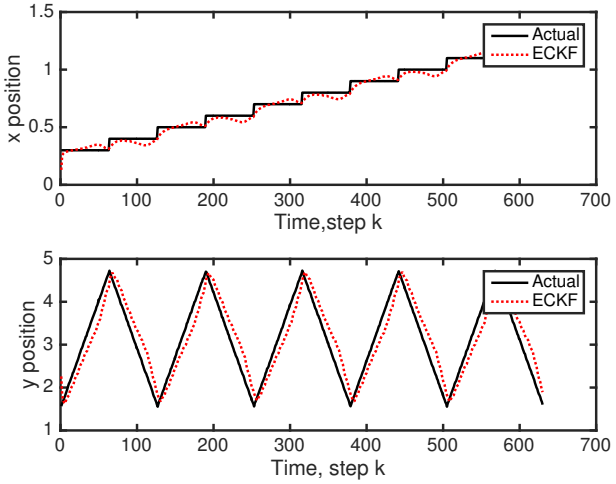

Figure 3.4: Tracking results with triggering threshold $\delta = 0.05$

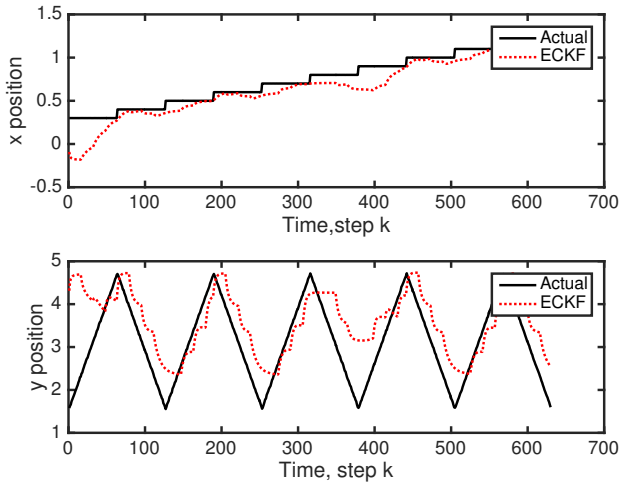

Figure 3.5: Tracking results with triggering threshold $\delta > 0.1$

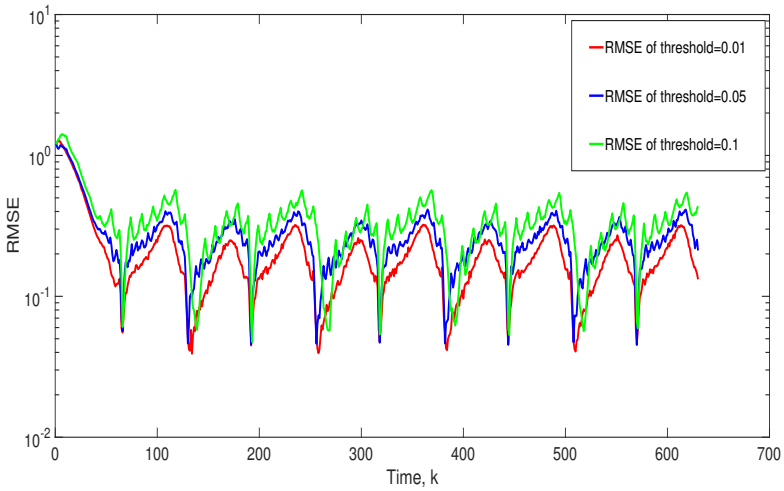

Figure 3.6: RMSE results with different event-triggered thresholds

and remote filters. We consider "send-on-delta" triggering mechanism which reduces the feedback communication between the sensors and the remote state estimators compared to the other triggering schemes. The event-triggered nonlinear filter gain is derived to reduce the estimation error and make the error covariance matrix bounded. Applied to nonlinear system model, our results show excellent tracking of the true states, despite an impressive communication reduction between the sensors and the remote filter.

Table 3.1: **Algorithm 1.** Event-Triggered Discrete-Time Cubature Kalman Filter

Time update steps:

The mean x_0 and covariance P_0 of initial state are both known.

1) Factorize:

$\hat{P}_k = S_k S_k^T$

2) Derive the Cubature Points:

$X_{i,k} = S_k \xi_i + \hat{x}_k \quad i = 1, 2, ..., 2n_x$

3) Propagate the Points:

$X^*_{i,k+1|k} = f(X_{i,k}, u_k) \quad i = 1, 2, ..., 2n_x$

4) Estimate the predicted state:

$\hat{x}_{k+1|k} = \frac{1}{2n_x} \sum_{i=1}^{2n_x} X^*_{i,k+1|k}$

5) Calculate the predicted state error covariance:

$\hat{P}_{k+1|k} = \frac{1}{2n_x} \sum_{i=1}^{2n_x} X^*_{i,k+1|k} X^{*T}_{i,k+1|k} - \hat{x}_{k+1|k} \hat{x}^T_{k+1|k} + Q_k$

Measurement update steps:

1) Factorize:

$\hat{P}_{k+1|k} = S_{k+1|k} S_{k+1|k}$

2) Calculate the Cubature points:

$X_{i,k+1|k} = S_{k+1|k} \xi_i + \hat{x}_{k+1|k} \qquad i = 1, 2, ..., 2n_x$

3)Propagate the points:

$Y_{i,k+1|k} = h(X_{i,k+1|k}, u_{k+1})$

4)Predicted the measurement:

$\hat{y}_{k+1|k} = \frac{1}{2n_x} \sum_{i=1}^{2n_x} Y_{i,k+1|k}$

5) Calculate the innovation covariance matrix:

$\hat{P}_{yy,k+1} = \frac{1}{2n_x} \sum_{i=1}^{2n_x} Y_{i,k+1|k} Y^T_{i,k+1|k} - \hat{y}_{k+1|k} \hat{y}^T_{k+1|k} + R_{k+1}$

6) Calculate the cross-covariance matrix:

$\hat{P}_{xy,k+1} = \frac{1}{2n_x} \sum_{i=1}^{2n_x} X_{i,k+1|k} Y^T_{i,k+1|k} - \hat{x}_{k+1|k} \hat{y}^T_{k+1|k}$

7) Compute the filter gain:

$K_{k+1} = \Big(1 + a_1(1 - \gamma_{k+1})\Big) \hat{P}_{xy,k+1}$

$\times \Big[(1 + a_1(1 - \gamma_{k+1})) \hat{P}^T_{xy,k+1} \hat{P}^{-1}_{k+1|k} \hat{P}_{xy,k+1}$

$+(1 + a_2(1 - \gamma_{k+1})) R_{k+1} + (1 + a_1^{-1} + a_2^{-1})(1 - \gamma_{k+1}) \delta I \Big]^{-1}$

8) Estimate the updated state:

$\hat{x}_{k+1} = \hat{x}_{k+1|k} + K_{k+1}(\overline{y}_{k+1} - \hat{y}_{k+1|k})$

9) Compute the state error covariance:

$\overline{P}_{k+1} = \Big(1 + a_1(1 - \gamma_{k+1})\Big)(I - K_{k+1} P^T_{xy,k+1} P^{-1}_{k+1|k})$

$\times \hat{P}_{k+1|k} (I - K_{k+1} P^T_{xy,k+1} P^{-1}_{k+1|k})^T +$

$\Big(1 + a_2(1 - \gamma_{k+1})\Big) K_{k+1} R_{k+1} K^T_{k+1} +$

$(1 - \gamma_{k+1})(1 + a_1^{-1} + a_2^{-1}) K_{k+1} \lambda_{k+1} \delta I K^T_{k+1}$

Chapter 4

Event-triggered Discrete-time Cubature Kalman filter in the presence of packet dropouts

In this chapter,[1] we develop an event-triggered discrete time Cubature Kalman filter applicable to high dimensional nonlinear dynamic system with strong nonlinearities when the packet drop outs occur during data transmission in the communication channels. We show that by choosing a proper event-triggered threshold and properly tuning the threshold of the event-triggered mechanism and the rate of the packet dropout, the proposed method reduces the number of data transmission between the sensors and the state estimator with respect to traditional discrete time Cubature Kalman filter. In addition, we develop a complete theory to show the boundedness of the state estimation error, estimation error covariance and the stochastic stability of the proposed filter. A lower bound for the communication rate is also obtained to guarantee the convergence of the proposed filter.

The remainder of this chapter is as follows. In Section 4.1, the nonlinear system model is defined, and we introduce the event-triggered rule, the packet dropout and the CKF. In Section 4.2, we will design a discrete-time event-triggered CKF for nonlinear systems. In Section 4.3, we study the boundedness of the state estimation error. In Section 4.3, we illustrate our results using a simulated example.

[1]The results of this chapter has been accepted for publication in the article: M. Kooshkbaghi, H. J. Marquez, "Event-Triggered Discrete-Time Cubature Kalman Filter for Nonlinear Dynamical Systems with Packet Dropout," *IEEE Transactions on Automatic Control* Sep. 2019

4.1 Problem formulation

4.1.1 System model

In this chapter, recalling from *Chapter 3*, we consider the following nonlinear discrete-time model, equations (4.1) and (4.2), with the current transmitted measurement,(4.3), defined in *Chapter 3*, as follows,

$$x_{k+1} = f(x_k, u_k) + \omega_k, \tag{4.1}$$

$$y_{k+1} = h(x_{k+1}) + \nu_{k+1}, \tag{4.2}$$

$$\bar{y}_k = y_k + (1 - \gamma_k)(\overline{y} - y_k), \tag{4.3}$$

4.1.2 Packet dropouts

Packet dropouts can occur during data transmission through the communication channel resulting in data losses. We define λ_k to be the binary random variable modelling packet dropout:

$$\lambda_k = \begin{cases} 1 & \text{data is received} \\ 0 & \text{otherwise.} \end{cases} \tag{4.4}$$

Measurements are received by the state estimator if and only if $\lambda_k = 1$. Note that the packet dropout happens while data is transferred through the communication channel ($\gamma_k = 1$). We assume throughout this thesis that the packet dropout rate is unknown, and we define the packet arrival rate, or packet delivery rate, as follows,

$$\lambda = E[\lambda_k]. \tag{4.5}$$

The packet dropout rate affects the boundedness of the estimation error. Our goal is to design a discrete-time CKF to reduce the impact of the event-triggered mechanism and the packet dropout on the state estimation error.

Note 4.1: *Following references [19] and [63], we define the probability density distribution of the observation noise ν_k with respect to λ_k as follows,*

$$p(\nu_k|\lambda_k) = \begin{cases} N(0, R_k) & \lambda_k = 1 \\ N(0, \sigma^2 I) & \lambda_k = 0 \end{cases}, \tag{4.6}$$

where $\sigma \to \infty$.

We assume that the remote state estimator receives λ_k and γ_k, at each time step. This assumption has been used in many references [5, 6, 19, 63]. In the absence of observation, the state estimator receives no new information and it will not update the state estimation and the corresponding covariance.

4.2 Design of Discrete-time Event-triggered Cubature Kalman Filter with packet dropout

In this section, to derive the nonlinear filtering problem with the event-triggered mechanism and the packet dropout, the linearization with first order approximation is implemented to facilitate the following discussion.

Theorem 4.1: *Consider the system* (4.1)-(4.2) *along with the current transmitted measurement (measurement transmitted under the event-triggered mechanism)* (4.3) *and the packet dropout parameter,* λ_k*. Under these conditions, the CKF estimation error covariance* $\hat{P}_{k+1}$*, and the filter gain are given by:*

$$\begin{aligned}\hat{P}_{k+1} =&(I - K_{k+1}\lambda_{k+1}B_{k+1})\hat{P}_{k+1|k}(I - K_{k+1}\lambda_{k+1}B_{k+1})^T + K_{k+1}\lambda_{k+1}R\lambda_{k+1}^T K_{k+1}^T \\ &+ K_{k+1}\lambda_{k+1}(1-\gamma_{k+1})E\{e_{k+1}e_{k+1}^T\}\lambda_{k+1}^T K_{k+1}^T + (1-\gamma_{k+1})E\Big\{(I - K_{k+1} \\ &\times \lambda_{k+1}B_{k+1})\widetilde{x}_{k+1|k}e_{k+1}^T\lambda_{k+1}^T K_{k+1}^T + K_{k+1}\lambda_{k+1}e_{k+1}\tilde{x}_{k+1|k}^T(I - K_{k+1}\lambda_{k+1} \\ &\times B_{k+1})^T - K_{k+1}\lambda_{k+1}\nu_{k+1}e_{k+1}^T\lambda_{k+1}^T K_{k+1}^T - K_{k+1}\lambda_{k+1}e_{k+1}\nu_{k+1}^T\lambda_{k+1}^T K_{k+1}^T\Big\}.\end{aligned} \tag{4.7}$$

$$\begin{aligned}K_{k+1} = &\Big(1 + a_1(1-\gamma_{k+1})\Big)\lambda_{k+1}\hat{P}_{k+1|k}B_{k+1}^T\Bigg[\Big(1 + a_1(1-\gamma_{k+1})\Big)B_{k+1}\hat{P}_{k+1|k}B_{k+1}^T \\ &+ \Big(1 + a_2(1-\gamma_{k+1})\Big)R_{k+1} + (1 + a_1^{-1} + a_2^{-1})(1-\gamma_{k+1})\delta I\Bigg]^{-1}.\end{aligned} \tag{4.8}$$

In this expression, $B_{k+1} = \beta_{k+1}H_{k+1}$*, where* $H_{k+1} = \frac{\partial h(x)}{\partial x}|_{x=\hat{x}_{k+1|k}}$ *is the Jacobian matrix and* $\beta_{k+1} = diag(\beta_{1,k+1}, \beta_{2,k+1}, ..., \beta_{n_y k+1})$ *is an unknown diagonal matrix representing the error incurred in neglecting the higher order terms.* $\widetilde{x}_{k+1|k}$ *and* $\hat{P}_{k+1|k}$ *are the prediction error and the prediction error covariance, respectively.* a_1 *and* a_2 *are two positive arbitrary parameters.*

Proof. Note that recalling from *Chapter 3*, by substituting (4.3) in (3.13) and considering the packet dropout in the communication channels, the state estimation and the estimation error are as follows,

$$\hat{x}_{k+1} = \hat{x}_{k+1|k} + K_{k+1}\lambda_{k+1}\Big(\widetilde{y}_{k+1|k} - (1-\gamma_{k+1})e_{k+1}\Big). \tag{4.9}$$

$$\widetilde{x}_{k+1} = \widetilde{x}_{k+1|k} - K_{k+1}\lambda_{k+1}\Big(\widetilde{y}_{k+1|k} - (1-\gamma_{k+1})e_{k+1}\Big). \tag{4.10}$$

Substituting $\widetilde{y}_{k+1|k}$ from (3.12), in (4.10) we have,

$$\widetilde{x}_{k+1} =(I - \lambda_{k+1}K_{k+1}B_{k+1})\widetilde{x}_{k+1|k} - \lambda_{k+1}K_{k+1}\Big(\nu_{k+1} - (1-\gamma_{k+1})e_{k+1}\Big). \tag{4.11}$$

Finally, considering (3.11), the estimation of the prediction state is as follows,

$$\widetilde{x}_{k+1|k} = A_k(I - K_k\lambda_k B_k)\widetilde{x}_{k|k-1} - A_k K_k\lambda_k\nu_k + A_k K_k\lambda_k(1-\gamma_k)e_k + \omega_k. \tag{4.12}$$

The estimation error covariance matrix is $\hat{P}_{k+1} = E\{\widetilde{x}_{k+1}\tilde{x}_{k+1}^T\}$. Substituting (4.11) in $\hat{P}_{k+1}$, we obtain (4.7). The following inequalities follow immediately by application of *Lemma 3.1* for any $a_1 > 0$ and $a_2 > 0$:

$$\begin{aligned}(I - K_{k+1}\lambda_{k+1}B_{k+1})\widetilde{x}_{k+1|k}e_{k+1}^T\lambda_{k+1}^T K_{k+1}^T + K_{k+1}\lambda_{k+1}e_{k+1}\tilde{x}_{k+1|k}^T(I - K_{k+1}\lambda_{k+1}B_{k+1})^T \leq \\ a_1(I - K_{k+1}\lambda_{k+1}B_{k+1})\widetilde{x}_{k+1|k}\tilde{x}_{k+1|k}^T(I - K_{k+1}\lambda_{k+1}B_{k+1})^T + a_1^{-1}K_{k+1}\lambda_{k+1}e_{k+1}e_{k+1}^T\lambda_{k+1}^T K_{k+1},\end{aligned} \tag{4.13}$$

$$\begin{aligned}&- K_{k+1}\lambda_{k+1}\nu_{k+1}e_{k+1}^T\lambda_{k+1}^T K_{k+1}^T - K_{k+1}\lambda_{k+1}e_{k+1}\nu_{k+1}^T\lambda_{k+1}^T K_{k+1}^T \\ &\leq a_2 K_{k+1}\lambda_{k+1}\nu_{k+1}\nu_{k+1}^T\lambda_{k+1}^T K_{k+1}^T + a_2^{-1}K_{k+1}\lambda_{k+1}e_{k+1}e_{k+1}^T\lambda_{k+1}^T K_{k+1}.\end{aligned} \tag{4.14}$$

Substituting (4.13) and (4.14) into (4.7) we have,

$$\begin{aligned}&\hat{P}_{k+1} \leq (I - K_{k+1}\lambda_{k+1}B_{k+1})\hat{P}_{k+1|k}(I - K_{k+1}\lambda_{k+1}B_{k+1})^T + K_{k+1}\lambda_{k+1}R_{k+1}\lambda_{k+1}^T K_{k+1}^T \\ &+ K_{k+1}\lambda_{k+1}(1-\gamma_{k+1})E\{e_{k+1}e_{k+1}^T\}(1-\gamma_{k+1})^T\lambda_{k+1}^T K_{k+1}^T + (1-\gamma_{k+1})E\Big\{a_1(I \\ &- K_{k+1}\lambda_{k+1}B_{k+1})\widetilde{x}_{k+1|k}\tilde{x}_{k+1|k}^T(I - K_{k+1}\lambda_{k+1}B_{k+1})^T + a_1^{-1}K_{k+1}\lambda_{k+1}e_{k+1}e_{k+1}^T\lambda_{k+1}^T K_{k+1}^T \\ &+ a_2 K_{k+1}\lambda_{k+1}\nu_{k+1}\nu_{k+1}^T\lambda_{k+1}^T K_{k+1}^T + a_2^{-1}K_{k+1}\lambda_{k+1}e_{k+1}e_{k+1}^T\lambda_{k+1}^T K_{k+1}^T\Big\}.\end{aligned} \tag{4.15}$$

It follows that the upper bound of the error covariance matrix can be written as follows:

$$\begin{aligned}\overline{P}_{k+1} =&\Big(1 + a_1(1-\gamma_{k+1})\Big)(I - K_{k+1}\lambda_{k+1}B_{k+1})\hat{P}_{k+1|k}(I - K_{k+1}\lambda_{k+1}B_{k+1})^T \\ &+ \Big(1 + a_2(1-\gamma_{k+1})\Big)K_{k+1}\lambda_{k+1}R_{k+1}\lambda_{k+1}^T K_{k+1}^T + (1-\gamma_{k+1})(1 + a_1^{-1} + a_2^{-1})K_{k+1} \\ &\times \lambda_{k+1}\delta I\lambda_{k+1}^T K_{k+1}^T.\end{aligned} \tag{4.16}$$

The upper bound of the error covariance matrix is minimized when its matrix derivative with respect to the gain matrix is zero, *i.e.* $\frac{\partial\overline{P}_{k+1}}{\partial K_{k+1}} = 0$, which leads to the filter gain (4.8).

$$\frac{\partial tr\overline{P}_{k+1}}{\partial K_{k+1}} = 0 \tag{4.17}$$

solving (4.17) we obtain the filter gain (4.8), which completes the proof. ■

Remark 4.1: *The estimation error and the estimation error covariance matrix of the classical CKF are as follows,*

$$\widetilde{x}_k = \widetilde{x}_{k|k-1} - K_k\widetilde{y}_{k|k-1},$$

$$\hat{P}_k = (I - K_k B_k)\hat{P}_{k|k-1}(I - K_k B_k)^T + K_k R K_k^T.$$

Comparing (4.10) *and* (4.7) *to the classical CKF we see that the event-triggered mechanism introduces additional terms affecting the upper and the lower bounds of the estimation error and the estimation error covariance, respectively. These changes affect the design of the filter gain and the boundedness of the estimation error. In the next sections, we study the boundedness of the proposed filter estimation error in the presence of the event-triggered mechanism and packet dropout.*

Table 4.1, provides the algorithm of the proposed Discrete-Time Event-triggered Cubature Kalman Filter. Note that the DECKF is a derivative-free filter, which does not require computation of the Jacobian matrix.

In the next section we study how the event-triggered mechanism affects the boundedness of the estimation error of the event-triggered CKF.

4.3 Boundedness of the estimation error for the even-triggered CKF

In this section, we study the stochastic stability of the proposed CKF. We assume that the linearized form of the system (4.1)-(4.2) is uniformly observable [23], and that the following conditions are satisfied [12]:

$$\begin{aligned}
&\hat{q}_{\min} I \leq \hat{Q}_k; Q_k \leq q_{\max} I; f_{\min}^2 I \leq F_k F_k^T \leq f_{\max}^2 I \\
&r_{\min} I \leq R_k \leq r_{\max}; \alpha_{\min}^2 f_{\min}^2 I \leq A_k A_k^T \leq \alpha_{\max}^2 f_{\max}^2 I \\
&\beta_{\min}^2 I \leq \beta_k \beta_k^T \leq \beta_{\max}^2 I; \beta_{\min}^2 h_{\min}^2 I \leq B_k B_k^T \leq \beta_{\max}^2 h_{\max}^2 I \\
&h_{\min}^2 I \leq H_k H_k^T \leq h_{\max}^2 I; \alpha_{\min}^2 I \leq \alpha_k \alpha_k^T \leq \alpha_{\max}^2 I,
\end{aligned} \tag{4.18}$$

where $f_{\min}, f_{\max}, h_{\min}, h_{\max}, \beta_{\min}, \beta_{\max}, \alpha_{\min}, \alpha_{\max} \neq 0$, and $r_{\max}, q_{\max}, \hat{q}_{\min}, \hat{r}_{\min} > 0$ are all real numbers.

Lemma 4.1: *Assume that there is a stochastic process $V_k(\xi_k)$ with the following conditions:*

$$\upsilon_{\min} \|\xi_k\|^2 \leq V_k(\xi_k) \leq \upsilon_{\max} \|\xi_k\|^2, \tag{4.19}$$

$$E[V_k(\xi_k)|\xi_{k-1}] - V_{k-1}(\xi_{k-1}) \leq \mu - \tau V_{k-1}(\xi_{k-1}), \tag{4.20}$$

where $\upsilon_{\min}, \upsilon_{\max}, \mu > 0$ and $0 < \tau \leq 1$ and all are real numbers. Then the stochastic process is exponentially bounded in mean square sense, i.e.

$$E[\|\xi_k\|^2] \leq \frac{\upsilon_{\max}}{\upsilon_{\min}} E[\|\xi_0\|^2](1-\tau)^k + \frac{\mu}{\upsilon_{\min}} \sum_{i=1}^{k-1} (1-\tau)^i. \tag{4.21}$$

Proof. The proof is straightforward, [24]. ■

Table 4.1: **Algrithm 1.** Discrete-Time Event-Triggered Cubature Kalman Filter

Time update:
The mean x_0 and covariance P_0 of initial state are both known.
Step 1: Factorize:
$\hat{P}_k = S_k S_k^T$
Step 2: Calculate the Cubature Points:
$X_{i,k} = S_k \xi_i + \hat{x}_k \qquad i = 1, 2, ..., 2n_x$
Step3: Propagate the Cubature Points:
$X^*_{i,k+1\|k} = f(X_{i,k}, u_k) \qquad i = 1, 2, ..., 2n_x$
Step 4: Estimate the predicted state:
$\hat{x}_{k+1\|k} = \frac{1}{2n_x} \sum_{i=1}^{2n_x} X^*_{i,k+1\|k}$
Step 5: Calculate the predicted state error covariance:
$\hat{P}_{k+1\|k} = \frac{1}{2n_x} \sum_{i=1}^{2n_x} X^*_{i,k+1\|k} X^{*T}_{i,k+1\|k} - \hat{x}_{k+1\|k} \hat{x}^T_{k+1\|k} + Q_k$
Measurement update:
Step 1: Factorize:
$\hat{P}_{k+1\|k} = S_{k+1\|k} S_{k+1\|k}$
Step 2: Calculate the Cubature points:
$X_{i,k+1\|k} = S_{k+1\|k} \xi_i + \hat{x}_{k+1\|k} \qquad i = 1, 2, ..., 2n_x$
Step 3: Calculate the propagate Cubature points:
$Y_{i,k+1\|k} = h(X_{i,k+1\|k}, u_{k+1}) \qquad i = 1, 2, ..., 2n_x$
Step 4: Estimate the predicted measurement:
$\hat{y}_{k+1\|k} = \frac{1}{2n_x} \sum_{i=1}^{2n_x} Y_{i,k+1\|k}$
Step 5: Calculate the innovation covariance matrix:
$\hat{P}_{yy,k+1} = \frac{1}{2n_x} \sum_{i=1}^{2n_x} Y_{i,k+1\|k} Y^T_{i,k+1\|k} - \hat{y}_{k+1\|k} \hat{y}^T_{k+1\|k} + R_{k+1}$
Step 6: Calculate the cross-covariance matrix:
$\hat{P}_{xy,k+1} = \frac{1}{2n_x} \sum_{i=1}^{2n_x} X_{i,k+1\|k} Y^T_{i,k+1\|k} - \hat{x}_{k+1\|k} \hat{y}^T_{k+1\|k}$
Step 7: Compute the filter gain:
$K_{k+1} = (1 + a_1(1 - \gamma_{k+1}))\lambda_{k+1} \hat{P}_{xy,k+1}$
$\times[(1 + a_1(1 - \gamma_{k+1}))\hat{P}^T_{xy,k+1} \hat{P}^{-1}_{k+1\|k} \hat{P}_{xy,k+1}$
$+(1 + a_2(1 - \gamma_{k+1}))R_{k+1} + (1 + a_1^{-1} + a_2^{-1})(1 - \gamma_{k+1})\delta I]^{-1}$
Step 8: Estimate the updated state:
$\hat{x}_{k+1} = \hat{x}_{k+1\|k} + K_{k+1}\lambda_{k+1}(\overline{y}_{k+1} - \hat{y}_{k+1\|k})$
Step 9: Compute the upper bound of state estimation error covariance:
$\overline{P}_{k+1} = (1 + a_1(1 - \gamma_{k+1}))(I - K_{k+1}\lambda_{k+1} P^T_{xy,k+1} P^{-1}_{k+1\|k})$
$\times \hat{P}_{k+1\|k}(I - K_{k+1}\lambda_{k+1} P^T_{xy,k+1} P^{-1}_{k+1\|k})^T +$
$(1 + a_2(1 - \gamma_{k+1}))\lambda_{k+1} K_{k+1} R_{k+1} K^T_{k+1} +$
$(1 - \gamma_{k+1})(1 + a_1^{-1} + a_2^{-1}) K_{k+1}\lambda_{k+1}\delta I K^T_{k+1}$

Theorem 4.2: *Assuming that the system* (4.1)-(4.2) *is uniformly observable and the inequalities* (4.18) *are satisfied, if the packet arrival probability has a lower bound*

$$\lambda > 1 - \frac{1}{\alpha_{\max}^2 f_{\max}^2 (1 + a_1(1-\gamma))}, \tag{4.22}$$

where $\gamma := \limsup_{N->\infty} \frac{1}{N+1} \sum_{k=0}^{N} E(\gamma_k)$ *is the average communication rate, then the error covariance matrix satisfies the following bound:*

$$E[\overline{P}_{k+1}] \leq E[\hat{P}_{k+1|k}] \leq \overline{p} I, \tag{4.23}$$

where $\overline{p} > 0$.

Proof. State estimation error and the error covariance matrix are updated with new/old data, so it is trivial that $E[\overline{P}_{k+1}] \leq E[\hat{P}_{k+1|k}]$. In addition, recalling from *Chapter 3* and according to (3.11) the prediction error covariance matrix is

$$E[\hat{P}_{k+1|k}] = E[A_k \hat{P}_k A_k^T + Q_k]. \tag{4.24}$$

Taking the upper bound of $\hat{P}_k$, (4.16), into account we have,

$$E[\hat{P}_{k+1|k}] \leq E[A_k \overline{P}_k A_k^T + Q_k]. \tag{4.25}$$

Substituting $\overline{P}_k$ and K_k in (4.25) we have,

$$\begin{aligned} E[\hat{P}_{k+1|k}] \leq E\Bigg[A_k \Bigg(& \hat{P}_{k|k-1} - \Big(1 + a_1(1-\gamma_k)\Big) \lambda_k \hat{P}_{k|k-1} B_k^T \Big[\Big(1 + a_1(1-\gamma_k)\Big) B_k \\ & \times \hat{P}_{k|k-1} B_k^T + \Big(1 + a_2(1-\gamma_k)\Big) R_k + (1 + a_1^{-1} + a_2^{-1})(1-\gamma_k)\delta I \Big]^{-1} \\ & \times B_k \hat{P}_{k|k-1} \Bigg) A_k^T + Q_k \Bigg]. \end{aligned} \tag{4.26}$$

Using the inequality $(A+B)^{-1} > A^{-1} - A^{-1}BA^{-1}$, and defining $A = \Big(1 + a_1(1-\gamma_k)\Big) B_k \hat{P}_{k|k-1} B_k^T$, and $B = (1 + a_2(1-\gamma_k))R_k + (1 + a_1^{-1} + a_2^{-1})(1-\gamma_k)\delta I$, according to the bounds of the matrices in (4.18), we obtain,

$$E[\hat{P}_{k+1|k}] < \alpha_{\max}^2 f_{\max}^2 \Big(1 + a_1(1-\gamma)\Big)(1-\lambda)\hat{P}_{k|k-1} + \Big(\frac{\lambda \alpha_{\max}^2 f_{\max}^2 r_{\max}}{\beta_{\min}^2 h_{\min}^2} + \hat{q}\Big) I_n, \tag{4.27}$$

where $r_{\max} = \max \parallel (1 + a_2(1-\gamma_k))R_k + (1 + a_1^{-1} + a_2^{-1})(1-\gamma_k)\delta I \parallel$. According to this, we have, $E[\hat{P}_{2|1}] < \alpha_{\max}^2 f_{\max}^2 (1 + a_1(1-\gamma))(1-\lambda)\overline{p} I_n + \overline{p} I_n$, where $\overline{p} = \max\{\parallel \hat{P}_{1|0} \parallel , \frac{\lambda \alpha_{\max}^2 f_{\max}^2 r_{\max}}{\beta_{\min}^2 h_{\min}^2} + \hat{q}\}$, and $E[\hat{P}_{1|0}] > 0$. Iterating and using an induction algorithm, we obtain,

$$E[\hat{P}_{k+1|k}] < \overline{p} \sum_{i=0}^{k} [\alpha_{\max}^2 f_{\max}^2 (1 + a_1(1-\gamma))(1-\lambda)]^i. \tag{4.28}$$

The proposed filter converges when $\lambda > 1 - \frac{1}{\alpha_{\max}^2 f_{\max}^2 (1+a_1(1-\gamma))}$. This completes the proof. ■

Remark 4.2: *The lower bound of the packet delivery rate is related to the average communication rate or the event-triggered threshold. Thus, by properly tuning the threshold we can guarantee the boundedness of the error covariance matrix and the estimation error.*

Note 4.2: Application of *L*emma 3.1 considerably simplifies computation of the error covariance matrix upper bound and/or filter gain, albeit introducing some conservatism in the filter design. If chosen appropriately, the parameters a_1 and a_2 can help reduce such conservatism. Note that the filter gain always minimizes $\overline{P}_{k+1}$ for any value of a_1 and a_2 and provides the optimal filter gain. The tradeoff in the selection of a_1 can be summarized as follows: According to *Theorem 4.2*, if the packet arrival probability λ has a lower bound $\lambda > 1 - \frac{1}{\alpha_{\max}^2 f_{\max}^2 (1+a_1(1-\gamma))}$, then the error covariance matrix satisfies the bound (4.23). Since λ is given, to satisfy this bound, a_1 should be chosen to minimize the right hand side of this inequality. If a_1 is chosen very large ($a_1 >> 1$), then the right hand side approaches 1, which means that the system cannot tolerate packet dropouts. On the other hand, very small values of a_1 result in large values of the error covariance matrix (4.16). Thus, a_1 should be chosen in the range $0 < a_1 < 1$. The larger a_1 within this range, the lower the tolerance to packet dropouts. A similar tradeoff exists for a_2.

Theorem 4.3: *Consider the nonlinear system* (4.1)-(4.2) *with event-triggered data transmission and the packet dropout and assume that inequalities* (4.18) *are satisfied. If*

$$0 < p_{\min} I \leq \overline{P}_{k+1|k+1} \leq \hat{P}_{k+1|k} \leq p_{\max} I, \tag{4.29}$$

and for some $\varepsilon > 0$, $E[\|\widetilde{x}_{1|0}\|^2] \leq \varepsilon$, *then the prediction error* $\widetilde{x}_{k+1|k}$ *is bounded in mean square sense.*

Proof. The proof of *Theorem 4.3* consists of showing that the conditions of *Lemma 4.1* are satisfied. Defining the Lyapunov function as follows,

$$V_{k+1}(\widetilde{x}_{k+1|k}) = \widetilde{x}_{k+1|k}^T \hat{P}_{k+1|k}^{-1} \widetilde{x}_{k+1|k}. \tag{4.30}$$

Theorem 2 in [4], shows that (4.29) holds. Assuming those bounds are $p_{\min}$ and $p_{\max}$ we have:

$$\upsilon_{\min} \|\widetilde{x}_{k+1|k}\|^2 \leq V_{k+1}(\widetilde{x}_{k+1|k}) \leq \upsilon_{\max} \|\widetilde{x}_{k+1|k}\|^2, \tag{4.31}$$

where $\upsilon_{\min} = \frac{1}{p_{\max}}$, and $\upsilon_{\max} = \frac{1}{p_{\min}}$. Consider now the second condition of *Lemma 4.1*. We need to find real numbers τ_k, and μ_k such that $0 < \tau_k < 1$ and $\mu_k > 0$, respectively.

Using (4.12), the predicted state error covariance is given by,

$$\hat{P}_{k+1|k} = E\{\widetilde{x}_{k+1|k}\tilde{x}^T_{k+1|k}\} = \hat{Q}_k + \Big[A_k(I - \lambda_k K_k B_k)\Big]\hat{P}_{k|k-1}\Big[A_k(I - \lambda_k K_k B_k)\Big]^T, \quad (4.32)$$

where,

$$\begin{aligned}\hat{Q}_k =& \Delta P_{k|k-1} + (A_k K_k)\lambda_k R_k (A_k K_k)^T + Q_k + (1-\gamma_k)E\{M_k e_k^T N_k^T + N_k e_k M_k^T \\ &+ N_k e_k e_k^T N^T\},\end{aligned} \quad (4.33)$$

$M = [A_k(I - K_k\lambda_k B_k)\widetilde{x}_{k|k-1} - A_k K_k \lambda_k \upsilon_k + \omega_k]$, $N = (A_k K_k \lambda_k)$, and $\Delta P_{k|k-1}$ shows the difference between step 5 of time update part of Table 4.1 , and (4.32). (4.32) can be rewritten as follows,

$$\begin{aligned}\hat{P}_{k+1|k} =& [A_k(I - K_k\lambda_k B_k)]\Big\{[A_k(I - K_k\lambda_k B_k)]^{-1}\hat{Q}_k[A_k(I - K_k\lambda_k B_k)]^{-T} \\ &+ \hat{P}_{k|k-1}\Big\}[A_k(I - K_k\lambda_k B_k)]^T.\end{aligned} \quad (4.34)$$

Setting $\Upsilon_k = [A_k(I - K_k\lambda_k B_k)]^T \hat{Q}_k^{-1}[A_k(I - K_k\lambda_k B_k)]$ and considering the characteristics of the matrix norm and the assumptions in (4.18), we have,

$$\Upsilon_k \leq \frac{[(\alpha_{\max} f_{\max})(1 + \lambda_k \beta_{\max} h_{\max}\hat{K})]^2}{\hat{q}_{\min}},$$

where the upper bound of $\hat{K}$ is,

$$\|K_k\| \leq [p_{\max}\beta_{\max}h_{\max}][(\beta_{\min}h_{\min})^2 p_{\min} + r_{\min}]^{-1}.$$

Using properties of matrix inverse and taking the inverse of Υ_k and substituting in (4.34), we obtain the following inequality [24],

$$[A_k(I - \lambda K_k B_k)]^T \hat{P}^{-1}_{k+1|k}[A_k(I - \lambda K_k B_k)] \leq (1 - \tau_k)\hat{P}^{-1}_{k|k-1}, \quad (4.35)$$

where,

$$(1 - \tau_k) = \Big[1 + \frac{\hat{q}_{\min}}{[(\alpha_{\max} f_{\max})(1 + \beta_{\max} h_{\max}\hat{K})]^2 p_{\max}}\Big]^{-1} > 0. \quad (4.36)$$

It is easy to observe that $0 < \tau_k < 1$. Substituting (4.12) into $V_{k+1}(\widetilde{x}_{k+1|k})$, the conditional expectation is as follows:

$$\begin{aligned}E\{V_{k+1}(\widetilde{x}_{k+1|k})|\widetilde{x}_{k+1|k}\} =& \mu_k + \widetilde{x}^T_{k|k-1}[A_k(I - \lambda_k K_k B_k)]^T \hat{P}^{-1}_{k+1|k} \\ &\times [A_k(I - \lambda_k K_k B_k)]\widetilde{x}_{k|k-1},\end{aligned} \quad (4.37)$$

where,

$$\begin{aligned}\mu_k =& E\Big\{\upsilon_k^T[A_k\lambda_k K_k]^T\hat{P}_{k+1|k}^{-1}A_k\lambda_k K_k\upsilon_k+\omega_k^T\hat{P}_{k+1|k}^{-1}\omega_k|\widetilde{x}_{k+1|k}\Big\}+(1-\gamma_k)\\ &\times\Bigg(E\Big\{(A_k\lambda_k K_k e_k)^T\hat{P}_{k+1|k}^{-1}A_k\lambda_k K_k e_k+\omega_k^T\hat{P}_{k+1|k}^{-1}A_k\lambda_k K_k e_k\\ &+(A_k\lambda_k K_k e_k)^T\hat{P}_{k+1|k}^{-1}\omega_k+e_k^T\lambda_k^T K_k^T A_k^T\hat{P}_{k+1|k}^{-1}A_{_k}\lambda_k K_k\upsilon_k+e_k^T\lambda_k^T K_k^T A_k^T\hat{P}_{k+1|k}^{-1}\\ &\times[A_k(I-\lambda_k K_k B_k)]\widetilde{x}_{k|k-1}+\widetilde{x}_{k|k-1}^T[A_k(I-\lambda_k K_k B_k)]^T\hat{P}_{k+1|k}^{-1}A_k\lambda_k K_k e_k\\ &-\upsilon_k^T[A_k\lambda_k K_k]^T\hat{P}_{k+1|k}^{-1}A_k\lambda_k K_k e|\widetilde{x}_{k+1|k}\}\Bigg)\end{aligned} \tag{4.38}$$

Both sides of μ_k are scalars. Using *Lemma 3.1* and computing the trace of μ_k we have,

$$\begin{aligned}\mu_k \le tr\Bigg\{&([A_k\lambda_k K_k]^T\hat{P}_{k+1|k}^{-1}A_k\lambda_k K_k R_k)+(\hat{P}_{k+1|k}^{-1}Q_k)+(1-\gamma_k)\\ &\times\Big\{(\lambda_k^T K_k^T A_k^T\hat{P}_{k+1|k}^{-1}A_k\lambda_k K_k\delta I)+a_3\Big([\hat{P}_{k+1|k}^{-1}A_{_k}(I-\lambda_k K_k B_k)]\hat{P}_{k|k-1}\\ &\times[\hat{P}_{k+1|k}^{-1}A_k(I-\lambda_k K_k B_k)]^T\Big)+a_4(\hat{P}_{k+1|k}^{-1}Q_k[\hat{P}_{k+1|k}^{-1}]^T)\\ &+a_5(\hat{P}_{k+1|k}^{-1}A_k\lambda_k K_k R_k[\hat{P}_{k+1|k}^{-1}A_{_k}\lambda_k K_k]^T)\\ &+(a_3^{-1}+a_4^{-1}+a_5^{-1})(A_k\lambda_k K_k\delta I[A_k\lambda_k K_k]^T)\Bigg\}.\end{aligned} \tag{4.39}$$

a_3, a_4, and a_5 are positive scalars. It is immediate that μ_k is positive and it has an upper bound $\mu_{\max}$. Substituting (4.35) in (4.37), and taking account of $V_{k+1}(\widetilde{x}_{k+1|k})$ and (4.39) we have,

$$E[V_{k+1}(\widetilde{x}_{k+1|k})|\widetilde{x}_{k+1|k}]-V_k(\widetilde{x}_{k|k-1})\le\mu_{\max}-\tau V_k(\widetilde{x}_{k|k-1}).$$

Thus, according to *Lemma 4.1*, $\widetilde{x}_{k+1|k}$, is bounded in mean square sense. ■

Note 4.3: *Inequalities* (4.31), (4.36) *and* (4.39) *are satisfied for any value of the parameters α_k and β_k, while the value of the upper and lower bound of the inequalities may change. Thus, we conclude that the stability of the filter does not depend on the values α_k and β_k.*

From (3.11), and the assumptions in (4.18), we conclude that the mean squared error of the estimation is as follows,

$$E\{\|\widetilde{x}_k\|^2\}\le(f_{\min}\alpha_{\min})^{-2}E\{\left\|\widetilde{x}_{k+1|k}\right\|^2+\|\omega_k\|^2\} \tag{4.40}$$

Note that, according to *Theorem 4.3*, the upper bound of μ_k in (4.39) depends on the event-triggered threshold, which affects on the upper bound of $E[\left\|\widetilde{x}_{k+1|k}\right\|^2]$ (*Lemma 4.1*). Thus, by choosing a proper event-triggered mechanism, one can limit the upper bound of the estimation error (4.40).

4.4 Simulation Results

In this section, we consider an application of the CKF to the air traffic control problem given in [8]. The state of the aircraft at time k is $x_k = [\eta_k, \dot{\eta_k}, y_k, \dot{y_k}, \Psi]^T$, where Ψ is the turn rate, η and y, represent position, and $\dot{\eta}$ and $\dot{y}$ represent the velocities along the x-axis and y-axis, respectively. The kinematics of the turning motion is modelled by the following nonlinear process and measurement equations,

$$x_{k+1} = \begin{pmatrix} 1 & \frac{\sin(\Psi T)}{\Psi} & 0 & \frac{-(1-\cos(\Psi T))}{\Psi} & 0 \\ 0 & \cos(\Psi T) & 0 & -\sin(\Psi T) & 0 \\ 0 & \frac{(1-\cos(\Psi T))}{\Psi} & 1 & \frac{\sin(\Psi T)}{\Psi} & 0 \\ 0 & \sin(\Psi T) & 0 & \cos(\Psi T) & 0 \\ 0 & 0 & 0 & 0 & 1 \end{pmatrix} x_k + \omega_k. \tag{4.41}$$

The radar, stationed at [20000, 20000] metres measures the range (position) r, and the bearing θ.

$$z_{k+1} = \begin{pmatrix} r_k \\ \theta_k \end{pmatrix} = \begin{pmatrix} \sqrt{x^2_{1_{k+1}} + x^2_{3_{k+1}}} \\ tan^{-1} \frac{x_{3_{k+1}}}{x_{1_{k+1}}} \end{pmatrix} + \nu_k. \tag{4.42}$$

T is the time-interval which is assumed to be 1 sec in our simulations. The process noise $w_k \sim N(0, Q)$ is white noise with zero mean and covariance $Q = \text{diag}[q_1 M \quad q_1 M \quad q_2 T]$, where $M = [\frac{T^3}{3} \quad \frac{T^2}{2}; \frac{T^2}{2} \quad T]$, $q_1 = 0.1 m^2 s^{-3}$ and $q_2 = 1.75 * 10^{-4} s^{-3}$, respectively. The measurement noise, $v_k \sim N(0, R)$, is white noise with zero mean and covariance $R = \text{diag}[100 \quad 10]$. a_1 and a_2 are considered 0.02.

Scenario A: In this scenario, we consider the event-triggered CKF without packet dropout using different threshold values. The initial state value is as follows,

$x_0 = \text{diag}[10^4 m \ 150 m s^{-1} \ 3.5 * 10^4 m \ 0 m s^{-1} \ -3^o s^{-1}]^T$. The initial error covariance is as follows, $\hat{P}_0 = \text{diag}[100 m^2 \ 10 m^2 s^{-2} \ 100 m^2 \ 10 m^2 s^{-2} \ 0.1 \text{rad}^{\ 2} s^{-2}]$.

The initial state estimate $\hat{x}_0$ is chosen randomly from $N(x_0, \hat{P}_0)$ in each run. We set $\lambda = 1$ in step 7, 8, and 9 of Table 4.1, to represent the absence of packet dropouts. Figure 4.1.(a) shows the results of the target tracking with the event-triggered threshold of 100, 500, 1000. The resulting number of data transmission events are 180, 142, and 70, respectively.

Comparison between tracking results shows that by properly tuning the event-triggered mechanism threshold, a desired estimation quality can be achieved while communication rate is reduced dramatically.

The simulation results in Figure 4.3(a) with different initial values, $x_0 = diag[10^3 m \ 300 m s^{-1} \ 10^3 m \ 0 m s^{-1} \ -2^o s^{-1}]^T$ and $P_{0|0} = diag[100 m^4 \ 10 m^4 s^{-2} \ 100 m^4 \ 10 m^4 s^{-2} \ 0.1 rad^2 s^{-2}]$ show that, as expected, a smaller event-triggered threshold results in better estimations.

Scenario B: We repeat scenario A but we include the packet dropouts assuming rates of 0.2, Figure 4.1(b) and 0.5, Figure 4.1(c). When the packet dropout occurs we have $\lambda_k = 0$, resulting in a filter gain $K_k = 0$, and consequently no update in the estimate of the state, in step 8 of Table 4.1.

The results show that, as expected, when the packet dropout rate increases for the same event-triggered mechanism threshold, the quality of the tracking deteriorates. Figure 4.3.(b) shows the tracking result with and without packet dropout assuming a fixed event-triggered threshold of 500, with different initial values.

Once again, we see that as the packet dropout rate increases, the quality of the estimate deteriorates, however the tracking error remains bounded.

To compare the filter performance under different conditions, we use the root-mean square error (RMSE) of the states. As an example, for the position, we define the RMSE in position at time k , as

$$RMSE_{position}(k) = \sqrt{\frac{1}{N}\sum_{n=1}^{N}(\eta_k^n - \hat{\eta}_k^n)^2 + (y_k^n - \hat{y}_k^n)^2}.$$

(η_k^n, y_k^n) and $(\hat{\eta}_k^n, \hat{y}_k^n)$ are the true and estimated states at the n-th Monte Carlo run, respectively. We make 20 independent Monte Carlo runs. Figure 4.2 shows the performance comparison without packet dropout and with packet dropout rates of 0.2 and 0.5 for the fixed event-triggered threshold of 500, based on 20 Monte Carlo runs.

As expected, performance degrades as the packet dropout rate increases. However, the figure also shows that by properly tuning the event-triggered threshold for the given packet dropout rate, one can achieve acceptable state estimation results.

Figure 4.4 compares the estimation error of the DECKF and DEUKF. We do not present the tracking results of the EKF because of the limitations mentioned in *Chapter 3* and the *Appendix*. Note that, the dimension of the states used here is higher than three, and the scaling factor of UKF is $k = -2$ which results in non-positive covariance which halts the operation, so we assume that $k = 1$. The figure shows significantly better results for the DECKF compared to EUKF.

4.5 Summary

In this chapter, we developed a new discrete-time event-triggered Cubature Kalman Filter (CKF) for the nonlinear dynamic systems over a wireless network with the packet dropout in the transmission lines. We developed a complete theory to derive the lower bound of the packet delivery rate, so the proposed filter could ensure that the prediction error covariance

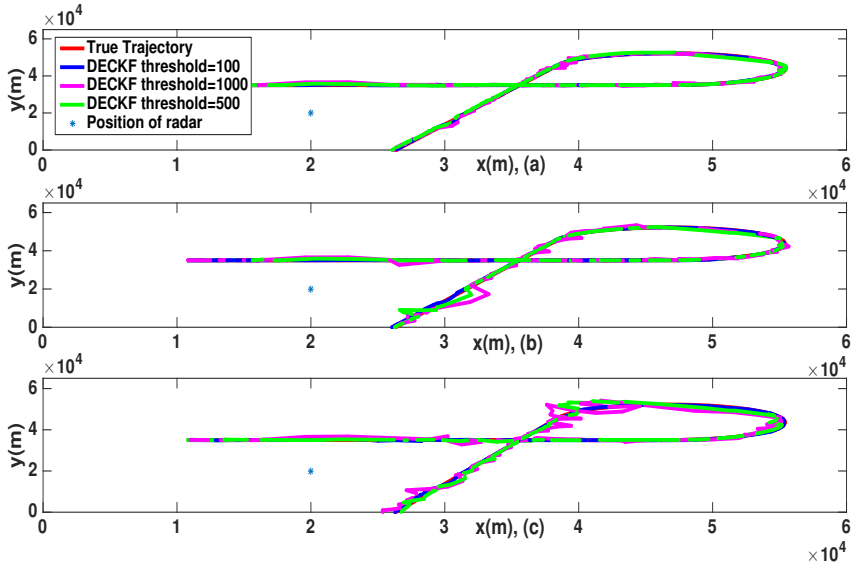

Figure 4.1: Tracking results of DECKF (a) without packet dropout. (b) packet dropout rate: 0.2. (c) packet dropout rate: 0.5.

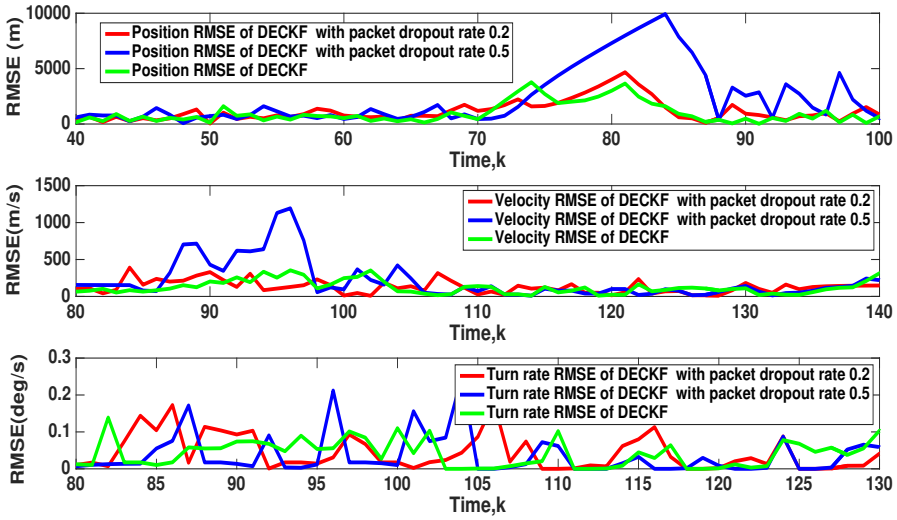

Figure 4.2: Position,Velocity and Turn rate RMSE of DECKF with and without packet dropout

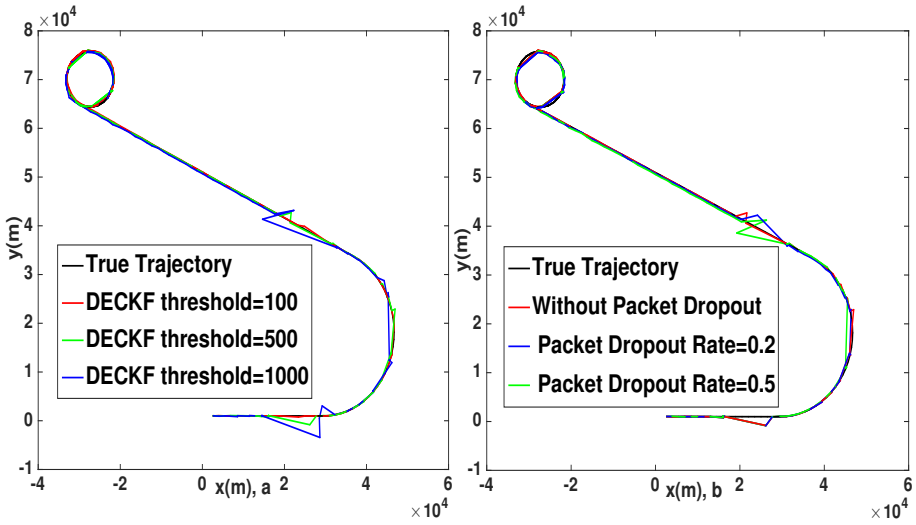

Figure 4.3: Tracking results of DECKF (a) without packet dropout. (b) event-triggered threshold 500 with packet dropout

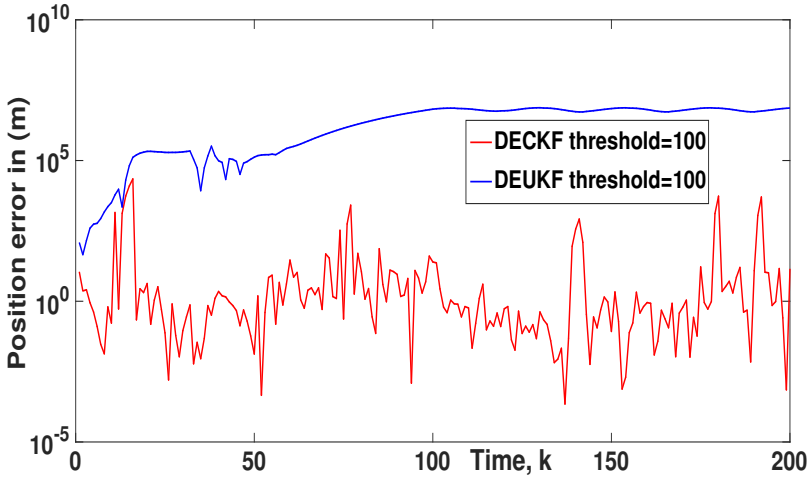

Figure 4.4: Position MSE of DECKF and DEUKF

is bounded when the packet delivery rate has a lower bound. We then showed that the estimation error can be guaranteed to be bounded by properly tuning the threshold of the event-triggered mechanism. An example is given to illustrate the filter's performance.

Chapter 5

Event-Triggered Cubature Kalman Filter for One Step Randomly Delayed Measurements

In this chapter we develop a new event-triggered cubature Kalman filter for discrete-time high dimensional nonlinear systems with strong nonlinearities under the assumption that the sensors exchange data via imperfect communication channels and the measurements are randomly delayed by one sampling time.

We first discuss the difficulties involved in dealing with time-delays in the context of state estimation and formulate the need for a new algorithm. Then we show that using the proposed event-triggered cubature Kalman filter and properly tuning the event-triggered threshold, can lead to accurate estimates of the state despite time delays, while reducing transmission of information between system and filter. An example shows the effectiveness of the proposed algorithm.

5.1 Problem formulation

The nonlinear discrete-time system model and the nonlinear measurement model are described as follows,

$$x_{k+1} = f(x_k, u_k) + \omega_k, \tag{5.1}$$

$$z_{k+1} = h(x_{k+1}) + \nu_{k+1}, \tag{5.2}$$

where $x_k \in \mathbb{R}^{n_x}$ is the state vector, and $z_k \in \mathbb{R}^{n_z}$ is the measurement vector. Other parameters are defined in *Chapter 2*. Recalling from *Chapter 3*, we consider that our system works under even-triggered mechanism. So, the current transmitted measurement

(5.3) is as follows,

$$\bar{z}_k = z_k + (1 - \gamma_k)(\overline{z} - z_k) \tag{5.3}$$

where z_k is the current measurement and $\overline{z}$ is the last sent measurement. $\bar{z}_k$ is the current transmitted measurement after the triggering condition is satisfied.

5.1.1 Delay

In this subsection, we summarize the derivation of the Gaussian filter for the system with one randomly delay measurement described in (5.1)-(5.2). Note that the one-step randomly delayed measurement model is as follows,

$$y_{k+1} = (1 - \sigma_{k+1})z_{k+1} + \sigma_{k+1}z_k, \tag{5.4}$$

where, $\{\sigma_k; k > 1\}$ is a sequence of uncorrelated Bernoulli random variables which can be 0 or 1 with,

$$\begin{aligned} &p(\sigma_k = 1) = E[\sigma_k] = p_k, \\ &p(\sigma_k = 0) = 1 - E[\sigma_k] = 1 - p_k, \\ &E[(\sigma_k - p_k)^2] = (1 - p_k)p_k. \end{aligned} \tag{5.5}$$

It is worth mentioning that the one-step posterior predictive PDF of the state, $p(x_{k+1}|Y_k)$, and the one-step posterior predictive PDF of the delayed measurement, $p(y_{k+1}|Y_k)$, are assumed to be Gaussian, where $Y_{k+1} = \{y_i\}_{i=1}^{k+1}$, shows the set of the available measurements. The statistics of the observation at time k depends on both statistics of x_{k-1} and ν_{k-1}.

To derive the filter with measurement delays, we should consider jointly the state and noise vectors. Thus, we define the following augmented vector as $x^a_{k+1} = \begin{pmatrix} x_{k+1} \\ \nu_{k+1} \end{pmatrix}$. The conditional mean and the covariance are as follows,

$$\hat{x}^a_{k+1} = \begin{pmatrix} \hat{x}_{k+1} \\ \hat{\nu}_{k+1} \end{pmatrix} \quad ; \quad \hat{P}^a_{k+1} = \begin{pmatrix} \hat{P}_{k+1} & \hat{P}^{x\nu}_{k+1} \\ (\hat{P}^{x\nu}_{k+1})^T & \hat{P}^{\nu\nu}_{k+1} \end{pmatrix} \tag{5.6}$$

where, $\hat{P}^{\nu\nu}_{k+1} = E[\tilde{\nu}_{k+1}\tilde{\nu}^T{}_{k+1}|Y_{k+1}]$, $\hat{P}^{x\nu}_{k+1} = E[\tilde{x}_{k+1}\tilde{\nu}^T{}_{k+1}|Y_{k+1}]$. In addition, ν_{k+1} is uncorrelated to Y_k, so the prediction state $\hat{x}^a_{k+1|k}$ and the prediction covariance $\hat{P}^a_{k+1|k}$ are as follows,

$$\hat{x}^a_{k+1|k} = \begin{pmatrix} \hat{x}_{k+1|k} \\ 0_{m\times 1} \end{pmatrix} \quad ; \quad \hat{P}^a_{k+1|k} = \begin{pmatrix} \hat{P}_{k+1|k} & 0_{n\times m} \\ 0_{m\times n} & R_{k+1} \end{pmatrix} \tag{5.7}$$

where m is the dimensionality of the measurement noise. So we need to derive $\hat{P}^{x\nu}_{k+1}$, $\hat{P}_{k+1}$, and $\hat{P}^{\nu\nu}_{k+1}$ to find the augmented covariance. First we use linearization to facilitate the filter

derivation. Linearization of $f(x_k)$ and $h(x_k)$ around $x_k = \hat{x}_k$ yields to the following,

$$x_{k+1} \approx f_k(\hat{x}_k) + A_k(x_k - \hat{x}_k) + \omega_k \tag{5.8}$$

$$z_k \approx h_k(\hat{x}_k) + B_k(x_k - \hat{x}_k) + \nu_k \tag{5.9}$$

where, $A_k = \alpha_k F_k$, and $B_k = \beta_k H_k$. $F_k = \frac{\partial f(x)}{\partial x}|_{x=\hat{x}_k}$ and $H_k = \frac{\partial h(x)}{\partial x}|_{x=\hat{x}_k}$ are the Jacobian matrix, $\alpha_k = \text{diag}(\alpha_{1,k}, \alpha_{2,k}, ..., \alpha_{n_x k})$, and $\beta_{k+1} = \text{diag}(\beta_{1,k}, \beta_{2,k}, ..., \beta_{n_y k})$ are unknown diagonal matrix representing the error incurred in neglecting the higher order terms of the Taylor series. Moreover the predicted state and covariance are as follows,

$$\hat{x}_{k+1|k} = f_k(\hat{x}_k) \tag{5.10}$$

$$\hat{P}_{k+1|k} = A_k \hat{P}_k A_k^T + Q_k. \tag{5.11}$$

Next, linearizing $h_{k+1}(x_{k+1})$ around $x_{k+1} = \hat{x}_{k+1|k}$ we have,

$$z_{k+1} \approx h_{k+1}(\hat{x}_{k+1|k}) + B_{k+1}(x_{k+1} - \hat{x}_{k+1|k}) + \nu_{k+1}. \tag{5.12}$$

where $B_{k+1} = \beta_k H_{k+1}$, and $H_{k+1} = \frac{\partial h(x)}{\partial x}|_{x=\hat{x}_{k+1|k}}$.

Now we summarize the equations which are used in the developing of the Gaussian filter for the system described by (5.1) and (5.2) with randomly delayed measurements as follows [41],

$$\hat{x}_{k+1} = \hat{x}_{k+1|k} + K_{k+1}^x \tilde{y}_{k+1|k}, \tag{5.13}$$

$$\hat{y}_{k+1|k} = (1 - p_{k+1})\hat{z}_{k+1|k} + p_{k+1}\hat{z}_k \tag{5.14}$$

$$\tilde{y}_{k+1|k} = (1 - \sigma_{k+1})(z_{k+1} - \hat{z}_{k+1|k}) + \sigma_{k+1}(z_k - \hat{z}_k) + (\sigma_{k+1} - p_{k+1})(\hat{z}_k - \hat{z}_{k+1|k}), \tag{5.15}$$

$$\hat{P}_{k+1} = \hat{P}_{k+1|k} - K_{k+1}^x \hat{P}_{k+1|k}^{yy} (K_{k+1}^x)^T, \tag{5.16}$$

$$K_{k+1}^x = \hat{P}_{k+1|k}^{xy} (\hat{P}_{k+1|k}^{yy})^{-1}, \tag{5.17}$$

$$\hat{P}_{k+1|k}^{xy} = E[\tilde{x}_{k+1} \tilde{y}_{k+1|k}^T | Y_k] = (1 - p_{k+1})\hat{P}_{k+1|k}^{xz} + p_{k+1}\hat{P}_{k+1,k}^{xz}, \tag{5.18}$$

$$\hat{P}_{k+1|k}^{xz} = E[\tilde{x}_{k+1|k} \tilde{z}_{k+1|k}^T | Y_k] = \hat{P}_{k+1|k} B_{k+1}^T, \tag{5.19}$$

$$\hat{P}^{xz}_{k+1,k} = E[\tilde{x}_{k+1|k}\tilde{z}^T_k|Y_k] = A_k\hat{P}_k B^T_k + A_k\hat{P}^{x\nu}_k, \tag{5.20}$$

$$\hat{\nu}_{k+1} = K^{\nu}_{k+1}\tilde{y}_{k+1|k}, \tag{5.21}$$

$$\hat{P}^{\nu\nu}_{k+1} = R_{k+1} - K^{\nu}_{k+1}\hat{P}^{yy}_{k+1|k}(K^{\nu}_{k+1})^T, \tag{5.22}$$

$$K^{\nu}_{k+1} = \hat{P}^{\nu y}_{k+1|k}(\hat{P}^{yy}_{k+1|k})^{-1}, \tag{5.23}$$

$$\hat{P}^{\nu y}_{k+1|k} = E[\nu_{k+1}\tilde{y}^T_{k+1|k}|Y_k] = (1-p_{k+1})R_{k+1}, \tag{5.24}$$

$$\hat{P}^{x\nu}_{k+1} = E[\tilde{x}_{k+1}\tilde{\nu}^T_{k+1}|Y_k] = -K^x_{k+1}\hat{P}^{yy}_{k+1|k}(K^{\nu}_{k+1})^T, \tag{5.25}$$

$$\hat{P}^{yy}_{k+1|k} = (1-p_{k+1})\hat{P}^{zz}_{k+1|k} + p_{k+1}\hat{P}^{zz}_{k+1|k} + (1-p_{k+1})p_{k+1}(\hat{z}_{k+1|k} - \hat{z}_k)(\hat{z}_{k+1|k} - \hat{z}_k)^T, \tag{5.26}$$

$$\hat{P}^{zz}_{k+1|k} = E[\tilde{z}_{k+1|k}\tilde{z}^T_{k+1|k}|Y_k] = B_{k+1}\hat{P}_{k+1|k}B^T_{k+1} + R_{k+1}, \tag{5.27}$$

$$\hat{P}^{zz}_k = E[\tilde{z}_k\tilde{z}^T_k|Y_k] = B_k\hat{P}_k B^T_k + B_k\hat{P}^{x\nu}_k + (B_k\hat{P}^{x\nu}_k)^T + \hat{P}^{\nu\nu}_k, \tag{5.28}$$

$$\hat{z}_{k+1|k} = E[z_{k+1}|Y_k] = h_{k+1}(\hat{x}_{k+1|k}), \tag{5.29}$$

$$\hat{z}_k = E[z_k|Y_k] = h_{k+1}(\hat{x}_k) + \hat{\nu}_k, \tag{5.30}$$

where K^x_{k+1} and K^{ν}_{k+1} express the gain matrices of the filtering estimated state and measurement noise, respectively.

5.2 The DECKF with One-Step Randomly Delayed Measurements

In this section, we develop the discrete-time event-triggered cubature Kalman filter in the presence of delay in the communication channels. Note that we should derive the Kalman gain to reduce the estimation error and the error covariance matrix considering one step randomly delayed measurements.

Theorem 5.1: *Consider the system* (5.1) *and* (5.2) *with the defined current transmitted measurement* (5.3)*. Assume that the measurement are transmitted with one step randomly*

delay through the communication channels.The state estimator gain can be obtained as follows,

$$K_{k+1} = O(T)^{-1} \tag{5.31}$$

where, O and T are equal to the following,

$$O = m_1(1-p_{k+1})B_{k+1}\hat{P}_{k+1|k} + p_{k+1}A_k\hat{P}_kB_{k+1}^T + p_{k+1}A_k\hat{P}^{x\nu}{}_k \tag{5.32}$$

$$\begin{aligned} T = {} & p_{k+1}B_k\hat{P}^{x\nu}{}_k + p_{k+1}(B_k\hat{P}^{x\nu}{}_k)^T + m_1(1-p_{k+1})B_{k+1}\hat{P}_{k+1|k}B_{k+1}^T + m_2(1-p_{k+1})R_{k+1} \\ & + m_3p_{k+1}B_k\hat{P}_kB_k^T + m_4p_{k+1}\hat{P}^{\nu\nu}{}_k + m_5(1-p_{k+1})(1-\gamma_{k+1})\delta + m_6p_{k+1}(1-\gamma_k)\delta \\ & + p_{k+1}(1-p_{k+1})(\hat{z}_k - \hat{z}_{k+1|k})(\hat{z}_k - \hat{z}_{k+1|k})^T \end{aligned} \tag{5.33}$$

where, $m_1 = (1 + a_1(1-\gamma_{k+1}) + a_5(1-\gamma_k))$, $m_2 = (1 + a_2(1-\gamma_{k+1}) + a_6(1-\gamma_k))$, $m_3 = (1 + a_3(1-\gamma_{k+1}) + a_7(1-\gamma_k))$, $m_4 = (1 + a_4(1-\gamma_{k+1}) + a_8(1-\gamma_{k+1}))$, $m_5 = (1+a_1^{-1}+a_2^{-1}+a_3^{-1}+a_4^{-1})$, $m_6 = (1+a_5^{-1}+a_6^{-1}+a_7^{-1}+a_8^{-1})$. $a_1 - a_8$ are arbitrary positive parameters.

Proof. Substituting (5.3) in (5.4), the current transmitted measurement is as follows,

$$\bar{y}_{k+1} = (1-\sigma_{k+1})\Big[z_{k+1} + (1-\gamma_{k+1})(\overline{z} - z_{k+1})\Big] + \sigma_{k+1}\Big[z_k + (1-\gamma_k)(\overline{z} - z_k)\Big] \tag{5.34}$$

Substituting (5.9), (5.12) and (5.14) in (5.34), the measurement prediction error can be written as follows,

$$\begin{aligned} \bar{y}_{k+1} - \hat{y}_{k+1|k} = \widetilde{y}_{k+1|k} = {} & (1-\sigma_{k+1})\Big[B_{k+1}(x_{k+1} - \hat{x}_{k+1|k}) + \nu_{k+1}\Big] + \sigma_{k+1}\Big[B_k(x_k - \hat{x}_k) + \nu_k \\ & - \hat{\nu}_k\Big] + (\sigma_{k+1} - p_{k+1})\Big[h_k(\hat{x}_k) - h_{k+1}(\hat{x}_{k+1|k}) + \hat{\nu}_k\Big] + (1-\sigma_{k+1})(1-\gamma_{k+1})e_{k+1} \\ & + \sigma_{k+1}(1-\gamma_k)e_k \end{aligned} \tag{5.35}$$

Using $\widetilde{x}_{k+1}$ from (2.25), and considering (5.35), the estimation error can be written as follows,

$$\begin{aligned} \widetilde{x}_{k+1} = {} & \Big(I - K_{k+1}(1-\sigma_{k+1})B_{k+1}\Big)\widetilde{x}_{k+1|k} - K_{k+1}\Big((1-\sigma_{k+1})\nu_{k+1} + \sigma_{k+1}[B_k(\widetilde{x}_k) + \widetilde{\nu}_k] \\ & + (\sigma_{k+1} - p_{k+1})[h_k(\hat{x}_k) - h_{k+1}(\hat{x}_{k+1|k}) + \hat{\nu}_k] + (1-\sigma_{k+1})(1-\gamma_{k+1})e_{k+1} \\ & + \sigma_{k+1}(1-\gamma_k)e_k\Big) \end{aligned} \tag{5.36}$$

so the estimation error covariance matrix can be written as follows,

$$\begin{aligned}
\hat{P}_{k+1} = E\{\widetilde{x}_{k+1}\widetilde{x}_{k+1}^T\} &= \Big(I - K_{k+1}(1-p_{k+1})B_{k+1}\Big)\hat{P}_{k+1|k}\Big(I - K_{k+1}(1-p_{k+1})B_{k+1}\Big)^T \\
&+ (1-p_{k+1})K_{k+1}R_{k+1}K_{k+1}^T + p_{k+1}K_{k+1}B_k\hat{P}_k(K_{k+1}B_k)^T + p_{k+1}K_{k+1}\hat{P}^{\nu\nu}{}_kK_{k+1}^T \\
&+ p_{k+1}(1-p_{k+1})K_{k+1}(\hat{z}_k - \hat{z}_{k+1|k})(\hat{z}_k - \hat{z}_{k+1|k})^TK_{k+1}^T + (1-p_{k+1})K_{k+1}(1-\gamma_{k+1}) \\
&\times \delta K_{k+1}^T + p_{k+1}\Big((1-\gamma_k)K_{k+1}\delta K_{k+1}^T + K_{k+1}B_k\hat{P}^{x\nu}{}_kK_{k+1}^T + K_{k+1}(K_{k+1}B_k\hat{P}^{x\nu}{}_k)^T \\
&- A_k\hat{P}_kB_{k+1}^TK_k^T - B_{k+1}K_{k+1}\hat{P}_k^TA_k^T - A_k\hat{P}^{x\nu}{}_kK_{k+1}^T - K_{k+1}\hat{P}^{x\nu}{}_kA_k^T\Big) + (1-\gamma_{k+1}) \\
&\times E\Bigg\{ - \Big(I - K_{k+1}(1-\sigma_{k+1})B_{k+1}\Big)\widetilde{x}_{k+1|k}e_{k+1}^T(1-\sigma_{k+1})^TK_{k+1}^T + (1-\sigma_{k+1})K_{k+1}\nu_{k+1} \\
&\times e_{k+1}^T(1-\sigma_{k+1})^TK_{k+1}^T + \sigma_{k+1}K_{k+1}B_k(\widetilde{x}_k)e_{k+1}^T(1-\sigma_{k+1})^TK_{k+1}^T + \sigma_{k+1}K_{k+1}\widetilde{\nu}_ke_{k+1}^T \\
&\times (1-\sigma_{k+1})^TK_{k+1}^T - (1-\sigma_{k+1})K_{k+1}e_{k+1}\widetilde{x}_{k+1|k}^T\Big(I - K_{k+1}(1-\sigma_{k+1})B_{k+1}\Big)^T \\
&+ (1-\sigma_{k+1})K_{k+1}e_{k+1}((1-\sigma_{k+1})\nu_{k+1})^TK_{k+1}^T + (1-\sigma_{k+1})K_{k+1}e_{k+1}(\sigma_{k+1}B_k(\widetilde{x}_k))^TK_{k+1}^T \\
&+ (1-\sigma_{k+1})K_{k+1}e_{k+1}(\sigma_{k+1}\widetilde{\nu}_k)^TK_{k+1}^T\Bigg\} + (1-\gamma_k)E\Bigg\{\Big(I - K_{k+1}(1-\sigma_{k+1})B_{k+1}\Big)\widetilde{x}_{k+1|k} \\
&\times e_k^T(\sigma_{k+1})^TK_{k+1}^T + (1-\sigma_{k+1})K_{k+1}\nu_{k+1}e_k^T(\sigma_{k+1})^TK_{k+1}^T + \sigma_{k+1}K_{k+1}B_k(\widetilde{x}_k)e_k^T(\sigma_k)^TK_{k+1}^T \\
&+ \sigma_{k+1}K_{k+1}\widetilde{\nu}_ke_k^T(\sigma_{k+1})^TK_{k+1}^T + \sigma_{k+1}K_{k+1}e_k\Big(I - K_{k+1}(1-\sigma_{k+1})B_{k+1})\widetilde{x}_{k+1|k}\Big)^T \\
&+ \sigma_{k+1}K_{k+1}e_k((1-\sigma_{k+1})\nu_{k+1})^TK_{k+1}^T + \sigma_{k+1}K_{k+1}e_k(\sigma_{k+1}B_k(\widetilde{x}_k))^TK_{k+1}^T \\
&+ \sigma_{k+1}K_{k+1}e_k(\sigma_{k+1}\widetilde{\nu}_k)^TK_{k+1}^T\Bigg\}
\end{aligned} \tag{5.37}$$

using *Lemma 3.1* of *Chapter 3* we have the following equations,

$$\begin{aligned}
&E\Bigg\{ - \Big(I - K_{k+1}(1-\sigma_{k+1})B_{k+1}\Big)\widetilde{x}_{k+1|k}e_{k+1}^T(1-\sigma_{k+1})^TK_{k+1}^T \\
&- (1-\sigma_{k+1})K_{k+1}e_{k+1}\Big((I - K_{k+1}(1-\delta_{k+1})B_{k+1})\widetilde{x}_{k+1|k}\Big)^T\Bigg\} \leq \\
&E\Bigg\{a_1(I - K_{k+1}(1-p_{k+1})B_{k+1})\hat{P}_{k+1|k}(I - K_{k+1}(1-p_{k+1})B_{k+1})^T \\
&+ a_1^{-1}(1-p_{k+1})K_{k+1}\delta K_{k+1}^T\Bigg\},
\end{aligned} \tag{5.38}$$

$$\begin{aligned}
&E\Bigg\{(1-\sigma_{k+1})K_{k+1}\nu_{k+1}e_{k+1}^T(1-\sigma_{k+1})^TK_{k+1}^T + (1-\sigma_{k+1})K_{k+1}e_{k+1}((1-\sigma_{k+1})\nu_{k+1})^TK_{k+1}^T\Bigg\} \\
&\leq E\Bigg\{a_2(1-p_{k+1})K_{k+1}R_{k+1}(K_{k+1})^T + a_2^{-1}(1-p_{k+1})K_{k+1}\delta K_{k+1}^T\Bigg\},
\end{aligned} \tag{5.39}$$

$$E\Bigg\{\sigma_{k+1}K_{k+1}B_k(\widetilde{x}_k)e_{k+1}^T(1-\sigma_{k+1})^TK_{k+1}^T+(1-\sigma_{k+1})K_{k+1}e_{k+1}(\sigma_{k+1}B_k(\widetilde{x}_k))^TK_{k+1}^T\Bigg\}$$
$$\leq E\Bigg\{a_3p_{k+1}K_{k+1}B_k\hat{P}_k(K_{k+1}B_k)^T+a_3^{-1}(1-p_{k+1})K_{k+1}\delta K_{k+1}^T\Bigg\}, \tag{5.40}$$

$$E\Bigg\{\delta_{k+1}K_{k+1}\widetilde{\nu}_ke_{k+1}^T(1-\sigma_{k+1})^TK_{k+1}^T+(1-\sigma_{k+1})K_{k+1}e_{k+1}(\sigma_{k+1}\widetilde{\nu}_k)^TK_{k+1}\Bigg\}$$
$$\leq E\Bigg\{a_4p_{k+1}K_{k+1}\hat{P}^{\nu\nu}{}_kK_{k+1}^T+a_4^{-1}(1-p_{k+1})K_{k+1}\delta K_{k+1}^T\Bigg\}, \tag{5.41}$$

$$E\Bigg\{(I-K_{k+1}(1-\sigma_{k+1})B_{k+1})\widetilde{x}_{k+1|k}e_k^T(\sigma_{k+1})^TK_{k+1}^T+\sigma_{k+1}K_{k+1}e_k$$
$$\times((I-K_{k+1}(1-\sigma_{k+1})B_{k+1})\widetilde{x}_{k+1|k})^T\Bigg\}\leq E\Bigg\{a_5(I-K_{k+1}(1-p_{k+1})B_{k+1})\hat{P}_{k+1|k} \tag{5.42}$$
$$\times(I-K_{k+1}(1-p_{k+1})B_{k+1})^Ta_5^{-1}p_{k+1}K_{k+1}\delta K_{k+1}^T\Bigg\},$$

$$E\Bigg\{(1-\sigma_{k+1})K_{k+1}\nu_{k+1}e_k^T(\sigma_{k+1})^TK_{k+1}^T+\sigma_{k+1}K_{k+1}e_k((1-\sigma_{k+1})\nu_{k+1})^TK_{k+1}\Bigg\}^T$$
$$\leq E\Bigg\{a_6(1-p_{k+1})K_{k+1}R_{k+1}(K_{k+1})^T+a_6^{-1}p_{k+1}K_{k+1}\delta K_{k+1}^T\Bigg\}, \tag{5.43}$$

$$E\Bigg\{\sigma_{k+1}K_{k+1}B_k(\widetilde{x}_k)e_k^T(\sigma_{k+1})^TK_{k+1}^T+\sigma_{k+1}K_{k+1}e_k(\sigma_{k+1}B_k(\widetilde{x}_k))^TK_{k+1}^T\Bigg\}$$
$$E\Bigg\{\leq a_7p_{k+1}K_{k+1}B_k\hat{P}_k(K_{k+1}B_k)^T+a_7^{-1}p_{k+1}K_{k+1}\delta K_{k+1}^T\Bigg\}, \tag{5.44}$$

$$E\Bigg\{\sigma_{k+1}K_{k+1}\widetilde{\nu}_ke_k^T(\sigma_{k+1})^TK_{k+1}^T+\sigma_{k+1}K_{k+1}e_k(\sigma_{k+1}\widetilde{\nu}_k)^TK_{k+1}^T\Bigg\}$$
$$\leq E\Bigg\{a_8p_{k+1}K_{k+1}\hat{P}^{\nu\nu}{}_kK_{k+1}^T+a_8^{-1}p_{k+1}K_{k+1}\delta K_{k+1}^T\Bigg\}, \tag{5.45}$$

where $a_1-a_8>0$. Inserting (5.38)-(5.45) in (5.37), the upper bound of the estimation error

covariance $\overline{P}_{k+1}$ is as follows,

$$\begin{aligned}
\overline{P}_{k+1} &= \Big(1 + a_1(1-\gamma_{k+1}) + a_5(1-\gamma_k)\Big)(I - K_{k+1}(1-p_{k+1})B_{k+1})\hat{P}_{k+1|k} \\
&\times (I - K_{k+1}(1-p_{k+1})B_{k+1})^T - p_{k+1}(A_k\hat{P}_k B_{k+1}^T K_{k+1}^T + B_{k+1}K_{k+1}\hat{P}_k^T A_k^T) \\
&- p_{k+1}(A_k\hat{P}^{x\nu}{}_k K_{k+1}^T + K_{k+1}\hat{P}^{x\nu}{}_k A_k^T) + \Big(1 + a_2(1-\gamma_{k+1}) + a_6(1-\gamma_k)\Big)(1-p_{k+1}) \\
&\times K_{k+1}R_{k+1}(K_{k+1})^T + \Big(1 + a_3(1-\gamma_{k+1}) + a_7(1-\gamma_k)\Big)p_{k+1}K_{k+1}B_k\hat{P}_k(K_{k+1}B_k)^T \\
&+ \Big(1 + a_4(1-\gamma_{k+1}) + a_8(1-\gamma_k)\Big)p_{k+1}K_{k+1}\hat{P}^{\nu\nu}{}_k K_{k+1}^T + p_{k+1}(1-p_{k+1})K_{k+1} \\
&\times (\hat{z}_k - \hat{z}_{k+1|k})(\hat{z}_k - \hat{z}_{k+1|k})^T K_{k+1}^T + (1 + a_1^{-1} + a_2^{-1} + a_3^{-1} + a_4^{-1}) \\
&\times (1-p_{k+1})(1-\gamma_{k+1})K_{k+1}\delta K_{k+1}^T + (1 + a_5^{-1} + a_6^{-1} + a_7^{-1} + a_8^{-1})p_{k+1}(1-\gamma_k)K_{k+1} \\
&\times \delta K_{k+1}^T + p_{k+1}(K_{k+1}B_k\hat{P}_k^{x\nu}K_{k+1}^T + K_{k+1}(K_{k+1}B_k\hat{P}^{x\nu}{}_k)^T)
\end{aligned} \tag{5.46}$$

The filter gain (5.31) can be derived by $\frac{\partial \overline{P}_{k+1}}{\partial K_{k+1}} = 0$, which completes the proof. ■

In the next subsection, we describe the discrete-time event-triggered cubature Kalman filter algorithm with one step randomly delayed measurements. In some steps of the algorithm, we need to obtain the upper bound of $\hat{P}_{k+1|k}^{yy}$. From (5.35) we have,

$$\begin{aligned}
\hat{P}_{k+1|k}^{yy} &= (1-p_{k+1})\hat{P}_{k+1|k}^{zz} + p_{k+1}\hat{P}_k^{zz} + (1-p_{k+1})p_{k+1}(\hat{z}_{k+1|k} - \hat{z}_k)(\hat{z}_{k+1|k} - \hat{z}_k)^T \\
&+ (1-p_{k+1})(1-\gamma_{k+1})\delta + p_{k+1}(1-\gamma_k)\delta + (1-p_{k+1})(1-\gamma_{k+1})E\{\tilde{z}_{k+1|k}^T e_{k+1} \\
&+ e_{k+1}^T\tilde{z}_{k+1|k}\} + p_{k+1}(1-\gamma_k)E\{\tilde{z}_k^T e_{k+1} + e_{k+1}^T\tilde{z}_k\}
\end{aligned} \tag{5.47}$$

where $\hat{P}_{k+1|k}^{zz} = E[\tilde{z}_{k+1|k}\tilde{z}_{k+1|k}^T|Y_k]$, $\hat{P}_k^{zz} = E[\tilde{z}_k\tilde{z}_k^T|Y_k]$. Using *Lemma 3.1*, the upper bound of $\hat{P}_{k+1|k}^{yy}$ can be written as follows,

$$\begin{aligned}
\overline{P}_{k+1|k}^{yy} &= (1-p_{k+1})\Big(1 + b_1(1-\gamma_{k+1})\Big)\hat{P}_{k+1|k}^{zz} + p_{k+1}\Big(1 + b_2(1-\gamma_k)\Big)\hat{P}_k^{zz} + (1-p_{k+1})p_{k+1} \\
&\times (\hat{z}_{k+1|k} - \hat{z}_k)(\hat{z}_{k+1|k} - \hat{z}_k)^T + (1-p_{k+1})(1-\gamma_{k+1}) \\
&\times (1 + b_1^{-1})\delta + p_{k+1}(1-\gamma_k)(1 + b_2^{-1})\delta
\end{aligned} \tag{5.48}$$

where, $b_1, b_2 > 0$.

5.2.1 DECKF with One Step Randomly Delayed Measurements Algorithm

The event-triggered cubature Kalman filter with one-step randomly delayed measurements recursively propagates the first two-order moments, namely, the mean $\hat{x}_{k+1}^a$ and covariance, $\hat{P}_{k+1}^a$, by the following steps,

First we should initialize the mean, $(\hat{x}_0^a)^T = [\hat{x}_0 \quad 0]^T$ and the covariance $\hat{P}_0^a = \begin{bmatrix} \hat{P}_0 & 0 \\ 0 & R_0 \end{bmatrix}$. Then we should follow time update steps and measurement update steps to derive the $\hat{P}_{k+1}^{x\nu}$, $\hat{P}_{k+1}$, and $\hat{P}_{k+1}^{\nu\nu}$ to find the augmented covariance in (5.6). Note that the proposed DECKF is a derivative-free filter, which does not require computation of the Jacobian matrix. Suppose that $\hat{P}_{k+1|k}$ is the predicted state error covariance matrix, then based on $\hat{P}_{k+1|k}^{xy} = \hat{P}_{k+1|k} B_{k+1}^T$, one can derive the following $B_{k+1} = (\hat{P}_{k+1|k}^{xy})^T (\hat{P}_{k+1|k})^{-1}$ [39], where $\hat{P}^{xy}{}_{k+1|k}$ is the cross-covariance matrix. So the algorithm of DECKF with one-step randomly delayed measurement can be written as follows,

Time-Update:

1) Factorize $\hat{P}^a{}_k = S_k^a (S_k^a)^T$ to calculate the cubature points,

$$X_{i,k} = [(\xi_{i,k}^x)^T \quad (\xi_{i,k}^\nu)^T]^T = S_k^a \xi_i + \hat{x}^a{}_k$$

where $i = 1, 2, ..., L$ and $L = 2(n+m)$. n, m show the dimensionality of the states, and measurement noise, respectively. $\xi_{i,k}^x$ and $\xi_{i,k}^\nu$ are the state and noise cubature points.

2) Propagate the Cubature Points,

$$X_{i,k+1|k}^{*x} = f(\xi_{i,k}^x, u_k)$$

$$\Upsilon_{i,k+1|k}^{*x} = h(\xi_{i,k}^x, u_k)$$

3) Estimate the predicted state and the predicted state error covariance as follows,

$$\hat{x}_{k+1|k} = \frac{1}{2L} \sum_{i=1}^{2L} X_{i,k+1|k}^{*x}$$

$$\hat{P}_{k+1|k} = \frac{1}{2L} \sum_{i=1}^{2L} X_{i,k+1|k}^{*x} (X_{i,k+1|k}^{*x})^T - \hat{x}_{k+1|k} \hat{x}_{k+1|k}^T + Q_k$$

Measurement Update:

1) Factorize $\hat{P}_{k+1|k} = S_{k+1|k} S_{k+1|k}^T$ to calculate the Cubature points,

$$X_{i,k+1|k} = S_{k+1|k} \xi_i + \hat{x}_{k+1|k} \qquad i = 1, 2, ..., 2n$$

2) Propagate Cubature points as follows,

$$Y_{i,k+1|k} = h(X_{i,k+1|k}, u_{k+1}) \qquad i = 1, 2, ..., 2n$$

3) Compute the measurement means and covariances, $\hat{z}_{k+1|k}$, $\hat{z}_k$, $\hat{P}_{k+1|k}^{zz}$, $\hat{P}_k^{zz}$, $\hat{P}_{k+1|k}^{xz}$, and $\hat{P}_{k+1,k}^{xz}$ by the following equations,

$$\hat{z}_{k+1|k} = \frac{1}{2n} \sum_{i=1}^{2n} Y_{i,k+1|k}$$

$$\hat{\hat{z}}_k = \frac{1}{2L}\sum_{i=1}^{2L}(\Upsilon^{*x}_{i,k+1|k} + \xi^{\nu}_{i,k})$$

$$\hat{P}^{zz}_{k+1|k} = \frac{1}{2n}\sum_{i=1}^{2n} Y_{i,k+1|k}Y^T_{i,k+1|k} - \hat{\hat{z}}_{k+1|k}\hat{\hat{z}}^T_{k+1|k} + R_{k+1}$$

$$\hat{P}^{zz}_{k} = \frac{1}{2L}\sum_{i=1}^{2L}(\Upsilon^{*x}_{i,k+1|k} + \xi^{\nu}_{i,k})(\Upsilon^{*x}_{i,k+1|k} + \xi^{\nu}_{i,k})^T - \hat{\hat{z}}_{k}(\hat{\hat{z}}_{k})^T$$

$$\hat{P}^{xz}_{k+1|k} = \frac{1}{2n}\sum_{i=1}^{2n} X_{i,k+1|k}Y^T_{i,k+1|k} - \hat{x}_{k+1|k}\hat{\hat{z}}^T_{k+1|k}$$

$$\hat{P}^{xz}_{k+1,k} = \frac{1}{2L}\sum_{i=1}^{2L} X^{*x}_{i,k+1|k}(\Upsilon^{*x}_{i,k+1|k} + \xi^{\nu}_{i,k})^T - \hat{x}_{k+1|k}\hat{\hat{z}}^T_{k+1|k}$$

where $\hat{P}^{xz}_{k+1|k} = E[\tilde{x}_{k+1|k}\tilde{\hat{z}}^T_{k+1|k}|Y_k]$ and $\hat{P}^{xz}_{k+1,k|k} = E[\tilde{x}_{k+1|k}\tilde{\hat{z}}^T_{k}|Y_k]$.

4) Calculate the measurement, measurement noise means and covariances by the following equations,

$$\hat{\nu}_{k+1} = K^{\nu}_{k+1}\tilde{y}_{k+1|k}$$

$$K^{\nu}_{k+1} = P^{\nu y}_{k+1|k}(\overline{P}^{yy}_{k+1|k})^{-1}$$

$$\hat{P}^{\nu y}_{k+1|k} = (1-p_{k+1})(1+(1-\gamma_{k+1}))R_{k+1}$$

$$\hat{P}^{\nu\nu}_{k+1} = R_{k+1} - K^{\nu}_{k+1}\overline{P}^{yy}_{k+1|k}(K^{\nu}_{k+1})^T$$

$$\begin{aligned}\overline{P}^{yy}_{k+1|k} = (1-p_{k+1})\Big((1+b_1(1-\gamma_{k+1}))\hat{P}^{zz}_{k+1|k} + p_{k+1}(\hat{\hat{z}}_{k+1|k} - \hat{\hat{z}}_k)(\hat{\hat{z}}_{k+1|k} - \hat{\hat{z}}_k)^T \\ + (1+b_1^{-1})(1-\gamma_k)\delta\Big) + p_{k+1}((1+b_2(1-\gamma_k))\hat{P}^{zz}_{k} + p_{k+1}(1-\gamma_k)(1+b_2^{-1})\delta\end{aligned}$$

5) Compute the filter gain: $K_{k+1} = O(T)^{-1}$,where

$$O = m_1(1-p_{k+1})(\hat{P}^{xz}_{k+1|k})^T(\hat{P}_{k+1|k})^{-1}\hat{P}_{k+1|k} + p_{k+1}\hat{P}^{xz}_{k+1,k},$$

and,

$$\begin{aligned}T = {} & p_{k+1}(\hat{P}^{xz}_{k|k-1})^T(\hat{P}_{k|k-1})^{-1}\hat{P}^{x\nu}{}_k + p_{k+1}\Big((\hat{P}^{xz}_{k|k-1})^T(\hat{P}_{k|k-1})^{-1}\hat{P}^{x\nu}{}_k\Big)^T + m_1(1-p_{k+1})(\hat{P}^{xz}_{k+1|k})^T \\ & \times(\hat{P}_{k+1|k})^{-1}\hat{P}_{k+1|k}\Big((\hat{P}^{xz}_{k+1|k})^T(\hat{P}_{k+1|k})^{-1}\Big)^T + m_2(1-p_{k+1})R_{k+1} + m_3p_{k+1}(\hat{P}^{xz}_{k|k-1})^T(\hat{P}_{k+1|k})^{-1} \\ & \times\hat{P}_k\Big((\hat{P}^{xz}_{k|k-1})^T(\hat{P}_{k|k-1})^{-1}\Big)^T + m_4p_{k+1}\hat{P}^{\nu\nu}{}_k + m_5(1-p_{k+1})(1-\gamma_{k+1})\delta + m_6p_{k+1}(1-\gamma_k)\delta \\ & + p_{k+1}(1-p_{k+1})(\hat{\hat{z}}_k - \hat{\hat{z}}_{k+1|k})(\hat{\hat{z}}_k - \hat{\hat{z}}_{k+1|k})^T\end{aligned}$$

6) Estimate $\hat{P}^{x\nu}_{k+1}$ as follows,

$$\hat{P}^{x\nu}_{k+1} = -K_{k+1}\overline{P}^{yy}_{k+1|k}(K^{\nu}_{k+1})^T$$

7) Estimate the updated state:

$$\hat{x}_{k+1} = \hat{x}_{k+1|k} + K_{k+1}(\overline{y}_{k+1} - \hat{y}_{k+1|k})$$

8) Compute the upper bound of estimation error covariance:

$$\begin{aligned}
\overline{P}_{k+1} &= \Big(1 + a_1(1-\gamma_{k+1}) + a_5(1-\gamma_k)\Big)\Big(I - K_{k+1}(1-p_{k+1})(\hat{P}^{xz}_{k+1|k})^T(\hat{P}_{k+1|k})^{-1}\Big)\hat{P}_{k+1|k} \\
&\times \Big(I - K_{k+1}(1-p_{k+1})(\hat{P}^{xz}_{k+1|k})^T(\hat{P}_{k+1|k})^{-1}\Big)^T - p_{k+1}\Big(\hat{P}^{xz}_{k+1,k}K^T_{k+1} + K_{k+1}(\hat{P}^{xz}_{k+1,k})^T\Big) \\
&+ \Big(1 + a_2(1-\gamma_{k+1}) + a_6(1-\gamma_k)\Big)(1-p_{k+1})K_{k+1}R_{k+1}(K_{k+1})^T + \Big(1 + a_3(1-\gamma_{k+1}) \\
&+ a_7(1-\gamma_k)\Big)p_{k+1}\Big(K_{k+1}(\hat{P}^{xz}_{k|k-1})^T(\hat{P}_{k|k-1})^{-1}\hat{P}_k(K_{k+1}(\hat{P}^{xz}_{k|k-1})^T(\hat{P}_{k|k-1})^{-1})^T + \Big(1 \\
&+ a_4(1-\gamma_{k+1}) + a_8(1-\gamma_k)\Big)K_{k+1}\hat{P}^{\nu\nu}{}_k K^T_{k+1} + (1-p_{k+1})K_{k+1}(\hat{z}_k - \hat{z}_{k+1|k})(\hat{z}_k - \hat{z}_{k+1|k})^T \\
&\times K^T_{k+1}\Big) + (1 + a_1^{-1} + a_2^{-1} + a_3^{-1} + a_4^{-1})(1-p_{k+1})K_{k+1}(1-\gamma_{k+1})K_{k+1}\delta K^T_{k+1} \\
&+ p_{k+1}\Big((1 + a_5^{-1} + a_6^{-1} + a_7^{-1} + a_8^{-1})(1-\gamma_k)K_{k+1}\delta K^T_{k+1} + K_{k+1}\hat{P}^{xz^T}_{k|k-1}(\hat{P}_{k|k-1})^{-1}\hat{P}^{x\nu}_k \\
&\times K^T_{k+1} + K_{k+1}(\hat{P}^{xz^T}_{k|k-1}(\hat{P}_{k|k-1})^{-1}\hat{P}^{x\nu}{}_k)^T K^T_{k+1}\Big)
\end{aligned}$$

So, the augmented mean and covariance in (5.6) can be calculated.

5.3 Numerical implementation and verification

In this section the effectiveness of the proposed method is illustrated by simulation results. We consider the univariate non-stationary growth model under event-triggered mechanism with one randomly delayed measurement. We study the performance of the DECKF that we proposed in Section 5.2 and we compare the results to the DECKF that we proposed in *Chapter 3* under different condition, namely different triggering threshold values. A univariate non-stationary growth model is modelled as follows,

$$\begin{aligned}
x_{k+1} &= 0.5x_k + 25\frac{x_k}{1+x_k^2} + 8cos(1.2k) + \omega_k \qquad k \geq 0 \\
z_k &= \frac{x_k^2}{20} + \nu_k \qquad k \geq 1
\end{aligned} \tag{5.49}$$

The initial value of the state, x_0, is a Gaussian variable with zero mean and variance of one. The process noise $w_k \sim N(0, Q)$ and the measurement noise $v_k \sim N(0, R)$ are the white noise with zero mean and covariance $Q = 10$ and $R = 1$, respectively. We use the root mean square error (RMSE) to compare the performance of the two filters in the presence of delay. RMSE at time k is,

$$RMSE(k) = \sqrt{\frac{1}{N}\sum_{n=1}^{N}(\eta_k^n - \hat{\eta}_k^n)^2},$$

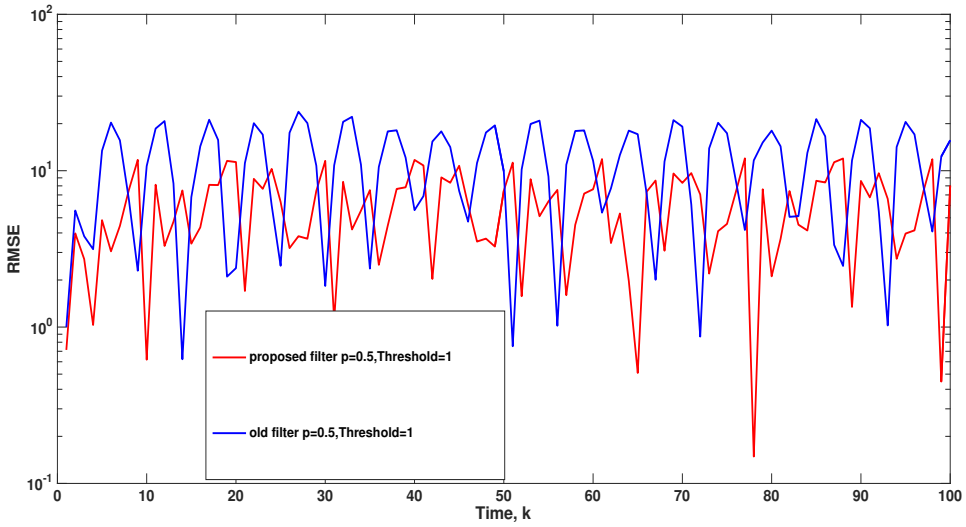

Figure 5.1: RMSE results of the filters with event-triggered threshold 1 and delay probability p=0.5

where η_k^n is the true, and $\hat{\eta}_k^n$ is the estimated state at the n-th Monte Carlo run, respectively.

In the first scenario, we consider that $p = 0.5$ and we compare the results of the filters with two different event-triggered thresholds of $\delta = 1$ and $\delta = 2$.

Figure 5.1 and Figure 5.2 show that the RMSE results of the proposed filter are lower than the filter proposed in *Chapter 3*, which means that the proposed filter has better estimation performance in the presence of delayed measurements, and the proposed gain matrix reduces the estimation error which improves the filter performance.

In the next scenario, we compare the performance of the proposed filter in the presence of different delay probabilities, namely $p = 0.2$ and $p = 0.5$, and different event-triggered thresholds, $\delta = 1$ and $\delta = 2$. The number of data transmissions are shown in Table.5.1. By comparing the results of the filter in Figure 5.3 and the Table.5.1, one can conclude the following: 1) increasing the triggering threshold and the delay probabilities, the estimation performance degrades, however, one can achieve a reasonable estimation quality by properly tuning the event-triggered threshold with respect to the delay probability. 2) By choosing a good triggering threshold, one can reduce the number of data transmission and communication burden while obtaining accurate state estimation results.

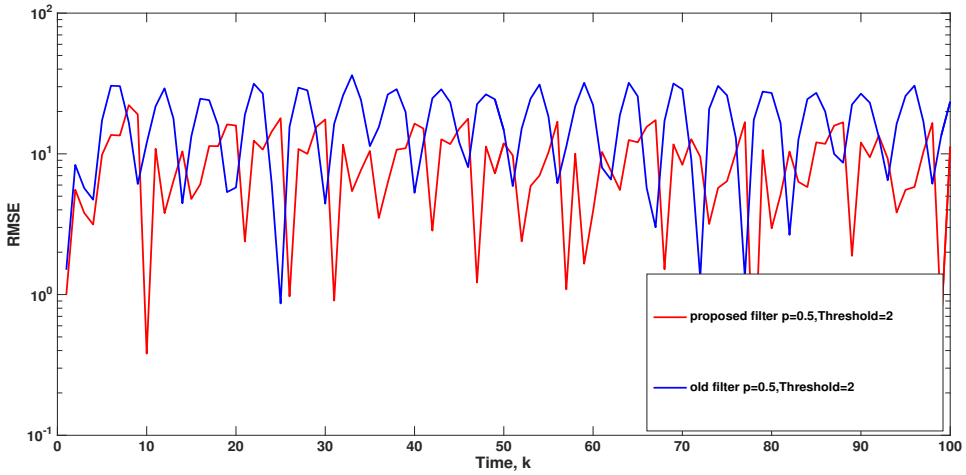

Figure 5.2: RMSE results of the filters with event-triggered threshold 2 and delay probability p=0.5

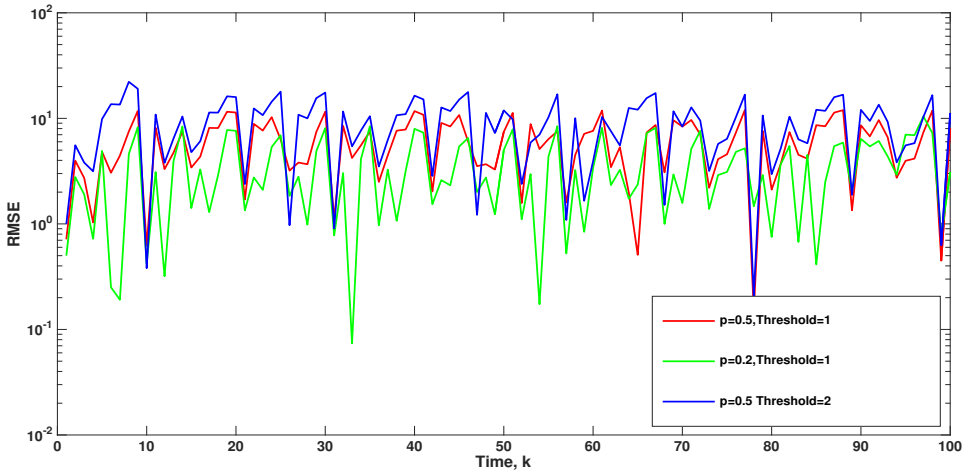

Figure 5.3: RMSE results of the proposed DECKF with different event-triggered threshold

Table 5.1: RMSE results of the proposed filter

Threshold value	Delay probability	number of data transmission
1	0.2	92
1	0.5	84
2	0.5	75

5.4 Summary

A new nonlinear filter algorithm for the filtering problems of high dimensional nonlinear systems under the event- triggered protocol with one-step delay in measurement is proposed. We show that when the communication channels are not perfect, the triggered measurements are transferred with delay and the state estimator can not be updated in real-time.

In the presence of delay in the communication, the previous data effects the filtering process, so a new filter gain should be achieved to consider the effects of the delayed measurements on the state estimation and to make the state estimation errors and the error covariance matrix bounded.

So, we develop a new filter algorithm to deal with this issue and we compare the estimation results of the proposed filter under different event-triggered conditions considering different delay probabilities. The simulation results show that by properly choosing the event-triggered threshold, one can guarantee the estimation quality while the extra communication burden would be decreased. Also, compared to the previously proposed filter, the new filter has less state estimation error in the presence of delay in the communication channels.

Chapter 6

Application of Discrete-Time Event-Triggered Cubature Kalman Filter to a Synchronous Machine

In this chapter, [1] our interest is in the application of the proposed event-triggered cubature Kalman filters in *Chapter 3* and *Chapter 5* to a synchronous generator using noisy signals from phasor measurement units (PMUs) devices. We show the advantage of employing the proposed cubature Kalman filters over the more established and more explored filters such as extended Kalman filters and unscented Kalman filters, frequently used in the literatures to estimate the states of synchronous machines.

We argue that better estimates can be obtained using the CKF and justify our claims in our simulations, both using periodic and event-triggered sampling. We show that the event-triggered approach allow us to obtain excellent estimates, while reducing the flow of information with respect to classical periodic systems.

First we study the application of the proposed nonlinear filter in *Chapter 3* with a well designed event-triggered mechanism and we show that the proposed filter can significantly reduce data communication between the PMUs and the remote filter while the estimation error is kept bounded, thus reducing potential network-related congestion issues.

Our solution makes use of a so-called "Send-on-Delta" type event-triggering condition in which a new sample is triggered if the measured signal deviates by "delta" from the most recent sample. Thus, the sensor node does not broadcast a new message while the sampled signal remains within a certain interval of confidence.

Then, we consider that the communication channels are not perfect and the measure-

[1] The results of this chapter has been published in the article: M. Kooshkbaghi, H. J. Marquez, and W. Xu, "Event-Triggered Approach to Dynamic State Estimation of a Synchronous Machine Using Cubature Kalman Filter," *IEEE Transactions on Control Systems Technology, DOI: 10.1109/TCST.2019.2923374.*

ments are transferred with one step random delay to the state estimator. We compare the estimation results of the proposed filter in *Chapter 5* with the proposed filter in *Chapter 3* and we show the performance improvement of the filter proposed in *Chapter 5*.

6.1 Dynamic of Single Machine Infinite Bus (SMIB)

Figure 6.1 shows a schematic of the system connection, in which synchronous machine connected to power distribution system via the transmission lines. The synchronous machine can be described by the following fourth-order nonlinear model [54, 55],

$$\begin{aligned}
\dot{\Psi}&=\omega_0\Delta\omega,\\
\Delta\dot{\omega}&=\frac{1}{J}(T_m - T_e - D\Delta\omega),\\
\dot{e}^{'}_q&=\frac{1}{T^{'}_{do}}(E_{fd} - e^{'}_q - (x_d - x^{'}_d)i_d),\\
\dot{e}^{'}_d&=\frac{1}{T^{'}_{qo}}(-e^{'}_d + (x_q - x^{'}_q)i_q),
\end{aligned} \tag{6.1}$$

where the variables are defined in Table 6.1. Note that the values are in (p.u), except when explicitly noted.

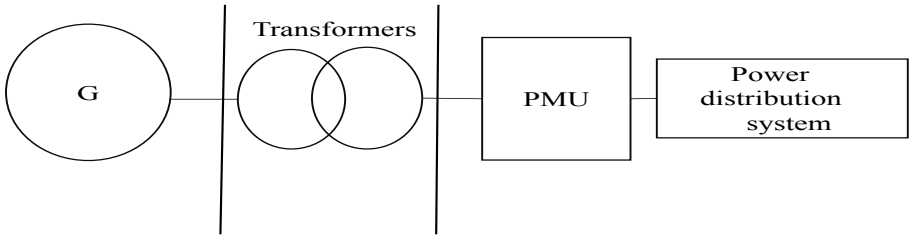

Figure 6.1: Synchronous Machine Interconnection.

Defining state variables, $\mathbf{x} = \begin{bmatrix} \Psi \\ \Delta\omega \\ e^{'}_q \\ e^{'}_d \end{bmatrix}$, and $\bar{\mathbf{u}} = \begin{bmatrix} T_m \\ E_{fd} \end{bmatrix} = \begin{bmatrix} \bar{u}_1 \\ \bar{u}_2 \end{bmatrix}$, equation (6.1) can be rewritten the state space form as follows,

$$\begin{aligned}
\dot{x}_1&=\omega_0 x_2,\\
\dot{x}_2&=\frac{1}{J}(\bar{u}_1 - T_e - Dx_2),\\
\dot{x}_3&=\frac{1}{T_{do}{}^{'}}\left(\bar{u}_2 - x_3 - (x_d - x^{'}_d)i_d\right),\\
\dot{x}_4&=\frac{1}{T_{qo}{}^{'}}\left(-x_4 + (x_q - x^{'}_q)i_q\right).
\end{aligned} \tag{6.2}$$

Table 6.1: Definition of Variables and Constants

Variables (pu)	**Definition**
d, q	Rotor direct axis and quadrature axis
D, J	Damping factor and inertia constant
$T_{do}^{'}$, $T_{qo}^{'}$	d and q axis transient open circuit time constants
T_m, T_e	Mechanical input and electrical torque
e_d ,e_q	Direct and quadratic axis voltage
Ψ(elec.rad)	First state, rotor angle with respect to the machine terminals (load angle)
$e_d^{'}$, $e_q^{'}$	Transient voltage of d- and q-axis
i_d, i_q ,E_{fd}	Direct and quadratic axis current, Field voltage
x_d, x_q	Direct and quadratic axis reactance
$x_d^{'}$, $x_q^{'}$	Direct and quadratic axis transient reactance
$\Delta\omega$, ω_0(elec.rad/s)	2nd state, rotor speed and nominal sync speed
V_t , P_t	Voltage and Active power at terminal bus

The electric air-gap torque T_e, is given by $T_e = P_t + R_a I_t^2$, and neglecting the stator resistance R_a, we have:

$$T_e \cong P_t = e_d i_d + e_q i_q. \tag{6.3}$$

The d-and q-axis voltages, (e_d, e_q), and currents, (i_d, i_q), are given by:

$$\begin{aligned} e_d &= V_t \sin\Psi, \\ e_q &= V_t \cos\Psi. \end{aligned} \tag{6.4}$$

$$\begin{aligned} i_d = I_t \sin(\Psi + \Phi) &= \frac{e_q^{'} - V_t \cos\Psi}{x_d^{'}}, \\ i_q = I_t \cos(\Psi + \Phi) &= \frac{V_t \sin\Psi}{x_q}. \end{aligned} \tag{6.5}$$

The terminal bus voltage and current are $E_T = V_t = \sqrt{e_d^2 + e_q^2}$, and $I_t = \sqrt{i_d^2 + i_q^2}$, respectively.

Replacing the variables, Ψ and $e_q^{'}$, with the state variables x_1 and x_3, (6.5) becomes,

$$\begin{aligned} i_d &= \frac{x_3 - V_t \cos x_1}{x_d^{'}}, \\ i_q &= \frac{V_t \sin x_1}{x_q}. \end{aligned} \tag{6.6}$$

Substituting (6.4) and (6.6) in (6.3), we obtain the electrical output power in terms of the states as follows:

$$T_e \cong P_t \cong \frac{V_t}{x_d^{'}} x_3 \sin x_1 + \frac{V_t^2}{2}\left(\frac{1}{x_q} - \frac{1}{x_d^{'}}\right) \sin 2x_1. \tag{6.7}$$

Finally, substituting (6.6) and (6.7) in (6.1), we obtain the state space model of the fourth-order nonlinear synchronous machine:

$$\dot{\mathbf{x}} = \frac{d}{dt}\begin{bmatrix} \Psi \\ \Delta\omega \\ e_q^{'} \\ e_d^{'} \end{bmatrix} = \begin{bmatrix} \dot{x}_1 \\ \dot{x}_2 \\ \dot{x}_3 \\ \dot{x}_4 \end{bmatrix},$$

$$\mathbf{u} = \begin{bmatrix} T_m \\ E_{fd} \\ V_t \end{bmatrix} = \begin{bmatrix} u_1 \\ u_2 \\ u_3 \end{bmatrix},$$

$$\dot{x}_1 = \omega_0 x_2,$$

$$\dot{x}_2 = \frac{1}{J}\Big[u_1 - \Big(\frac{u_3}{x_d^{'}} x_3 \sin x_1 + \frac{u_3^2}{2}(\frac{1}{x_q} - \frac{1}{x_d^{'}}) \sin 2x_1\Big) - Dx_2\Big],$$

$$\dot{x}_3 = \frac{1}{T_{do}^{'}}\left[u_2 - x_3 - (x_d - x_d^{'})(\frac{x_3 - u_3 \cos x_1}{x_d^{'}})\right],$$

$$\dot{x}_4 = \frac{1}{T_{qo}^{'}}\left[-x_4 + (x_q - x_q^{'})(\frac{u_3 \sin x_1}{x_q})\right],$$

$$y_1 = \frac{u_3}{x_d^{'}} x_3 \sin x_1 + \frac{u_3^2}{2}(\frac{1}{x_q} - \frac{1}{x_d^{'}}) \sin 2x_1. \tag{6.8}$$

The global structure of (6.8) can be represented as follows,

$$\begin{aligned} \dot{\mathbf{x}} &= f(\mathbf{x}, \mathbf{u}) + \mathbf{w}, \\ \mathbf{y} &= h(\mathbf{x}, \mathbf{u}) + \mathbf{v}. \end{aligned} \tag{6.9}$$

where f and h are the system and output functions, respectively. $\mathbf{x}$ is the state variable vector, $\mathbf{u}$ is the input vector, $\mathbf{w}$ and $\mathbf{v}$ are the process and the measurement noises. (6.9) can be written in discrete-time form (3.1) and (3.2) as follows,

$$\begin{aligned} x_{k+1} &= f(x_k, u_k) + \omega_k, \\ y_{k+1} &= h(x_{k+1}, u_{k+1}) + \nu_{k+1}. \end{aligned} \tag{6.10}$$

Note: *The filter operates with V_t, T_m, E_{fd}, and P_t as inputs, where P_t is obtained using a PMU. We assume that PMUs are installed at the terminal buses of the generator and provide measurements of the bus voltage and line current. Since the main objective of this section is to discuss the effect of the event-triggering mechanism on the CKF estimation of SMIB, we do not consider the dynamics of T_m, E_{fd}, and consider them instead as known inputs (see also [55–57]).* In the next section, we show the effectiveness of the proposed filters under different conditions, namely different triggering thresholds and delay probabilities in the communication channels.

6.2 Estimation Results

In this section, we apply the event-triggered CKF proposed in *Chapter 3* and *Chapter 5* to the derived fourth-order nonlinear synchronous generator model described by (6.8) to ensure the estimation performance of the proposed filters. The block diagram of the networked system with event-triggered cubature Kalman filter is shown in *Figure 6.2*. Note that

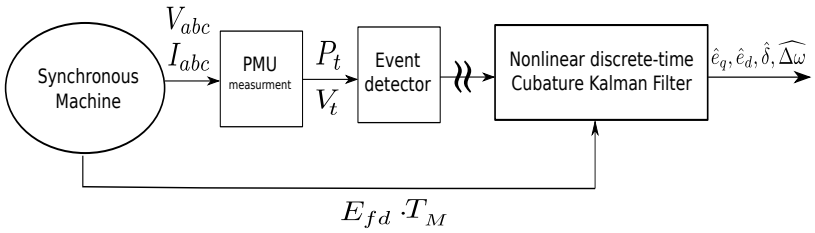

Figure 6.2: Block diagram of the overall networked system

although our example is applied to a single machine, the same approach is also applicable to a large scale system that includes multiple generators. Each of the generators can be described using the fourth-order model given by (6.8), [58].

The overall state space model (6.11) for all generators is high dimensional with high degree of nonlinearities.

$$\dot{x} = Ax + Bu + \phi(x), y = h(x). \tag{6.11}$$

$$A = \begin{bmatrix} 0 & \omega_0 I_G & 0 & 0 \\ 0 & \mathrm{diag}(\frac{-D}{J}) & 0 & 0 \\ 0 & 0 & \mathrm{diag}(\frac{-1}{T'_{do}}) & 0 \\ 0 & 0 & 0 & \mathrm{diag}(\frac{-1}{T'_{qo}}) \end{bmatrix},$$

$$B = \begin{bmatrix} 0 & 0 & 0 \\ \mathrm{diag}(\frac{1}{J}) & 0 & 0 \\ 0 & \mathrm{diag}(\frac{1}{T'_{do}}) & 0 \\ 0 & 0 & 0 \end{bmatrix},$$

$$\phi = \begin{bmatrix} 0 \\ -(\frac{u_3}{x'_d} x_3 \sin x_1 + \frac{u_3^2}{2}(\frac{1}{x_q} - \frac{1}{x'_d}) \sin 2x_1 \\ \frac{1}{T'_{do}}(-(x_d - x'_d)(\frac{x_3 - u_3 \cos x_1}{x'_d})) \\ \frac{1}{T'_{qo}}(-(x_q - x'_q)(\frac{u_3 \sin x_1}{x_q})) \end{bmatrix}.$$

The parameter G in matrix A is the number of the generators in the distribution system. Known parameters of the SMIB, and the active power produced by generator, P_t, which is accessible using a PMU device, are sent to the state estimator through the limited bandwidth communication channels. To reduce the communication burden, the measurement output,

Table 6.2: SMIB parameters amount

Parameters	**Value (pu)**	**Parameters**	**Value (pu)**
D ,J	0.05 ,10	x_d ,x_q	2.15,1.365
V , $\omega_{0nominal}$	1.02, 377	$x_d^{'}$,$x_q^{'}$	0.37 , 0.37
$T_{do}^{'}$, $T_{qo}^{'}$	0.131,0.01	T_m , E_{fd}	0.8, 2.4

P_t, is sent to the event detector to check the event-triggering condition. We study the effect of the event-triggering formulation on state estimation of the synchronous generator by using two separate scenarios; namely, with and without the event-triggered mechanism. We show that event-triggered data transmission leads to a significant reduction in transmission of information through the limited bandwidth communication channel, without significant deterioration in the quality of the estimated signals.

Scenario A: In this scenario, we apply the cubature Kalman filter without event-triggered mechanism and compare the results to the UKF. We achieve continuous flow of information by setting the event-triggering threshold parameter $\delta = 0$ in the SMIB system. We employ the system represented in *Figure 6.2* under the following conditions:

We assume T_m to be constant, E_{fd} is a step function, V_t and the observation signal, $P_t = (y_1)$, are the inputs to the nonlinear filter in each step through the communication channels, while $[\Psi, \Delta\omega, e_q, e_d]$ are the outputs, or estimated states, of the nonlinear filter. The values of the inputs and other SMIB parameters are shown in Table 6.2. The initial covariance matrix is $P_0 = diag([10^2 \quad 10^2 \quad 10^2 \quad 10^2])$. The process and measurement noise covariance matrices are $w_k \sim (0, Q_k) = (0, 10^{-2} \times I_{4\times4})$ and $v_k \sim (0, R_k) = (0, 10^{-2} \times I)$.

Figure 6.3 shows the result of the dynamic state estimation for the CKF without event-triggered mechanism using *MATLAB*. As expected, the results show the effectiveness of the CKF with all the states converge to the true values real states. In this scenario, the number of data transmission points between the remote CKF and the system is 120000.

Scenario B: In this scenario, to check the effectiveness of the proposed discrete time event-triggered cubature Kalman filter under time variant unknown input, we apply the proposed filter with different kinds of E_{fd} (constant, step) and mechanical input T_m (constant, step, ramp) with different event-triggered mechanism threshold to the SMIB system. The value of the parameters are as the previous subsection. T_m, E_{fd}, V_t and the observation signal, $P_t = (y_1)$, are the inputs of the nonlinear filter in each step. The measurable output $P_t = (y_1)$ is sent to event detector. a_1 and a_2 are considered 0.02. To obtain a desired trade-off between the estimation error and the number of data transfers, we compare different threshold values.

Figure 6.4 shows the results of the dynamic state estimation of the proposed filter with the event-triggered mechanism thresholds of $\delta = 0.05$, $\delta = 0.1$, and $\delta > 0.1$. We assume that the input signal E_{fd} is a step function while T_m is a constant. The state estimation results maintains good estimation properties for small values of the threshold parameter and only begins to diverge as the threshold increases over $\delta > 0.1$. The number of data transmission points between the remote cubature Kalman filter and the event detector, for event-triggered threshold of $\delta = 0.05$ and $\delta = 0.1$, reduces from 120000 to only 700 and 500 values, respectively. Comparison between the value of the event-triggered mechanism threshold and the number of data transfers is shown in Table. 6.3.

As the results show, it can be concluded that by properly tuning the event-triggered mechanism threshold, a desired estimation quality can be achieved while the communication rate is reduced dramatically.

To confirm the effectiveness of the proposed filter under general conditions, the simulations are repeated for two other conditions, the first for T_m= step and E_{fd}=constant (*Figure 6.5*), and the second for T_m= ramp and E_{fd}=step (*Figure 6.6*). The simulation results for different input conditions demonstrate the accuracy of the estimated states.

To compare various nonlinear filter performances, we use the root-mean square error (RMSE) of the states. For instance, for the first state, we define the RMSE in angle at time k, as

$$RMSE(k) = \sqrt{\frac{1}{N}\sum_{n=1}^{N}(\Psi_k^n - \hat{\Psi}_k^n)^2}, \tag{6.12}$$

where Ψ_k^n and $\hat{\Psi}_k^n$ are the true and estimated states at the n-th Monte Carlo run. We make 20 independent Monte Carlo runs. All the filters are initialized with the same condition in each run. *Figure 6.7* shows the performance comparison between the proposed discrete time event-triggered cubature Kalman filter (DECKF) and event-triggered UKF (EUKF) for different event-triggered threshold. We don't present the results of the EKF as it uses linearization which leads to large errors in state estimation results. Note that, as mentioned in the Appendix, UKF can be used in systems with dimension up to three. The dimension of the states used here is higher than three, so the weight of the centre sigma point is negative which result in non-positive covariance [8].

In this simulation, we assume that n+k=5 (which is used to select the sigma points and the weight of the sigma points) and the estimation results are not optimal, so the RMSEs estimated by DECKF are lower than the RMSEs estimated by EUKF. For both filters, DECKF and EUKF, the performance is degraded as the threshold increases, since

Table 6.3: Comparison between different Event-triggered threshold

Threshold value	Number of data transfers	Convergence
0 , 0.05, 0.1	120000, 700, 500	✓
Ψ >0.1	-	×

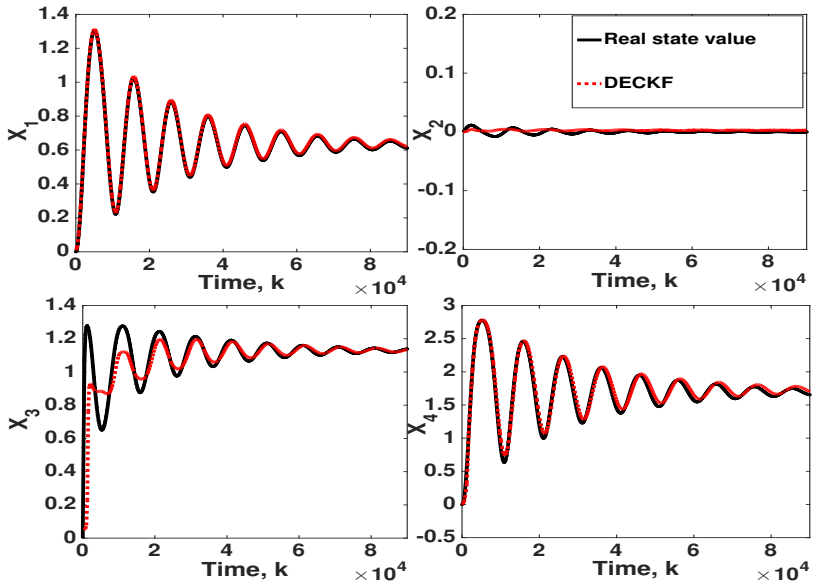

Figure 6.3: States estimation results of DECKF with no event-triggered mechanism and Efd= Step, Tm= Constant

less information would be transferred to state estimator as the threshold increases. For instance, the performance of DECKF with event-triggered threshold of 0.05 lies between CKF without event-triggered mechanism (event-triggered threshold equals to zero) and DECKF with event-triggered threshold of 0.1. As it is clear from the simulation result (*Figure 6.7*), the performance of the proposed filter, DECKF is better than the EUKF.

Scenario C: In this scenario, we compare the performance of the proposed filter in *Chapter 5* and the filter proposed in *Chapter 3*, in the presence of delay in the communication channels. We consider that the event-triggered threshold is 0.05 and the delay probability rate is 0.2. Figure 6.8 shows the RMSE results of the two proposed filters. As we mentioned before, in the presence of delay in the communication channels, the previous data affects the filtering process. The DECKF which is proposed in *Chapter 5* considers the effects of the delayed measurements on the state estimation process compared to the filter proposed in *Chapter 3*, thus the state estimation errors, the error covariance matrix of the DECKF of *Chapter 5* are less than those of the filter proposed in *Chapter 3*.

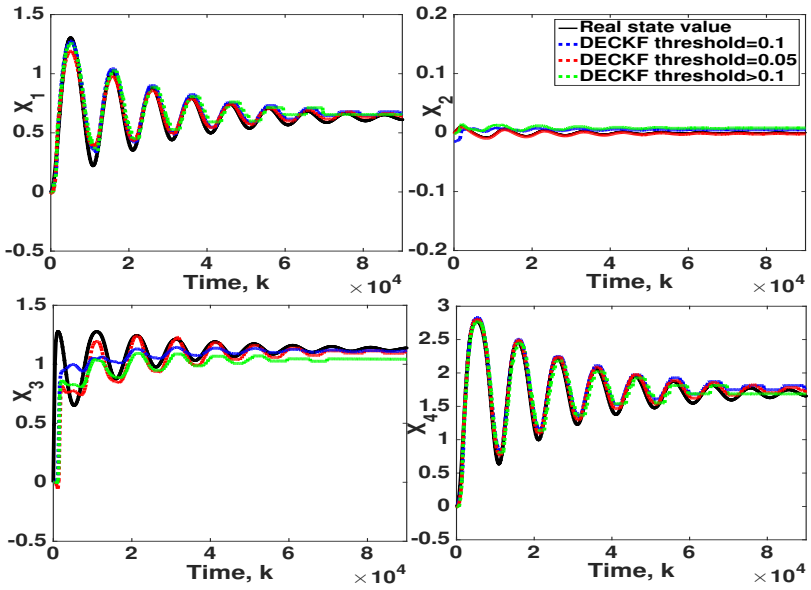

Figure 6.4: States estimation results of DECKF with different thresholds and Efd=Step, Tm= Constant

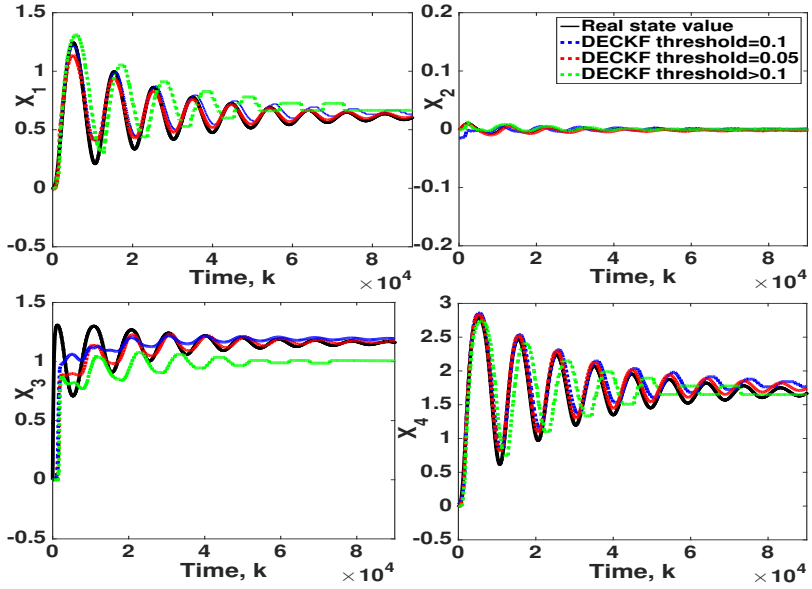

Figure 6.5: States estimation results of DECKF with different thresholds and Tm=Step, Efd=Constant

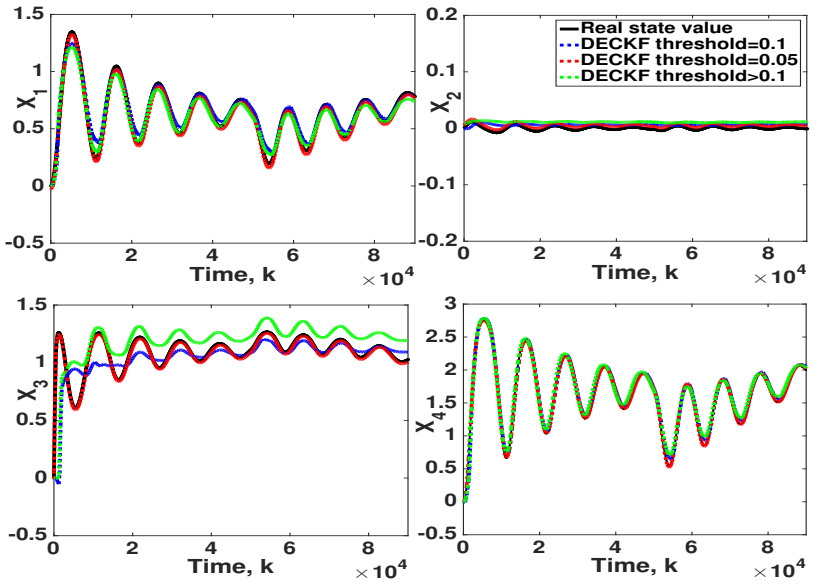

Figure 6.6: States estimation results of DECKF with different thresholds and Tm=Ramp, Efd=Stept

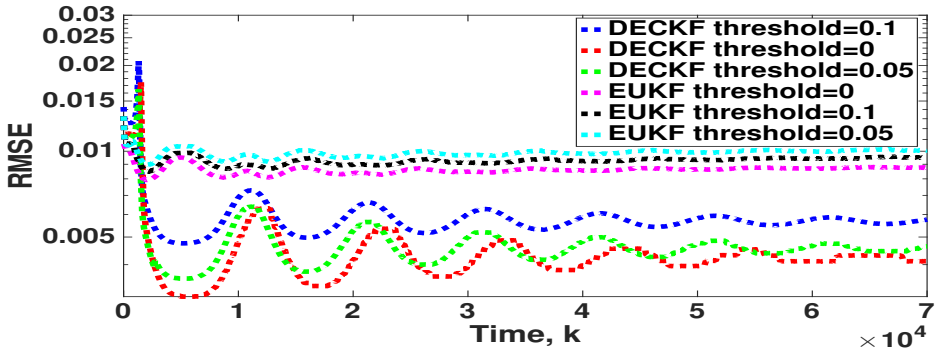

Figure 6.7: RMSEs of DECKF and EUKF with different threshold

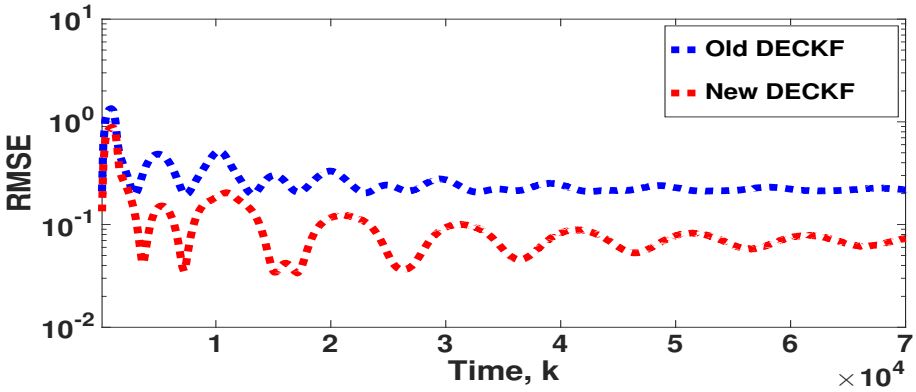

Figure 6.8: RMSEs of DECKF and EUKF with different threshold

6.3 Summary

In this chapter, we considered the dynamic state estimation of a synchronous generator using a discrete-time event-triggered cubature Kalman filter (DECKF). As mentioned in the introduction, the event-triggered formulation is an alternative to conventional periodic discrete-time sampling which can render similar performance while reducing communication between sensors and remote filters. Event-triggered systems are becoming predominant in applications in which communication between components is established via a communication channel, with the consequent communication restrictions, such as smart grid applications, etc. Applied to a fourth-order nonlinear model of a synchronous generator, our results show excellent tracking of the true states, despite an impressive communication reduction between the sensors and the remote filter. More specifically: comparison of a discrete-time cubature Kalman filter with periodic sampling, and the event-triggered formulation, shows that using a conservative triggering threshold ($\delta = 0.05$), we obtain nearly undistinguishable performance despite reducing communication to less than 1%. The article explicitly reinforces the use of the cubature Kalman filter as opposed to the more established and well explored extended Kalman filter and unscented Kalman filter. To justify our claims, we compare the cubature Kalman filter presented here to the unscented Kalman filter and show that the cubature filter provides a more accurate estimate of the true states, both using periodic sampling and/or event-triggered sampling.

In addition, we study the effectiveness of the proposed filter in *Chapter 5* in the presence of delay in the communication channels. We show that the proposed filter has less estimation error and provide better estimation of the states compared to the previously proposed filters.

Chapter 7

Strong Tracking Discrete-Time Event-Triggered Cubature Kalman Filter with Packet Dropout

In this chapter, [1] a new filtering algorithm, a strong tracking discrete-time event-triggered cubature Kalman filter (STDECKF), is developed to reduce the amount of data transmission between the measuring sensors and the remote state estimator and to reduce the low accuracy of the filtering.

This filter uses the strong tracking filtering technology to improve the performance of cubature Kalman filter in the presence of *sudden changes in the states of nonlinear system*. The time-varying fading factor is derived from the orthogonality principle conditions and it tunes the predicted state error covariance and the gain of the filter based on the residuals between available and predicted measurements which improves the filtering performance. We show that the estimation error is bounded provided that the event-triggered threshold is properly tuned with respect to the packet dropout rate and the proposed filter displays higher accuracy when compared to its DECKF (non-adaptive) counterpart.

The remainder of the chapter is as follows. In Section 7.1, we define the nonlinear system model, and we define the event-triggered data transferring mechanism, the packet dropout and the strong tracking filter. In Section 7.2, we will develop a strong tracking discrete-time event-triggered cubature Kalman filter for nonlinear systems and we study the boundedness of the state estimation error. In Section 7.3, we compare the results of the proposed filter with the previous filter by using a simulated example.

[1] The results of this chapter has been submitted for publication in the article: M. Kooshkbaghi, H. J. Marquez,"Strong Tracking Discrete-Time Event-Triggered Cubature Kalman Filter for Nonlinear Dynamical Systems with Packet Dropout," *Internationa Journal of Robust and Nonlinear Control, September 2019.*

7.1 Problem formulation

7.1.1 System Model

Consider the nonlinear discrete-time system and the nonlinear measurement model given in (7.1) and (7.2), respectively.

$$x_{k+1} = f(x_k, u_k) + \omega_k \tag{7.1}$$

$$y_{k+1} = h(x_{k+1}) + \nu_{k+1} \tag{7.2}$$

In addition, recalling from *Chapter 3* and *Chapter 4*, the current transmitted measurement (7.3) and the packet dropout binary random variable (7.4), are defined as follows,

$$\bar{y}_k = y_k + (1 - \gamma_k)(\overline{y} - y_k) \tag{7.3}$$

$$\lambda_k = \begin{cases} 1 & \text{data is received} \\ 0 & \text{otherwise} \end{cases} \tag{7.4}$$

7.1.2 Strong Tracking Filter (STF)

As mentioned in the introduction, the strong tracking filters display important characteristics, making them attractive in many applications. When there are sudden changes in the states, nonlinear filters such as EKF, UKF, or CKF have poor estimation performance. Strong tracking filters introduce a fading factor based on the residual to reduce the influence of the history data and to modify the predicted state error covariance matrix, the gain matrix and the model of the system in real time. To derive STF, we use the *Extended Orthogonality Principle* which defines as follows,

Definition 7.1: Extended Orthogonality Principle

For the discrete-time nonlinear systems, the optimal state estimation can be achieved by the following extended orthogonality principle [59],

$$E\{(x_{k+1} - \hat{x}_{k+1|k+1})(x_{k+1} - \hat{x}_{k+1|k+1})^T\} = min \tag{7.5}$$

such that,

$$E\{\widetilde{y}_{k+j+1|k+j}\widetilde{y}^T_{k+1|k}\} = 0 \qquad k = 0, 1, ... \quad j = 1, 2, ... \tag{7.6}$$

To modify the state error covariance matrix at time k, the time-varying fading factor, Λ_k, is introduced as follows to adjust the predicted state error covariance matrix in the real time,

$$\hat{P}_k = \Lambda_{k+1}\hat{P}_k \tag{7.7}$$

where $\hat{P}_k$ is the error covariance matrix and Λ_k is obtained by solving the (7.5) and (7.6). The predicted state error covariance is as follows,

$$\hat{P}_{k+1|k} = \Lambda_{k+1} A_k \hat{P}_k A_k^T + Q_k \tag{7.8}$$

As mentioned in [61] and [60], DECKF has the highest accuracy among all variations of the Kalman filters applicable to nonlinear systems (UKF and EKF) for high dimensional systems, but may present deviations from the true state in the presence of sudden changes in the states. To overcome this problem, a strong tracking discrete-time event-triggered cubature Kalman filter is proposed. Note that the strong tracking filter can not be directly applied to the DECKF algorithm, so in the next section, STDECKF algorithm based on the extended orthogonality principle is developed.

7.2 Strong Tracking Filter Discrete-Time Event-Triggered Cubature Kalman Filter

In this section, a suboptimal fading factor , Λ_k is derived to modify the discrete-time event-triggered cubature Kalman filter to have a strong tracking estimation of the states of the nonlinear system. Note that the linearization with first order approximation is implemented to facilitate the following discussion.

Theorem 7.1: *Consider the system* (7.1) *and* (7.2) *with the defined event-triggered mechanism* (7.3) *and the packet dropout* (7.4)*. Using the cubature Kalman filter state estimator, the sub-optimal time-varying fading factor can be calculated as follows,*

$$\Lambda_{k+1} = max\{1, \frac{tr[N_{k+1}]}{tr[M_{k+1}]}\}, \tag{7.9}$$

and N_{k+1} *and* M_{k+1} *can be defined as follows,*

$$\begin{aligned} N_{k+1} &= \Big((1 + a_1(1-\gamma_{k+1})\Big)\lambda_{k+1} V_{k+1}^0 - \Big(1 + a_2(1-\gamma_{k+1})\Big) R_{k+1} \\ &-(1 + a_1^{-1} + a_2^{-1})(1-\gamma_{k+1})\delta I - \Big(1 + a_1(1-\gamma_{k+1})\Big) B_{k+1} Q_k B_{k+1}^T \end{aligned} \tag{7.10}$$

$$M_{k+1} = \Big(1 + a_1(1-\gamma_{k+1})\Big) B_{k+1} (A_k \hat{P}_k A_k^T) B_{k+1}^T \tag{7.11}$$

where, $A_k = \alpha_k F_k$*, and* $B_{k+1} = \beta_{k+1} H_{k+1}$*.* $F_k = \frac{\partial f(x)}{\partial x}|_{x=\hat{x}_k}$ *and* $H_{k+1} = \frac{\partial h(x)}{\partial x}|_{x=\hat{x}_{k+1|k}}$ *are the Jacobian matrix,* $\alpha_k = diag(\alpha_{1,k}, \alpha_{2,k}, ..., \alpha_{n_x k})$*, and* $\beta_{k+1} = diag(\beta_{1,k+1}, \beta_{2,k+1}, ..., \beta_{n_y k+1})$ *are unknown diagonal matrix representing the error incurred in neglecting the higher order terms of the Taylor series respectively.* $\beta_{min}^2 I \leq \beta_k \beta_k^T \leq \beta_{max}^2 I$ *and* $\alpha_{min}^2 I \leq \alpha_k \alpha_k^T \leq \alpha_{max}^2 I$

where $\beta_{min}, \beta_{max}, \alpha_{min}, \alpha_{max} \neq 0$. $V_{k+1}^{0} = E\{\widetilde{y}_{k+1|k}\widetilde{y}_{k+1|k}^{T}\}$ *is the residual covariance.* $a_1 > 0$ *and* $a_2 > 0$ *are two positive arbitrary parameters.*

The following *Remark* is used in the proof of *Theorem 7.1.*

Remark 7.1: *The innovation measurement at time k, denoted by* $\widetilde{y}_{k+1|k}$*, has the following features [46]:*

- *Zero mean: The innovation has zero mean* $E[\widetilde{y}_{k+1|k}] = 0$.
- *White sequence: Innovation is whitened measurement.*

$$E\{\widetilde{y}_{k+j+1|k+j}\widetilde{y}_{k+1|k}^{T}\} = 0 \qquad k = 0, 1, ... \quad j = 1, 2, ...$$

- *Uncorrelated with past measurements:*

$$E\{\widetilde{y}_{k+1|k}y_{k+1-j}^{T}\} = 0 \quad j = 1, 2, ...$$

Proof. Recalling from *Chapter 4*, the estimation error and the prediction error of the event-triggered system can be defined as follows:

$$\widetilde{x}_{k+1} = (I - \lambda_{k+1}K_{k+1}B_{k+1})\widetilde{x}_{k+1|k} - \lambda_{k+1}K_{k+1}\nu_{k+1} + \lambda_{k+1}K_{k+1}(1 - \gamma_{k+1})e_{k+1} \tag{7.12}$$

$$\widetilde{x}_{k+1|k} = A_k(I - K_k\lambda_k B_k)\widetilde{x}_{k|k-1} - A_k K_k \lambda_k \nu_k + A_k K_k \lambda_k (1 - \gamma_k)e_k + \omega_k. \tag{7.13}$$

where $e_k = \overline{y} - y_k$. In addition, the measurement prediction error can be written as follows,

$$\widetilde{y}_{k+1|k} = B_{k+1}A_k\widetilde{x}_k + B_{k+1}\omega_k + \nu_{k+1} \tag{7.14}$$

using a similar derivation method yields,

$$\widetilde{y}_{k+1+j|k+j} = B_{k+1+j}A_{k+j}\widetilde{x}_{k+j} + B_{k+1+j}\omega_{k+j} + \nu_{k+1+j} \tag{7.15}$$

The initial state x_0, ω_k and ν_k which generate the states and observations are mutually independent. Considering it into account and substituting (7.14) and (7.15) into (7.6), we have,

$$\begin{aligned} E\{\widetilde{y}_{k+1+j|k+j}\widetilde{y}_{k+1|k}^{T}\} &= E\Big\{(B_{k+1+j}A_{k+j}\widetilde{x}_{k+j} + B_{k+1+j}\omega_{k+j} + \nu_{k+1+j})\widetilde{y}_{k+1|k}^{T}\Big\} \\ &= E\Big\{(B_{k+1+j}A_{k+j}\widetilde{x}_{k+j})\widetilde{y}_{k+1|k}^{T}\Big\} \end{aligned} \tag{7.16}$$

(7.12) can be written as follows,

$$\widetilde{x}_{k+j} = (I - \lambda_{k+j}K_{k+j}B_{k+j})\widetilde{x}_{k+j|k+j-1} - \lambda_{k+j}K_{k+j}\nu_{k+j} + \lambda_{k+j}K_{k+j}(1 - \gamma_{k+j})e_{k+j} \tag{7.17}$$

substituting (7.17) into (7.16) yields,

$$E\{\widetilde{y}_{k+1+j|k+j}\widetilde{y}_{k+1|k}^{T}\} = E\Bigg\{ B_{k+1+j}A_{k+j}\Big[(I-\lambda_{k+j}K_{k+j}B_{k+j})\widetilde{x}_{k+j|k+j-1} - \lambda_{k+j}K_{k+j}\nu_{k+j} + \lambda_{k+j}K_{k+j}(1-\gamma_{k+j})e_{k+j}\Big]\widetilde{y}_{k+1|k}^{T}\Bigg\} \tag{7.18}$$

As we mentioned before the initial state x_0, ω_k and ν_k which generate the states and observations are mutually independent. Recall from *Chapter 3* we have, $\widetilde{x}_{k+1|k} = A_k\widetilde{x}_k+\omega_k$. Thus, substituting $\widetilde{x}_{k+j|k+j-1}$ into (7.18), yields,

$$E\{\widetilde{y}_{k+1+j|k+j}\widetilde{y}_{k+1|k}^{T}\} = E\Bigg\{ B_{k+1+j}A_{k+j}\Big[(I-\lambda_{k+j}K_{k+j}B_{k+j})A_{k+j-1}\widetilde{x}_{k+j-1} + \lambda_{k+j}K_{k+j}(1-\gamma_{k+j})e_{k+j}\Big]\widetilde{y}_{k+1|k}^{T}\Bigg\} \tag{7.19}$$

from (7.16) and (7.19), using the iterative operation, and considering the $\widetilde{y}_{k+1|k}^{T}$ features which are mentioned in *Remark 7.1*, the following form can be derived,

$$E\{\widetilde{y}_{k+1+j|k+j}\widetilde{y}_{k+1|k}^{T}\} = B_{k+1+j}A_{k+j}\prod_{i=2}^{j}(I-\lambda_{k+j}K_{k+j}B_{k+j})A_{k+j-1}E\Big\{[x_{k+1}-\hat{x}_{k+1}]\widetilde{y}_{k+1|k}^{T}\Big\} \tag{7.20}$$

recalling $\hat{x}_{k+1}$, (4.9), from *Chapter 4* and substituting it in $E\Big\{[x_{k+1}-\hat{x}_{k+1}]\widetilde{y}_{k+1|k}^{T}\Big\}$ of (7.20) we have,

$$E\Big\{[x_{k+1}-\hat{x}_{k+1}]\widetilde{y}_{k+1|k}^{T}\Big\} = E\Big\{[x_{k+1}-\hat{x}_{k+1|k}-K_{k+1}\lambda_{k+1}(\widetilde{y}_{k+1|k}-(1-\gamma_{k+1})e_{k+1})]\widetilde{y}_{k+1|k}^{T}\Big\} \tag{7.21}$$

considering the $\widetilde{y}_{k+1|k}^{T}$ features again, (7.21) can be written as follows,

$$\begin{aligned} E\Big\{[x_{k+1}-\hat{x}_{k+1}]\widetilde{y}_{k+1|k}^{T}\Big\} &= E\{\widetilde{x}_{k+1|k}\widetilde{y}_{k+1|k}^{T}\} - K_{k+1}\lambda_{k+1}E\{\widetilde{y}_{k+1|k}\widetilde{y}_{k+1|k}^{T}\} = \hat{P}_{xyk+1|k} \\ &\quad - K_{k+1}\lambda_{k+1}E\{\widetilde{y}_{k+1|k}\widetilde{y}_{k+1|k}^{T}\} = \hat{P}_{k+1|k}B_{k+1}^{T} - K_{k+1}\lambda_{k+1}V_{k+1}^{0} \end{aligned} \tag{7.22}$$

where $V_{k+1}^{0} = E\{\widetilde{y}_{k+1|k}\widetilde{y}_{k+1|k}^{T}\}$ is the residual covariance, and it can be estimated as

$$V_{k+1}^{0} = \begin{cases} \widetilde{y}_{1|0}\widetilde{y}_{1|0}^{T} & k=0 \\ \frac{\rho V_k^0+\widetilde{y}_{k+1|k}\widetilde{y}_{k+1|k}^{T}}{1+\rho} & k\geq 1 \end{cases}$$

where $0<\rho\leq 1$ is the forgetting factor and is generally set as $\rho = 0.95$.

Substituting K_{k+1}, (4.8), in (7.22) yields,

$$E\Big\{[\widetilde{x}_{k+1}\widetilde{y}^T_{k+1|k}]\Big\} = \hat{P}_{k+1|k}B^T_{k+1}\Bigg[I - \lambda_{k+1}\Big((1+a_1(1-\gamma_{k+1})\Big)\lambda_{k+1}\Big[\Big(1+a_1(1-\gamma_{k+1})\Big) \times B_{k+1}\hat{P}_{k+1|k}B^T_{k+1} + R_{k+1}\Big(1+a_2(1-\gamma_{k+1})\Big) + (1+a_1^{-1}+a_2^{-1})(1-\gamma_{k+1})\delta I\Big]^{-1})V^0_{k+1}\Bigg]. \tag{7.23}$$

Substituting (7.23) in (7.20) yields,

$$\begin{aligned} E\Big\{[\widetilde{y}_{k+j+1}\widetilde{y}^T_{k+1|k}]\Big\} = {} & B_{k+1+j}A_{k+j}\prod_{i=2}^{j}\Big((I-\lambda_{k+j}K_{k+j}B_{k+j})A_{k+j-1}\Big) \\ & \times \hat{P}_{k+1|k}B^T_{k+1}\Bigg[I - \lambda_{k+1}\Big((1+a_1(1-\gamma_{k+1})\Big)\lambda_{k+1} \\ & \times \Big[\Big(1+a_1(1-\gamma_{k+1})\Big)B_{k+1}\hat{P}_{k+1|k}B^T_{k+1} \\ & + \Big(1+a_2(1-\gamma_{k+1}\Big))R_{k+1} \\ & + (1+a_1^{-1}+a_2^{-1})(1-\gamma_{k+1})\delta I\Big]^{-1})V^0_{k+1}\Bigg]. \end{aligned} \tag{7.24}$$

An appropriate fading factor Λ_{k+1} should be chosen to satisfy the principle of extended orthogonality in (7.6). So we should have,

$$\begin{aligned} & \Bigg[I - \lambda_{k+1}\Big((1+a_1(1-\gamma_{k+1})\Big)\lambda_{k+1} \times \Big[\Big(1+a_1(1-\gamma_{k+1})\Big)B_{k+1}\hat{P}_{k+1|k}B^T_{k+1} \\ & + \Big(1+a_2(1-\gamma_{k+1})\Big)R_{k+1} + (1+a_1^{-1}+a_2^{-1})(1-\gamma_{k+1})\delta I\Big]^{-1})V^0_{k+1}\Bigg] = 0, \end{aligned} \tag{7.25}$$

which is equivalent to

$$\begin{aligned} & \lambda_{k+1}\Big((1+a_1(1-\gamma_{k+1})\Big)\lambda_{k+1}V^0_{k+1} - \Big(1+a_2(1-\gamma_{k+1})\Big)R_{k+1} \\ & - (1+a_1^{-1}+a_2^{-1})(1-\gamma_{k+1})\delta I = \Big(1+a_1(1-\gamma_{k+1})\Big)B_{k+1}\hat{P}_{k+1|k}B^T_{k+1}. \end{aligned} \tag{7.26}$$

Substituting (7.8) into (7.26) yields,

$$\begin{aligned} & \lambda_{k+1}\Big((1+a_1(1-\gamma_{k+1})\Big)\lambda_{k+1}V^0_{k+1} - \Big(1+a_2(1-\gamma_{k+1})\Big)R_{k+1} \\ & - (1+a_1^{-1}+a_2^{-1})(1-\gamma_{k+1})\delta I = \Big(1+a_1(1-\gamma_{k+1})\Big)B_{k+1}(\Lambda_{k+1}A_k\hat{P}_kA^T_k + Q_k)B^T_{k+1}. \end{aligned} \tag{7.27}$$

The traces of the both sides of (7.27) can be calculated as follows,

$$\begin{aligned} & tr\Bigg[\lambda_{k+1}\Big((1+a_1(1-\gamma_{k+1})\Big)\lambda_{k+1}V_{k+1}^0-\Big(1+a_2(1-\gamma_{k+1})\Big)R_{k+1}-(1+a_1^{-1}+a_2^{-1}) \\ & \times(1-\gamma_{k+1})\delta I-\Big(1+a_1(1-\gamma_{k+1})\Big)B_{k+1}Q_kB_{k+1}^T\Bigg] \\ & = tr\Bigg[\Lambda_{k+1}\Big(1+a_1(1-\gamma_{k+1})\Big)B_{k+1}(A_k\hat{P}_kA_k^T)B_{k+1}^T\Bigg]. \end{aligned} \tag{7.28}$$

Define

$$M_{k+1}=\Big(1+a_1(1-\gamma_{k+1})\Big)B_{k+1}(A_k\hat{P}_kA_k^T)B_{k+1}^T, \tag{7.29}$$

and

$$\begin{aligned} N_{k+1}=&\Big((1+a_1(1-\gamma_{k+1})\Big)\lambda_{k+1}V_{k+1}^0-(1+a_2(1-\gamma_{k+1}))R_{k+1} \\ &-(1+a_1^{-1}+a_2^{-1})(1-\gamma_{k+1})\delta I-\Big(1+a_1(1-\gamma_{k+1})\Big)B_{k+1}Q_kB_{k+1}^T. \end{aligned} \tag{7.30}$$

It follows that (7.28) is equivalent to $tr[\Lambda_{k+1}M_{k+1}]=tr[N_{k+1}]$, and the fading factor can be obtained by $\Lambda_{k+1}=\frac{tr[N_{k+1}]}{tr[M_{k+1}]}$. The fading factor is effective when $\Lambda_{k+1}\geq 1$, so the fading factor is calculated by $\Lambda_{k+1}=max\{1,\frac{tr[N_{k+1}]}{tr[M_{k+1}]}\}$ ■

STF requires calculation of the linearization of the nonlinear measurement (Hessian) matrix. To combine the STF with event-triggered Cubature Kalman filter and to propose a derivative-free STDECKF , the equivalent equation of the STF needs to be derived.

Suppose that $\hat{P}_{k+1|k}^l$ is the predicted state error covariance matrix before introducing fading factor, then based on $\hat{P}_{xy,k+1|k}=\hat{P}_{k+1|k}B_{k+1}^T$, one can derive the following $B_{k+1}=(\hat{P}_{xy,k+1|k}^l)^T(\hat{P}_{k+1|k}^l)^{-1}$ [39], where $\hat{P}_{xy,k+1|k}^l$ is the cross-covariance matrix without fading factor. So, N_{k+1} and M_{k+1} can be written as follows,

$$\begin{aligned} N_{k+1}=&\Big((1+a_1(1-\gamma_{k+1})\Big)\lambda_{k+1}V_{k+1}^0-\Big(1+a_2(1-\gamma_{k+1})\Big)R_{k+1}-(1+a_1^{-1}+a_2^{-1}) \\ &\times(1-\gamma_{k+1})\delta I-\Big(1+a_1(1-\gamma_{k+1})\Big)(\hat{P}_{xy,k+1|k}^l)^T(\hat{P}_{k+1|k}^l)^{-1}Q_k(\hat{P}_{k+1|k}^l)^{-1}(\hat{P}_{xy,k+1|k}^l), \end{aligned} \tag{7.31}$$

$$\begin{aligned} M_{k+1}=&\Big(1+a_1(1-\gamma_{k+1})\Big) \\ &\times\Big(\hat{P}_{yy,k+1|k}^l-R_{k+1}-(\hat{P}_{xy,k+1|k}^l)^T(\hat{P}_{k+1|k}^l)^{-1}Q_k(\hat{P}_{k+1|k}^l)^{-1}(\hat{P}_{xy,k+1|k}^l)\Big). \end{aligned} \tag{7.32}$$

In the following, we summarize the strong tracking discrete-time event-triggered cubature Kalman filter algorithm.

First we should initialize the mean, $(\hat{x}_0)$ and the covariance $\hat{P}_0$. Then we should follow time update steps and measurement update steps to derive the state estimation $\hat{x}_{k+1}$, the upper bound of the error covariance matrix $\overline{P}_{k+1}$ and the filter gain K_{k+1}.

Time-Update:

First we should factorize $\hat{P}_k = S_k(S_k)^T$ to calculate the cubature points, $X_{i,k} = S_k\xi_i + \hat{x}_k$, where $i = 1, 2, ..., 2n_x$.

Then we propagate the Cubature Points,

$$X^*{}_{i,k+1|k} = f(X_{i,k}, u_k) \tag{7.33}$$

To estimate the predicted state and the predicted state error covariance as follows,

$$\hat{x}_{k+1|k} = \frac{1}{2n_x}\sum_{i=1}^{2n_x} X^*{}_{i,k+1|k} \tag{7.34}$$

$$\hat{P}^l{}_{k+1|k} = \frac{1}{2n_x}\sum_{i=1}^{2n_x} X^*{}_{i,k+1|k}(X^*{}_{i,k+1|k})^T - \hat{x}_{k+1|k}\hat{x}^T_{k+1|k} + Q_k \tag{7.35}$$

Fading Factor Calculation :

Like the time update steps, first we factorize $\hat{P}^l_{k+1|k} = S^l_{k+1|k}S^l_{k+1|k}$ to calculate the cubature points $X^l_{i,k+1|k} = S^l_{k+1|k}\xi_i + \hat{x}_{k+1|k}$. Then we propagate the Cubature points as follows,

$$Y^l_{i,k+1|k} = h(X^l_{i,k+1|k}, u_{k+1}) \qquad i = 1, 2, ..., 2n_x \tag{7.36}$$

Now the the predicted measurement estimation $\hat{y}^l_{k+1|k}$, the innovation covariance matrix $\hat{P}^l_{yy,k+1|k}$ and the cross-covariance matrix $\hat{P}^l_{xy,k+1|k}$ are as follows,

$$\hat{y}^l_{k+1|k} = \frac{1}{2n_x}\sum_{i=1}^{2n_x} Y^l_{i,k+1|k} \tag{7.37}$$

$$\hat{P}^l_{yy,k+1|k} = \frac{1}{2n_x}\sum_{i=1}^{2n_x} Y^l_{i,k+1|k}Y^{lT}_{i,k+1|k} - \hat{y}^l_{k+1|k}\hat{y}^{lT}_{k+1|k} + R_{k+1} \tag{7.38}$$

$$\hat{P}^l_{xy,k+1|k} = \frac{1}{2n_x}\sum_{i=1}^{2n_x} X^l_{i,k+1|k}Y^{lT}_{i,k+1|k} - \hat{x}^l_{k+1|k}\hat{y}^{lT}_{k+1|k} \tag{7.39}$$

We can derive N_{k+1} and M_{k+1} as follows,

$$\begin{aligned} N_{k+1} = &\Big((1 + a_1(1 - \gamma_{k+1})\Big)\lambda_{k+1}V^0_{k+1} - \Big(1 + a_2(1 - \gamma_{k+1})\Big)R_{k+1} - (1 + a_1^{-1} + a_2^{-1}) \\ &\times (1 - \gamma_{k+1})\delta I - \Big(1 + a_1(1 - \gamma_{k+1})\Big)(\hat{P}^l_{xy,k+1|k})^T(\hat{P}^l_{k+1|k})^{-1}Q_k(\hat{P}^l_{k+1|k})^{-1}(\hat{P}^l_{xy,k+1|k}), \end{aligned} \tag{7.40}$$

$$\begin{aligned} M_{k+1} = &\Big(1 + a_1(1 - \gamma_{k+1})\Big) \\ &\times \Big(\hat{P}^l_{yy,k+1|k} - R_{k+1} - (\hat{P}^l_{xy,k+1|k})^T(\hat{P}^l_{k+1|k})^{-1}Q_k(\hat{P}^l_{k+1|k})^{-1}(\hat{P}^l_{xy,k+1|k})\Big). \end{aligned} \tag{7.41}$$

so the fading factor can be obtained as follows,

$$\Lambda_{k+1} = max\{1, \frac{tr[N_{k+1}]}{tr[M_{k+1}]}\} \tag{7.42}$$

Measurement update:

Now we use the fading factor derived in the previous step to update the measurement. First we calculate the predicted state error covariance as follows,

$$\hat{P}_{k+1|k} = \frac{\Lambda_{k+1}}{2n_x} \sum_{i=1}^{2n_x} X^*_{i,k+1|k} X^{*T}_{i,k+1|k} - \Lambda_{k+1} \hat{x}_{k+1|k} \hat{x}^T_{k+1|k} + Q_k \tag{7.43}$$

Then we factorize the error covariance matrix as $\hat{P}_{k+1|k} = S_{k+1|k} S_{k+1|k}$. Now we calculate the cubature points and we propagate the cubature points,

$$X_{i,k+1|k} = S_{k+1|k} \xi_i + \hat{x}_{k+1|k} \qquad i = 1, 2, ..., 2n_x \tag{7.44}$$

$$Y_{i,k+1|k} = h(X_{i,k+1|k}, u_{k+1}) \qquad i = 1, 2, ..., 2n_x \tag{7.45}$$

The predicted measurement estimate $\hat{y}_{k+1|k}$, the innovation covariance matrix $\hat{P}_{yy,k+1|k}$ and the cross-covariance matrix $\hat{P}_{xy,k+1|k}$ are as follows,

$$\hat{y}_{k+1|k} = \frac{1}{2n_x} \sum_{i=1}^{2n_x} Y_{i,k+1|k} \tag{7.46}$$

$$\hat{P}_{yy,k+1|k} = \frac{1}{2n_x} \sum_{i=1}^{2n_x} Y_{i,k+1|k} Y^T_{i,k+1|k} - \hat{y}_{k+1|k} \hat{y}^T_{k+1|k} + R_{k+1} \tag{7.47}$$

$$\hat{P}_{xy,k+1|k} = \frac{1}{2n_x} \sum_{i=1}^{2n_x} X_{i,k+1|k} Y^T_{i,k+1|k} - \hat{x}_{k+1|k} \hat{y}^T_{k+1|k} \tag{7.48}$$

Finally, we can derive the filter gain K_{k+1}, update the state estimation $\hat{x}_{k+1}$ and the upper bound of the state error covariance $\overline{P}_{k+1}$ as follows,

$$\begin{aligned} K_{k+1} = (1 + a_1(1 - \gamma_{k+1}))\lambda_{k+1} \hat{P}_{xy,k+1|k} [(1 + a_1(1 - \gamma_{k+1})) \hat{P}^T_{xy,k+1|k} \hat{P}^{-1}_{k+1|k} \hat{P}_{xy,k+1|k} \\ + (1 + a_2(1 - \gamma_{k+1}))R_{k+1} + (1 + a_1^{-1} + a_2^{-1})(1 - \gamma_{k+1})\delta I]^{-1} \end{aligned} \tag{7.49}$$

$$\hat{x}_{k+1} = \hat{x}_{k+1|k} + K_{k+1} \lambda_{k+1} (\overline{y}_{k+1} - \hat{y}_{k+1|k}) \tag{7.50}$$

$$\begin{aligned} \overline{P}_{k+1} = (1 + a_1(1 - \gamma_{k+1}))(I - K_{k+1} \lambda_{k+1} P^T_{xy,k+1|k} P^{-1}_{k+1|k}) \hat{P}_{k+1|k} \\ \times (I - K_{k+1} \lambda_{k+1} P^T_{xy,k+1|k} P^{-1}_{k+1|k})^T + (1 + a_2(1 - \gamma_{k+1}))\lambda_{k+1} K_{k+1} R_{k+1} K^T_{k+1} \\ + (1 - \gamma_{k+1})(1 + a_1^{-1} + a_2^{-1}) K_{k+1} \lambda_{k+1} \delta I K^T_{k+1} \end{aligned} \tag{7.51}$$

It is worth mentioning that the fading factor is designed to minimize the error covariance matrix in the presence of sudden changes in states. Using the following theorems, one can

show that by introducing the fading factor into the error covariance matrix and by properly tuning the triggering threshold, the boundedness of the error covariance matrix/estimation error can be guaranteed under some conditions.

Theorem 7.2: *Assuming that the system* (7.1) *and* (7.2) *is uniformly observable [23]. Recalling from Chapter 4,* (4.18)*, consider the following conditions are satisfied,*

$$\begin{aligned}
&\hat{q}_{min}I \leq \hat{Q}_k; Q_k \leq q_{max}I; r_{min}I \leq R_k \leq r_{max}I \\
&f_{min}^2 I \leq F_k F_k^T \leq f_{max}^2 I; \alpha_{min}^2 f_{min}^2 I \leq A_k A_k^T \leq \alpha_{max}^2 f_{max}^2 I \\
&h_{min}^2 I \leq H_k H_k^T \leq h_{max}^2 I; \beta_{min}^2 h_{min}^2 I \leq B_k B_k^T \leq \beta_{max}^2 h_{max}^2 I \\
&\beta_{min}^2 I \leq \beta_k \beta_k^T \leq \beta_{max}^2 I; \alpha_{min}^2 I \leq \alpha_k \alpha_k^T \leq \alpha_{max}^2 I
\end{aligned} \tag{7.52}$$

where $f_{min}, f_{max}, h_{min}, h_{max}, \beta_{min}, \beta_{max}, \alpha_{min}, \alpha_{max} \neq 0$ *, and* $r_{max}, q_{max}, \hat{q}_{min}, \hat{r}_{min} > 0$ *and all are real numbers.*

If the packet arrival probability has a lower bound,

$$\lambda > 1 - \frac{1}{\alpha_{max}^2 f_{max}^2 (1 + a_1(1-\gamma))},$$

where $\gamma := \lim_{N\to\infty} \frac{1}{N+1} \sum_{k=0}^{N} E(\gamma_k)$ is the average communication rate, the error covariance matrices will satisfy,

$$E[\overline{P}_{k+1}] \leq E[\hat{P}_{k+1|k}] \leq \overline{p} I, \tag{7.53}$$

where $\overline{p} > 0$.

Proof. We use the same procedure which is used in *Chapter 4* to prove this theorem. Recalling from *Chapter 3*, we have $\widetilde{x}_{k+1|k} = A_k \widetilde{x}_k + \omega_k$. According to this equation, $\widetilde{x}_{k+1|k}$, and the existence of an upper bound for the error covariance matrix $\overline{P}_k$, we have,

$$E[\hat{P}_{k+1|k}] \leq E[A_k \overline{P}_k A_k^T + Q_k] \tag{7.54}$$

Introducing the fading factor we have, $\overline{P}_k = \Lambda_k \overline{P}_k$. Substituting $\overline{P}_k$ and K_k from (7.51) and (7.49) in (7.54) we have,

$$\begin{aligned}
E[\hat{P}_{k+1|k}] \leq E\Bigg[& \Lambda_k A_k \Big(\hat{P}_{k|k-1} - (1 + a_1(1-\gamma_k)\Big) \lambda_k \hat{P}_{k|k-1} B_k^T \\
& \times \Big[\Big(1 + a_1(1-\gamma_k)\Big) B_k \hat{P}_{k|k-1} B_k^T + \Big(1 + a_2(1-\gamma_k)\Big) R_k \\
& + (1 + a_1^{-1} + a_2^{-1})(1-\gamma_k)\delta I \Big]^{-1} B_k \hat{P}_{k|k-1}) A_k^T + Q_k \Bigg]
\end{aligned} \tag{7.55}$$

Using this inequality $(A+B)^{-1} > A^{-1} - A^{-1}BA^{-1}$, and defining, $A = \Big(1 + a_1(1-\gamma_k)\Big) B_k \hat{P}_{k|k-1} B_k^T$, and $B = \Big(1 + a_2(1-\gamma_k)\Big) R_k + (1 + a_1^{-1} + a_2^{-1})(1-\gamma_k)\delta I$, according to

the bounds of the matrices in (7.52), we obtain,

$$E[\hat{P}_{k+1|k}] < \Lambda\alpha_{max}^2 f_{max}^2\Big(1 + a_1(1-\gamma)\Big)(1-\lambda)E[\hat{P}_{k|k-1}] + (\Lambda\frac{\lambda\alpha_{max}^2 f_{max}^2 r_{max}}{\beta_{min}^2 h_{min}^2} + \hat{q})I_n \tag{7.56}$$

where $r_{max} = max \parallel (1 + a_2(1-\gamma_k))R_k + (1 + a_1^{-1} + a_2^{-1})(1-\gamma_k)\delta I \parallel$. Assume that $E[\hat{P}_{1|0}] > 0$ and recursively, using an inductive method, the upper bound of the $\hat{P}_{k+1|k}$ can be achieved as follows,

$$E[\hat{P}_{k+1|k}] < \Bigg\{\Big[\alpha_{max}^2 f_{max}^2(1 + a_1(1-\gamma)(1-\lambda)\Big]^k \Lambda \parallel \hat{P}_{1|0} \parallel + (\Lambda\frac{\lambda\alpha_{max}^2 f_{max}^2 r_{max}}{\beta_{min}^2 h_{min}^2} + \hat{q}) \times \sum_{i=0}^{k-1}\Big[\alpha_{max}^2 f_{max}^2\Big(1 + a_1(1-\gamma)\Big)(1-\lambda)\Big]^i\Bigg\} I_n \tag{7.57}$$

Setting, $\overline{p} = max\Big\{\Lambda \parallel \hat{P}_{1|0} \parallel, \Lambda\frac{\lambda\alpha_{max}^2 f_{max}^2 r_{max}}{\beta_{min}^2 h_{min}^2} + \hat{q}\Big\}$ we have,

$$E[\hat{P}_{k+1|k}] < \overline{p}\sum_{i=0}^{k}\Big[\alpha_{max}^2 f_{max}^2(1 + a_1(1-\gamma))(1-\lambda)\Big]^i \tag{7.58}$$

The proposed filter converges when $\lambda > 1 - \frac{1}{\alpha_{max}^2 f_{max}^2(1+a_1(1-\gamma))}$. This completes the proof. ■

So, one can conclude that the fading factor may affect $\overline{p}$ while the lower bound of packet arrival rate is related to the average communication rate or the event-triggered threshold. Thus, by properly tuning the threshold we can guarantee the boundedness of the error covariance matrix/estimation error.

The boundedness of the DECKF under some conditions is studied as follows,

Theorem 7.3 : *Consider the nonlinear system* (7.1) *and* (7.2) *with event-triggered data transmission and the packet dropout. Assume that the condition is satisfied such that,*

$$p_{min} \leq \overline{P}_{k+1} \leq \hat{P}_{k+1|k} \leq p_{max}, \tag{7.59}$$

where p_{max} *and* $p_{min} > 0$ *. Assume that the initial prediction error,* $E[\|\widetilde{x}_{1|0}\|^2] \leq \varepsilon$*, is bounded, where* $\varepsilon > 0$*. Then the prediction error* $\widetilde{x}_{k+1|k}$ *and estimation error* $\widetilde{x}_k$ *are bounded in mean square sense.*

Proof. We use the same procedure which is used in *Chapter 4* to prove this theorem. First, recalling from *Chapter 4*, we introduce the following *Lemma 7.1* which is used in the proof.

Lemma 7.1: Assume that there is a stochastic process $V_k(\xi_k)$ with the following conditions:

$$\upsilon_{min}\|\xi_k\|^2 \leq V_k(\xi_k) \leq \upsilon_{max}\|\xi_k\|^2 \tag{7.60}$$

$$E[V_k(\xi_k)|\xi_{k-1}] - V_{k-1}(\xi_{k-1}) \leq \mu - \tau V_{k-1}(\xi_{k-1}) \tag{7.61}$$

where $\upsilon_{min}, \upsilon_{max}, \mu > 0$ and $0 < \tau \leq 1$ and all are real numbers. Then the stochastic process is exponentially bounded in mean square sense [24],

$$E[\|\xi_k\|^2] \leq \frac{\upsilon_{max}}{\upsilon_{min}} E[\|\xi_0\|^2](1-\tau)^k + \frac{\mu}{\upsilon_{min}} \sum_{i=1}^{k-1} (1-\tau)^i \tag{7.62}$$

Now, define the Lyapunov function as follows,

$$V_{k+1}(\widetilde{x}_{k+1|k}) = \widetilde{x}^T_{k+1|k} \hat{P}^{-1}_{k+1|k} \widetilde{x}_{k+1|k} \tag{7.63}$$

from the result of the Theorem 2 of [4], we have,

$$\upsilon_{min}\left\|\widetilde{x}_{k+1|k}\right\|^2 \leq V_{k+1}(\widetilde{x}_{k+1|k}) \leq \upsilon_{max}\left\|\widetilde{x}_{k+1|k}\right\|^2 \tag{7.64}$$

where $\upsilon_{min} = \frac{1}{p_{max}}$, and $\upsilon_{max} = \frac{1}{p_{min}}$. From (7.8) one can conclude that the lower and upper bounds of the $\hat{P}_{k+1|k}$, p_{min} and p_{max}, are affected by the fading factor.

The first condition of *Lemma 7.1* is satisfied. Now, we should find real numbers τ_k , and μ_k such that $0 < \tau_k < 1$ and $\mu_k > 0$, respectively. Using (7.13), the predicted state error covariance can be written as follows,

$$\begin{aligned} \hat{P}_{k+1|k} =& E\{\widetilde{x}_{k+1|k}\tilde{x}^T_{k+1|k}\} = \\ & \Big[A_k(I - \lambda_k K_k B_k)\Big]\hat{P}_{k|k-1}\Big[A_k(I - \lambda_k K_k B_k)\Big]^T + \hat{Q}_k \end{aligned} \tag{7.65}$$

where $\hat{Q}_k$ is $\Delta P_{k|k-1} + (A_k K_k)\lambda_k R_k (A_k K_k)^T + Q_k + (1-\gamma_k)E\Big\{O_k e_k^T S_k^T + S_k e_k O_k^T + S_k e_k e_k^T S^T\Big\}$, $O = \Big[A_k(I - K_k\lambda_k B_k)\widetilde{x}_{k|k-1} - A_k K_k \lambda_k \nu_k + \omega_k\Big]$, $S = (A_k K_k \lambda_k)$, and $\Delta P_{k|k-1}$ shows the difference between (7.43) and (7.65). (7.65) can be rewritten as follows,

$$\begin{aligned} \hat{P}_{k+1|k} = & \Big[A_k(I - K_k\lambda_k B_k)\Big]\Big\{\hat{P}_{k|k-1} + [A_k(I - K_k\lambda_k B_k)]^{-1} \\ & \times \hat{Q}_k[A_k(I - K_k\lambda_k B_k)]^{-T}\Big\}\Big[A_k(I - K_k\lambda_k B_k)\Big]^T \end{aligned} \tag{7.66}$$

setting $\Upsilon_k = \Big[A_k(I - K_k\lambda_k B_k)\Big]^T \hat{Q}_k^{-1}\Big[A_k(I - K_k\lambda_k B_k)\Big]$, and considering the characteristics of the matrix norm and the assumption in (7.52), we have,

$$\Upsilon_k \leq \frac{\Big[(\alpha_{max} f_{max})(1 + \lambda_k \beta_{max} h_{max}\hat{K})\Big]^2}{\hat{q}_{min}} \tag{7.67}$$

where the upper bound of $\hat{K}$ is,

$$\|K_k\| \leq [p_{max}\beta_{max}h_{max}][(\beta_{min}h_{min})^2 p_{min} + r_{min}]^{-1}$$

as we mentioned before the upper bounds of the $\hat{P}_{k+1|k}$, p_{min} and p_{max}, are affected by the fading factor which affect the upper bound of the filter gain $\hat{K}$. Using the matrix inverse laws and taking the inverse of Υ_k (or both sides of (7.67)) and substituting it in (7.66), it is possible to show that the following inequality is satisfied [24],

$$\Big[A_k(I - \lambda_k K_k B_k)\Big]^T \hat{P}^{-1}_{k+1|k}\Big[A_k(I - \lambda_k K_k B_k)\Big] \leq (1 - \tau_k)\hat{P}^{-1}_{k|k-1} \tag{7.68}$$

where

$$(1 - \tau_k) = \left[1 + \frac{\hat{q}_{min}}{\Big[(\alpha_{max}f_{max})(1 + \beta_{max}h_{max}\hat{K})\Big]^2 p_{max}}\right]^{-1} > 0 \tag{7.69}$$

It can be concluded that $0 < \tau_k < 1$ is always satisfied while the upper/lower bound value of p_{min} and p_{max} may be changed by introducing the fading factor. Substituting (7.13) into (7.63), the conditional expectation is as follows:

$$E\{V_{k+1}(\widetilde{x}_{k+1|k})|\widetilde{x}_{k+1|k}\} = \mu_k + \widetilde{x}^T_{k|k-1}\Big[A_k(I - \lambda_k K_k B_k)\Big]^T \hat{P}^{-1}_{k+1|k}\Big[A_k(I - \lambda_k K_k B_k)\Big]\widetilde{x}_{k|k-1} \tag{7.70}$$

where μ_k is as following,

$$\begin{aligned}
\mu_k &= E\Big\{\nu_k^T[A_k\lambda_k K_k]^T \hat{P}^{-1}_{k+1|k}A_k\lambda_k K_k\nu_k|\widetilde{x}_{k+1|k}\Big\} + E\Big\{\omega_k^T\hat{P}^{-1}_{k+1|k}\omega_k|\widetilde{x}_{k+1|k}\Big\} + (1 - \gamma_k) \\
&\times \Bigg(E\Big\{e_k^T\lambda_k^T K_k^T A_k^T\hat{P}^{-1}_{k+1|k}A_k\lambda_k K_k e_k|\widetilde{x}_{k+1|k}\Big\} + E\Big\{\widetilde{x}^T_{k|k-1}[A_k(I - \lambda_k K_k B_k)]^T\hat{P}^{-1}_{k+1|k} \\
&\times A_k\lambda_k K_k e_k|\widetilde{x}_{k+1|k}\Big\} - E\Big\{\nu_k^T[A_k\lambda_k K_k]^T\hat{P}^{-1}_{k+1|k}A_k\lambda_k K_k e_k|\widetilde{x}_{k+1|k}\Big\} \\
&+ E\Big\{\omega_k^T\hat{P}^{-1}_{k+1|k}A_k\lambda_k K_k e_k|\widetilde{x}_{k+1|k}\Big\} + E\Big\{e_k^T\lambda_k^T K_k^T A_k^T\hat{P}^{-1}_{k+1|k}[A_k(I - \lambda_k K_k B_k)]\widetilde{x}_{k|k-1}|\widetilde{x}_{k+1|k}\Big\} \\
&- E\Big\{e_k^T\lambda_k^T K_k^T A_k^T\hat{P}^{-1}_{k+1|k}A_{k}\lambda_k K_k\nu_k|\widetilde{x}_{k+1|k}\Big\} + E\Big\{e_k^T\lambda_k^T K_k^T A_k^T\hat{P}^{-1}_{k+1|k}\omega_k|\widetilde{x}_{k+1|k}\Big\}\Bigg)
\end{aligned} \tag{7.71}$$

both side of (7.71) are scalars. By applying the *Lemma 3.1*, the trace of μ_k is s follows,

$$\begin{aligned}
\mu_k \leq tr\Bigg\{&\Big([A_k\lambda_k K_k]^T\hat{P}^{-1}_{k+1|k}A_k\lambda_k K_k R_k\Big) + (\hat{P}^{-1}_{k+1|k}Q_k) + (1 - \gamma_k)\Big\{(\lambda_k^T K_k^T A_k^T\hat{P}^{-1}_{k+1|k}A_k\lambda_k K_k\delta I) \\
&+ a_3\Big([\hat{P}^{-1}_{k+1|k}A_{k}(I - \lambda_k K_k B_k)]\hat{P}_{k|k-1}[\hat{P}^{-1}_{k+1|k}A_k(I - \lambda_k K_k B_k)]^T\Big) + a_4(\hat{P}^{-1}_{k+1|k}Q_k[\hat{P}^{-1}_{k+1|k}]^T) \\
&+ a_5(\hat{P}^{-1}_{k+1|k}A_k\lambda_k K_k R_k[\hat{P}^{-1}_{k+1|k}A_{k}\lambda_k K_k]^T) + (a_3^{-1} + a_4^{-1} + a_5^{-1})(A_k\lambda_k K_k\delta I[A_k\lambda_k K_k]^T)\Bigg\}
\end{aligned} \tag{7.72}$$

where a_3, a_4, and a_5 are positive scalars. It is immediate that μ_k is positive and it has and upper bound μ_{max}. Insert (7.68) into (7.70), and considering (7.63), and (7.72) we have,

$$E[V_{k+1}(\widetilde{x}_{k+1|k})|\widetilde{x}_{k+1|k}] - V_k(\widetilde{x}_{k|k-1}) \leq \mu_{max} - \tau V_k(\widetilde{x}_{k|k-1}).$$

Thus, all of the conditions in *Lemma 7.1* are satisfied and the stochastic process, $\widetilde{x}_{k+1|k}$, is bounded in mean square sense. From the definition of $\widetilde{x}_{k+1|k}$, and the assumptions in (7.52), it is possible to show that the mean squared error of the estimation is as follows,

$$E\{\|\widetilde{x}_k\|^2\} \leq (f_{min}\alpha_{min})^{-2} E\{\left\|\widetilde{x}_{k+1|k}\right\|^2 + \|\omega_k\|^2\} \tag{7.73}$$

So the estimation error is upper bounded. It is worth mentioning that the upper bound value μ_{max} is affected by the event-triggered threshold and the fading factor which affects the upper bound (boundedness) of the $\widetilde{x}_{k+1|k}$ and $\widetilde{x}_{k+1}$. ■

It can be concluded that by introducing the fading factor to the error covariance matrix and by properly tuning the event-triggered threshold, the boundedness of the estimation error is guaranteed while the upper/lower bound of the inequalities may change.

7.3 Simulation Results

In this section we consider an illustrative example to verify the performance of the proposed STDECKF using the motion model of unmanned under water vehicle (UUV) adopted from [62]. A 4-DOF constant velocity kinematics model is used for tracking purposes as follows,

$$\begin{bmatrix} x \\ y \\ z \\ \psi \\ u \\ v \\ w \\ r \end{bmatrix}_k = \begin{bmatrix} x + uTcos(\psi) - vTsin(\psi) \\ y + uTsin(\psi) + vTcos(\psi) \\ z + wT \\ \psi + rT \\ u \\ v \\ w \\ r \end{bmatrix}_{k-1} + \omega_{k-1}, \tag{7.74}$$

where x, y, z and ψ show position and heading of UUV, and u, v, w, and r show the linear velocity and angular velocity of UUV. ω shows the noise of the system which is white noise, $\omega_k \sim N(0, Q)$, with zero mean and covariance $Q = \begin{bmatrix} 0.1 & 0.1 & 0.1 & 0.1 & 0.1 & 0.1 & 0.1 & 0.1 \end{bmatrix}$. The observation model is as follows,

$$\boldsymbol{z_k} = H\boldsymbol{x_k} + \nu_k, \tag{7.75}$$

where $\boldsymbol{x_k}$ and $\boldsymbol{z_k}$ are the state vector and the observation vector respectively. ν_k is observation noise which is white noise, $\nu_k \sim N(0, R)$, with zero mean and covariance

$R = \begin{bmatrix}10 & 10 & 10 & 10 & 10\end{bmatrix}$, and H is the observation matrix which can be defined as follows,

$$H = \begin{bmatrix} 0 & 0 & 1 & 0 & 0 & 0 & 0 & 0 \\ 0 & 0 & 0 & 1 & 0 & 0 & 0 & 0 \\ 0 & 0 & 0 & 0 & 1 & 0 & 0 & 0 \\ 0 & 0 & 0 & 0 & 0 & 1 & 0 & 0 \\ 0 & 0 & 0 & 0 & 0 & 0 & 1 & 0 \end{bmatrix} \tag{7.76}$$

Here we use three different scenarios to show the effectiveness of the proposed filter under different conditions, namely with different event-triggered mechanism threshold value and different packet dropout rate.

Scenario A:

In this scenario, we use the root mean square error (RMSE) to compare the performance of the STDECKF and the DECKF proposed in [60, 61] in the presence of different event-triggered threshold values and constant packet dropout rate.

The position RMSE is defined as follows,

$$RMSE_{(k)} = \sqrt{\frac{1}{N}\sum_{n=1}^{N}(x_k^n - \hat{x}_k^n)^2 + (y_k^n - \hat{y}_k^n)^2 + (z_k^n - \hat{z}_k{}^n)^2}$$

where, x_k^n, y_k^n, and z_k^n are the true, $\hat{x}_k^n$, $\hat{y}_k^n$, and $\hat{z}_k^n$ are the estimated states at the n-th Monte Carlo run, respectively. The initial values of x_0 and P_0 are as follows,

$$x_0 = \begin{bmatrix}2 & 3 & \pi/2 & \pi/3 & -1 & 3 & 1 & 1\end{bmatrix}$$

$$P_0 = \begin{bmatrix}0.01 & 0.01 & 0.01 & 0.01 & 0.1 & 0.1 & 0.1 & 0.1\end{bmatrix}$$

. The initial state estimate $\hat{x}_0$ is chosen randomly from $N(x_0, P_0)$ in each run. We make 20 independent Monte Carlo runs.

Figure 7.1.(a),(b),(c) show the RMSE results of the proposed STDECKF and the DECKF proposed in [60, 61] for different event-triggered threshold of $\lambda = 1, 2, 4$ and the constant packet dropout rate of 10%, respectively. The RMSE results show that although by increasing the event-triggered threshold value, the estimation quality will be degraded but the proposed STDECKF has better state estimation performance compared to DECEKF for the same triggering condition.

In addition, Figure 7.2 shows the trajectory tracking and RMSE results of the proposed STDECKF under the same condition. Note that the for different event-triggering threshold values of $\lambda = 1, 2, 4$, the number of data transmission reduces from 1000 (without event-triggered mechanism) to 900, 660 and 440, respectively. Comparison between tracking results shows that by properly tuning the event-triggered mechanism threshold, a desired

estimation quality can be achieved while communication rate is reduced dramatically.

Scenario B: To guarantee the performance improvement of the proposed filter, we repeat the simulation for other different conditions. Different from scenario A, now we consider that the packet dropout rates are different and the triggering threshold value is constant. We compare the RMSE results of STDECKF and DECKF in the presence of different packet dropout rate of 10% and 20% and the constant event-triggered threshold of $\lambda = 2$. Figure 7.1.(d) shows the comparison results. The RMSE results show the performance improvement of the proposed filter compared to the previously proposed DECKF for different conditions.

Scenario C: As we mentioned before, the developed STDECKF has better performance in the presence of sudden changes in the states compared to the previously proposed filters. So, to show the effectiveness of the proposed filter in tracking of the abrupt changes in the states, we repeat the simulation using STDECKF and DECKF in the presence of event-triggered threshold $\lambda = 1$ and the packet dropout rate 10%. As the Figure 7.3 shows, the proposed STDECKF can effectively track the abrupt motion of the state of the target compared to the previously proposed DECKF and the estimation trajectory converges better to the real trajectory.

So from the simulation results one can conclude that: (a) the proposed STDECKF has better performance and less estimation error in the presence of different conditions compared to the previously proposed filter, (b) the proposed filter has a good estimation quality despite the abrupt changes in the states, and (c) like the DECKF, the proposed STDECKF can achieve a desired estimation quality with less communication rate by properly choosing an event-triggered threshold value.

7.4 Summary

In this work, a strong tracking discrete-time event-triggered cubature Kalman filter for nonlinear dynamic system with packet dropout is developed. We show that the proposed filter reduces the amount of data transmission between the measuring sensors and the remote state estimator and it has better performance compared to other filters in the presence of sudden changes in the sates. The event-triggered mechanism reduces the amount of data transferring between the sensors and the remote cubature Kalman filter and we show that by choosing a proper event-triggered threshold and properly tuning the threshold of the

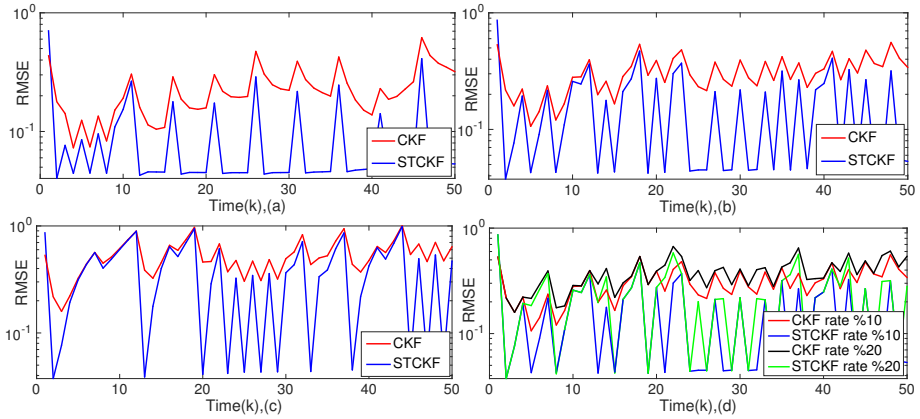

Figure 7.1: RMSE results of STDECKF and DECKF with different Event-Triggered Threshold (ETT) and Packet Dropout Rate (PDR), (a) ETT=1, PDR= 10%, (b) ETT=2, PDR=10%,(c) ETT=4, PDR=10%, (d) ETT=2, PDR=10% and 20%

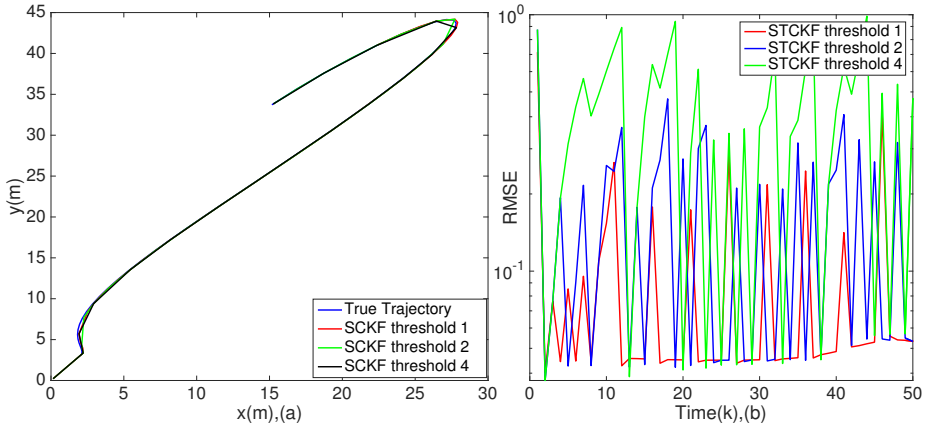

Figure 7.2: Trajectory tracking and RMSE results for event-triggered threshold of $\lambda = 1, 2, 4$, and packet dropout rate of 10%. (a)Trajectory tracking, (b)RMSE results

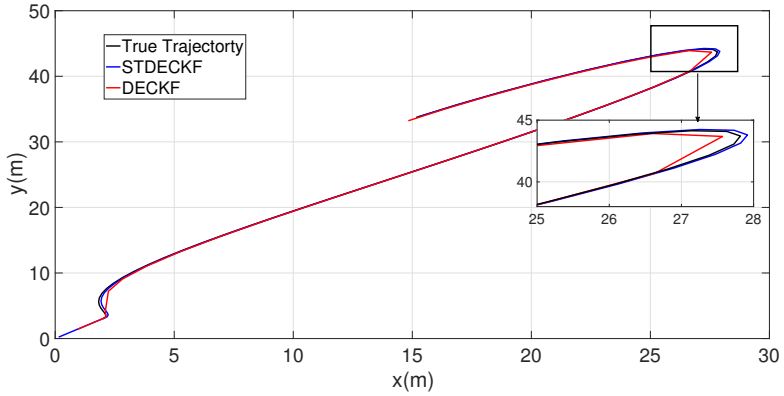

Figure 7.3: Trajectory tracking of the proposed STDECKF and the DECKF in [60]

event-triggered mechanism with respect to the rate of the packet dropout, the proposed method can guarantee the boundedness of the state estimation error, covariance and the stochastic stability of the system. Simulation results show the effectiveness of the proposed technique and we compared the improvement in the results to the DECKF.

Chapter 8

Strong Tracking Event-Triggered Filter with One Step Randomly Delayed Measurements

In this chapter, we focus on the filtering problem of the nonlinear discrete-time systems in the presence of one step randomly delayed measurements and sudden changes in the states. A new filtering algorithm, a strong tracking discrete-time event-triggered cubature Kalman filter (STDECKF), is proposed to send the data from the nonlinear system to the remote state estimator when some specific condition, namely triggering condition, is satisfied to reduce the amount of data transmissions in the communication channels and to reduce the estimation errors when there is randomly delay and/or sudden changes in the states during data transmission.

Based on the principle of extended orthogonality, the proposed strong tracking filter uses a time-variant fading factor to reduce the effect of the delayed measurement and the abrupt changes in the states on the the state prediction error covariance to improve the performance of cubature Kalman filter and to reduce the estimation errors.

The remainder of this chapter is as follows. Section 8.1, presents the problem statement. Section 8.2 introduces the derivation procedure of the strong tracking DECKF in the presence of delayed measurement and sudden changes in the states while the algorithm is described in Section 8.3. Simulation results are shown in Section 8.4 to show the effectiveness of the proposed filter.

8.1 Problem formulation

Consider the nonlinear discrete-time system model and the nonlinear measurement model as follows,

$$x_{k+1} = f(x_k, u_k) + \omega_k, \tag{8.1}$$

$$z_{k+1} = h(x_{k+1}) + \nu_{k+1}, \tag{8.2}$$

where $x_k \in \mathbb{R}^{n_x}$ is the state vector, and $z_k \in \mathbb{R}^{n_z}$ is the measurement vector. Other parameters are defined in *Chapter 2*. Assume that our system works under event-triggered mechanism and the communication channels are not perfect which might lead to delay in the transferring of the measurements to the remote state estimator. So, recalling from *Chapter 3*, the current transmitted measurement (8.3) is defined as follows,

$$\bar{z}_k = z_k + (1 - \gamma_k)(\overline{z} - z_k) \tag{8.3}$$

where z_k is the current measurement and $\overline{z}$ is the last sent measurement. $\bar{z}_k$ is the current transmitted measurement after the triggering condition is satisfied. In addition recalling from *Chapter 5*, if we have one-step randomly delay in the communication channels, the measurement is defined as follows,

$$y_{k+1} = (1 - \sigma_{k+1})z_{k+1} + \sigma_{k+1}z_k, \tag{8.4}$$

where, $\{\sigma_k; k > 1\}$ is a sequence of uncorrelated Bernoulli random variables which can be 0 or 1 with,

$$\begin{aligned} &p(\sigma_k = 1) = E[\sigma_k] = p_k, \\ &p(\sigma_k = 0) = 1 - E[\sigma_k] = 1 - p_k, \\ &E[(\sigma_k - p_k)^2] = (1 - p_k)p_k. \end{aligned} \tag{8.5}$$

8.2 Derivation of the STDECKF with One-Step Randomly Delayed Measurements

The proposed filter in *Chapter 5* with one-step randomly delayed measurement depends upon the past measurement data and it may lead to divergence in the state estimation in the presence of delay and sudden changes in the states. So, in this section, a suboptimal fading factor, Λ_k should be derived to modify the previous proposed discrete-time event-triggered cubature Kalman filter to eliminate the effect of past data on the estimation process and to have a strong tracking estimation of the states of the nonlinear system in

the presence of sudden changes in the states and one step randomly delayed measurement. Recalling from *Chapter 7*, the Λ_k is introduced as follows to the error covariance matrix,

$$\hat{P}_k = \Lambda_{k+1}\hat{P}_k \tag{8.6}$$

also, the predicted error covariance matrix is modified as follows,

$$\hat{P}_{k+1|k} = \Lambda_{k+1}A_k\hat{P}_kA_k^T + Q_k \tag{8.7}$$

where, $A_k = \alpha_k F_k$. $F_k = \frac{\partial f(x)}{\partial x}|_{x=\hat{x}_k}$ is the Jacobian matrix, $\alpha_k = \text{diag}(\alpha_{1,k}, \alpha_{2,k}, ..., \alpha_{n_x k})$ is unknown diagonal matrix representing the error incurred in neglecting the higher order terms of the Taylor series. In the following, we derive the Λ_{k+1}. Note that the linearization with first order approximation is implemented to facilitate the following discussion.

Theorem 8.1: *Consider the system* (8.1) *and* (8.2) *with the defined current transmitted measurement* (8.3). *Assume that the measurement are transmitted with one randomly delay through the communication channels* (8.4). *Using the cubature Kalman filter state estimator designed in Theorem 7.1, the sub-optimal time-varying fading factor can be calculated by*

$$\Lambda_{k+1} = max\{1, \frac{tr[N_{k+1}]}{tr[M_{k+1}]}\} \tag{8.8}$$

M_{k+1} *and* N_{k+1} *are as follows,*

$$M_{k+1} = m_1\Lambda_{k+1}\Big((1-p_{k+1})B_{k+1}A_k\hat{P}_kA_k^TB_{k+1}^T + m_3p_{k+1}B_k\hat{P}_kB_k^T\Big) \tag{8.9}$$

$$\begin{aligned} N_{k+1} &= m_1\lambda_{k+1}V_{k+1}^0 - p_{k+1}B_k\hat{P}^{x\nu}{}_k - p_{k+1}(B_k\hat{P}^{x\nu}{}_k)^T - m_2(1-p_{k+1})R_{k+1} - m_4p_{k+1}\hat{P}^{\nu\nu}{}_k \\ &\quad - m_5(1-p_{k+1})(1-\gamma_{k+1})\delta - m_6p_{k+1}(1-\gamma_k)\delta - p_{k+1}(1-p_{k+1})(\hat{z}_k - \hat{z}_{k+1|k}) \\ &\quad \times (\hat{z}_k - \hat{z}_{k+1|k})^T - m_1(1-p_{k+1})B_{k+1}Q_kB_{k+1}^T \end{aligned} \tag{8.10}$$

where, $m_1 = (1 + a_1(1-\gamma_{k+1}) + a_5(1-\gamma_k))$, $m_2 = (1 + a_2(1-\gamma_{k+1}) + a_6(1-\gamma_k))$, $m_3 = (1 + a_3(1-\gamma_{k+1}) + a_7(1-\gamma_k))$, $m_4 = (1 + a_4(1-\gamma_{k+1}) + a_8(1-\gamma_{k+1}))$, $m_5 = (1+a_1^{-1}+a_2^{-1}+a_3^{-1}+a_4^{-1})$, $m_6 = (1+a_5^{-1}+a_6^{-1}+a_7^{-1}+a_8^{-1})$. $a_1 - a_8$ are arbitrary positive parameters. Recalling from *Chapter 7*, $B_{k+1} = \beta_{k+1}H_{k+1}$ and $H_{k+1} = \frac{\partial h(x)}{\partial x}|_{x=\hat{x}_{k+1|k}}$ is the Jacobian matrix. $\beta_{k+1} = \text{diag}(\beta_{1,k+1}, \beta_{2,k+1}, ..., \beta_{n_y k+1})$ is unknown diagonal matrix representing the error incurred in neglecting the higher order terms of the Taylor series respectively. In addition, $B_k = \beta_k H_k$ and $H_k = \frac{\partial h(x)}{\partial x}|_{x=\hat{x}_k}$. $V_{k+1}^0 = E\{\widetilde{y}_{k+1|k}\widetilde{y}_{k+1|k}^T\}$ is the residual covariance.

Proof. First recalling from *Chapter 5*, $x_{k+1} - \hat{x}_{k+1|k}$ can be written as follows by using (5.8) and (5.10),

$$x_{k+1} - \hat{x}_{k+1|k} = A_k(x_k - \hat{x}_k) + \omega_k. \tag{8.11}$$

Substituting (8.11) in (5.35) results in (8.12) as follows,

$$\widetilde{y}_{k+1|k} = \Big[(1-\sigma_{k+1})B_{k+1}A_k + \sigma_{k+1}B_k\Big](x_k - \hat{x}_k) + (1-\sigma_{k+1})B_{k+1}\omega_k + (1-\sigma_{k+1})\nu_{k+1} + \sigma_{k+1}(\nu_k - \hat{\nu}_k) + (\sigma_{k+1} - p_{k+1})\Big[h_k(\hat{x}_k) - h_{k+1}(\hat{x}_{k+1|k}) + \hat{\nu}_k\Big] + g(e_k) \tag{8.12}$$

where $e_k = (\overline{z} - z_k)$ and $g(e_k) = (1-\sigma_{k+1})(1-\gamma_{k+1})e_{k+1} + \sigma_{k+1}(1-\gamma_k)e_k$. Using a similar derivation method yields,

$$\begin{aligned}\widetilde{y}_{k+1+j|k+j} = &\Big[(1-\sigma_{k+j+1})B_{k+j+1}A_{k+j} + \sigma_{k+j+1}B_{k+j}\Big](x_{k+j} - \hat{x}_{k+j}) + (1-\sigma_{k+j+1})B_{k+j+1} \\ &\times \omega_{k+j} + (1-\sigma_{k+j+1})\nu_{k+j+1} + \sigma_{k+j+1}(\nu_{k+j} - \hat{\nu}_{k+j}) + (\sigma_{k+j+1} - p_{k+j+1}) \\ &\Big[h_{k+j}(\hat{x}_{k+j}) - h_{k+j+1}(\hat{x}_{k+j+1|k+j}) + \hat{\nu}_{k+j}\Big] + g(e_{k+j})\end{aligned} \tag{8.13}$$

Note that the initial state x_0, ν_k and ω_k which generate the states and the observations are mutually independent. Considering these and the $\widetilde{y}_{k+1|k}$ features into account (*Remark 7.1*), to obtain the fading factor one should use the extended orthogonality principle, $E\{\widetilde{y}_{k+j+1|k+j}\widetilde{y}^T_{k+1|k}\} = 0$. So, by substituting (8.12) and (8.13) in $E\{\widetilde{y}_{k+j+1|k+j}\widetilde{y}^T_{k+1|k}\}$, we have,

$$E\Big\{\widetilde{y}_{k+1+j|k+j}\widetilde{y}^T_{k+1|k}\Big\} = \Big[(1-p_{k+j+1})B_{k+j+1}A_{k+j} + p_{k+j+1}B_{k+j}\Big]E\Big\{(x_{k+j} - \hat{x}_{k+j})\widetilde{y}^T_{k+1|k}\Big\} \tag{8.14}$$

Recalling from *Chapter 3*, the event-triggered state estimation can be written as follows,

$$\hat{x}_{k+1} = \hat{x}_{k+1|k} + K_{k+1}(\overline{y}_{k+1} - \hat{y}_{k+1|k}) \tag{8.15}$$

using (8.15) we can derive, $x_{k+j} - \hat{x}_{k+j}$ as the following,

$$\begin{aligned}x_{k+j} - \hat{x}_{k+j} &= x_{k+j} - \hat{x}_{k+j|k+j-1} - K_{k+j}\Big(\widetilde{y}_{k+j|k+j-1} - (1-\gamma_{k+j})e_{k+j}\Big) \\ &= \Big\{\Big[I - (1-\sigma_{k+j})B_{k+j}K_{k+j}\Big]A_{k+j-1} - K_{k+j}\sigma_{k+j}B_{k+j-1}\Big\} \\ &\times (x_{k+j-1} - \hat{x}_{k+j-1}) + \omega_{k+j-1} - K_{k+j}\Big\{(1-\sigma_{k+j})B_{k+j}\omega_{k+j-1} \\ &+ (1-\sigma_{k+j})\upsilon_{k+j} + \sigma_{k+j}(\upsilon_{k+j-1} - \hat{\upsilon}_{k+j-1}) + (\sigma_{k+j} - p_{k+j}) \\ &\times \Big[h_{k+j-1}(\hat{x}_{k+j-1}) - h_{k+j}(f_{k+j-1}(\hat{x}_{k+j-1})) + \hat{\upsilon}_{k+j-1}\Big] + g(e_{k+j-1}) \\ &- (1-\gamma_{k+j})e_{k+j}\Big\}\end{aligned} \tag{8.16}$$

substituting (8.16) in (8.14) and considering the features of $\widetilde{y}_{k+1|k}$ into account (*Remark*

7.1), we have the following,

$$E\{\widetilde{y}_{k+1+j|k+j}\widetilde{y}^T_{k+1|k}\} = \Big[(1-p_{k+j+1})B_{k+j+1}A_{k+j} + p_{k+j+1}B_{k+j}\Big]\Bigg\{\Big[I-(1-p_{k+j}) \times B_{k+j}K_{k+j}\Big]A_{k+j-1} - K_{k+j}p_{k+j}B_{k+j}\Bigg\} \times E\Big\{[x_{k+j-1}-\hat{x}_{k+j-1}]\widetilde{y}^T_{k+1|k}\Big\} \tag{8.17}$$

From (8.14) and (8.17) and using the iteration, we have,

$$E\{\widetilde{y}_{k+1+j|k+j}\widetilde{y}^T_{k+1|k}\} = \Big[(1-p_{k+j+1})B_{k+j+1}A_{k+j} + p_{k+j+1}B_{k+j}\Big] \prod_{i=2}^{j}\Bigg\{\Big[I-(1-p_{k+i})B_{k+i}K_{k+i}\Big]A_{k+i-1} - K_{k+i}p_{k+i}B_{k+i}\Bigg\} \times E\Bigg\{[x_{k+1}-\hat{x}_{k+1}]\widetilde{y}^T_{k+1|k}\Bigg\} \tag{8.18}$$

considering (8.15), $E\Big\{[x_{k+1}-\hat{x}_{k+1}]\widetilde{y}^T_{k+1|k}\Big\}$ of (8.18) can be written as follows,

$$\begin{aligned} E\Big\{[x_{k+1}-\hat{x}_{k+1}]\widetilde{y}^T_{k+1|k}\Big\} &= E\Bigg\{\Big[x_{k+1}-\hat{x}_{k+1|k}-K_{k+1}(\widetilde{y}_{k+1|k}-(1-\gamma_{k+1})e_{k+1})\Big]\widetilde{y}^T_{k+1|k}\Bigg\} \\ &= E\Big\{[x_{k+1}-\hat{x}_{k+1|k}]\widetilde{y}^T_{k+1|k}\Big\} - K_{k+1}E\{\widetilde{y}_{k+1|k}\widetilde{y}^T_{k+1|k}\} \\ &= \hat{P}^{xy}_{k+1|k} - K_{k+1}E\{\widetilde{y}_{k+1|k}\widetilde{y}^T_{k+1|k}\} = \hat{P}^{xy}_{k+1|k} - K_{k+1}V^0_{k+1}, \end{aligned} \tag{8.19}$$

where $V^0_{k+1} = E\{\widetilde{y}_{k+1|k}\widetilde{y}^T_{k+1|k}\}$ is the covariance of the residual which can be estimated as follows,

$$V^0_{k+1} = \begin{cases} \widetilde{y}_{1|0}\widetilde{y}^T_{1|0} & k=0 \\ \frac{\rho V^0_k + \widetilde{y}_{k+1|k}\widetilde{y}^T_{k+1|k}}{1+\rho} & k \geq 1 \end{cases} \tag{8.20}$$

Recalling from *Chapter 5*, by substituting (5.19) and (5.20) in (5.18) we have,

$$\hat{P}^{xy}_{k+1|k} = (1-p_{k+1})\hat{P}_{k+1|k}B^T_{k+1} + p_{k+1}(A_k\hat{P}_kB^T_k + A_k\hat{P}^{x\nu}_k) \tag{8.21}$$

where, $P^{\nu\nu}_{k+1} = E[\tilde{\nu}_{k+1}\tilde{\nu}^T{}_{k+1}|Y_{k+1}]$, $P^{x\nu}_{k+1} = E[\tilde{x}_{k+1}\tilde{\nu}^T{}_{k+1}|Y_{k+1}]$. So, substituting (8.21) in (8.19) we have,

$$\begin{aligned} E\Big\{[x_{k+1}-\hat{x}_{k+1|k+1}]\widetilde{y}^T_{k+1|k}\Big\} &= (1-p_{k+1})\hat{P}_{k+1|k}B^T_{k+1} + p_{k+1}(A_k\hat{P}_kB^T_k + A_kP^{x\nu}_k) \\ &\quad - K_{k+1}V^0_{k+1} \end{aligned} \tag{8.22}$$

From (5.31), the CKF gain with one step randomly delayed measurement can be written as follows,

$$\begin{aligned}K_{k+1} &= m_1\Big[(1-p_{k+1})B_{k+1}\hat{P}_{k+1|k} + p_{k+1}A_k\hat{P}_kB_{k+1}^T + p_{k+1}A_k\hat{P}^{x\nu}{}_k\Big] \\ &\times \Big[p_{k+1}B_k\hat{P}^{x\nu}{}_k + p_{k+1}(B_k\hat{P}^{x\nu}{}_k)^T + m_1(1-p_{k+1})B_{k+1}\hat{P}_{k+1|k}B_{k+1}^T + m_2(1-p_{k+1})R_{k+1} \\ &+ m_3p_{k+1}B_k\hat{P}_kB_k^T + m_4p_{k+1}\hat{P}^{\nu\nu}{}_k + m_5(1-p_{k+1})(1-\gamma_{k+1})\delta \\ &+ m_6p_{k+1}(1-\gamma_k)\delta + p_{k+1}(1-p_{k+1})(\hat{z}_k-\hat{z}_{k+1|k})(\hat{z}_k-\hat{z}_{k+1|k})^T\Big]^{-1}\end{aligned} \tag{8.23}$$

Substituting (8.23) in (8.22) we have,

$$\begin{aligned}E\Big\{[x_{k+1}-\hat{x}_{k+1}]\widetilde{y}_{k+1|k}^T\Big\} &= \Big\{(1-p_{k+1})\hat{P}_{k+1|k}B_{k+1}^T + p_{k+1}(A_k\hat{P}_kB_k^T + A_k\hat{P}_k^{x\nu})\Big\}\Big\{I \\ &- m_1V_{k+1}^0\Big[p_{k+1}B_k\hat{P}^{x\nu}{}_k + p_{k+1}(B_k\hat{P}^{x\nu}{}_k)^T + m_1(1-p_{k+1}) \\ &\times B_{k+1}\hat{P}_{k+1|k}B_{k+1}^T + m_2(1-p_{k+1})R_{k+1} + m_3p_{k+1}B_k\hat{P}_kB_k^T \\ &+ m_4p_{k+1}\hat{P}^{\nu\nu}{}_k + m_5(1-p_{k+1})(1-\gamma_{k+1})\delta + m_6p_{k+1}(1-\gamma_k)\delta \\ &+ p_{k+1}(1-p_{k+1})(\hat{z}_k-\hat{z}_{k+1|k})(\hat{z}_k-\hat{z}_{k+1|k})^T\Big]^{-1}\Big\}\end{aligned} \tag{8.24}$$

substituting (8.24) in (8.18) yields to the following,

$$\begin{aligned}E\{\widetilde{y}_{k+1+j|k+j}\widetilde{y}_{k+1|k}^T\} &= \Big[(1-p_{k+j+1})B_{k+j+1}A_{k+j} + p_{k+j+1}B_{k+j}\Big] \\ &\times \prod_{i=2}^{j}\Big\{[I-(1-p_{k+i})B_{k+i}K_{k+i}]A_{k+i-1} - K_{k+i}p_{k+i}B_{k+i}\Big\} \\ &\times \Big\{(1-p_{k+1})\hat{P}_{k+1|k}B_{k+1}^T + p_{k+1}(A_k\hat{P}_kB_k^T + A_k\hat{P}_k^{x\nu})\Big\} \\ &\times \Big\{I - m_1V_{k+1}^0[p_{k+1}B_k\hat{P}^{x\nu}{}_k + p_{k+1}(B_k\hat{P}^{x\nu}{}_k)^T + m_1(1-p_{k+1}) \\ &\times B_{k+1}\hat{P}_{k+1|k}B_{k+1}^T + m_2(1-p_{k+1})R_{k+1} + m_3p_{k+1}B_k\hat{P}_kB_k^T \\ &+ m_4p_{k+1}\hat{P}^{\nu\nu}{}_k + m_5(1-p_{k+1})(1-\gamma_{k+1})\delta + m_6p_{k+1}(1-\gamma_k)\delta \\ &+ p_{k+1}(1-p_{k+1})(\hat{z}_k-\hat{z}_{k+1|k})(\hat{z}_k-\hat{z}_{k+1|k})^T]^{-1}\Big\}\end{aligned} \tag{8.25}$$

A proper fading factor should be chosen such that the following equality holds,

$$I - m_1 V_{k+1}^0 \Bigg[p_{k+1} B_k \hat{P}^{x\nu}{}_k + p_{k+1} (B_k \hat{P}^{x\nu}{}_k)^T + m_1 (1-p_{k+1}) B_{k+1} \hat{P}_{k+1|k} B_{k+1}^T + m_2 (1-p_{k+1}) R_{k+1} + m_3 p_{k+1} B_k \hat{P}_k B_k^T + m_4 p_{k+1} \hat{P}^{\nu\nu}{}_k + m_5 (1-p_{k+1})(1-\gamma_{k+1})\delta + m_6 p_{k+1}(1-\gamma_k)\delta + p_{k+1}(1-p_{k+1})(\hat{z}_k - \hat{z}_{k+1|k})(\hat{z}_k - \hat{z}_{k+1|k})^T \Bigg]^{-1} = 0 \tag{8.26}$$

(8.26) can be written as follows,

$$m_1 \Big((1-p_{k+1}) B_{k+1} \hat{P}_{k+1|k} B_{k+1}^T + m_3 p_{k+1} B_k \hat{P}_k B_k^T \Big) = m_1 V_{k+1}^0 - p_{k+1} B_k \hat{P}^{x\nu}{}_k - p_{k+1} (B_k \hat{P}^{x\nu}{}_k)^T - m_2 (1-p_{k+1}) R_{k+1} - m_4 p_{k+1} \hat{P}^{\nu\nu}{}_k - m_5 (1-p_{k+1})(1-\gamma_{k+1})\delta - m_6 p_{k+1}(1-\gamma_k)\delta - p_{k+1}(1-p_{k+1})(\hat{z}_k - \hat{z}_{k+1|k})(\hat{z}_k - \hat{z}_{k+1|k})^T \tag{8.27}$$

Substituting (8.6) and (8.7) in (8.27) we have,

$$m_1 \Lambda_{k+1} \Big((1-p_{k+1}) B_{k+1} A_k \hat{P}_k A_k^T B_{k+1}^T + m_3 p_{k+1} B_k \hat{P}_k B_k^T \Big) = m_1 V_{k+1}^0 - p_{k+1} B_k \hat{P}^{x\nu}{}_k - p_{k+1} (B_k \hat{P}^{x\nu}{}_k)^T - m_2 (1-p_{k+1}) R_{k+1} - m_4 p_{k+1} \hat{P}^{\nu\nu}{}_k - m_5 (1-p_{k+1})(1-\gamma_{k+1})\delta - m_6 p_{k+1}(1-\gamma_k)\delta - p_{k+1}(1-p_{k+1})(\hat{z}_k - \hat{z}_{k+1|k})(\hat{z}_k - \hat{z}_{k+1|k})^T - m_1 (1-p_{k+1}) B_{k+1} Q_k B_{k+1}^T \tag{8.28}$$

The trace of both side of (8.28) can be calculated as follows,

$$tr \Bigg[m_1 \Lambda_{k+1} \Big((1-p_{k+1}) B_{k+1} A_k \hat{P}_k A_k^T B_{k+1}^T + m_3 p_{k+1} B_k \hat{P}_k B_k^T \Big) \Bigg] = tr \Bigg[m_1 V_{k+1}^0 - p_{k+1} B_k \hat{P}^{x\nu}{}_k - p_{k+1} (B_k \hat{P}^{x\nu}{}_k)^T - m_2 (1-p_{k+1}) R_{k+1} - m_4 p_{k+1} \hat{P}^{\nu\nu}{}_k - m_5 (1-p_{k+1})(1-\gamma_{k+1})\delta - m_6 p_{k+1}(1-\gamma_k)\delta - p_{k+1}(1-p_{k+1})(\hat{z}_k - \hat{z}_{k+1|k})(\hat{z}_k - \hat{z}_{k+1|k})^T - m_1 (1-p_{k+1}) B_{k+1} Q_k B_{k+1}^T \Bigg] \tag{8.29}$$

It follows that (8.29) is equivalent to $tr[\Lambda_{k+1} M_{k+1}] = tr[N_{k+1}]$, where M_{k+1} and N_{k+1} are as following,

$$M_{k+1} = m_1 \Lambda_{k+1} \Big((1-p_{k+1}) B_{k+1} A_k \hat{P}_k A_k^T B_{k+1}^T + m_3 p_{k+1} B_k \hat{P}_k B_k^T \Big) \tag{8.30}$$

$$N_{k+1} = m_1 V^0_{k+1} - p_{k+1} B_k \hat{P}^{x\nu}{}_k - p_{k+1}(B_k \hat{P}^{x\nu}{}_k)^T - m_2(1-p_{k+1})R_{k+1} - m_4 p_{k+1}\hat{P}^{\nu\nu}{}_k$$
$$- m_5(1-p_{k+1})(1-\gamma_{k+1})\delta - m_6 p_{k+1}(1-\gamma_k)\delta - p_{k+1}(1-p_{k+1})(\hat{z}_k - \hat{z}_{k+1|k})$$
$$\times (\hat{z}_k - \hat{z}_{k+1|k})^T - m_1(1-p_{k+1})B_{k+1}Q_k B^T_{k+1} \tag{8.31}$$

and the fading factor can be obtained by,

$$\Lambda_{k+1} = \frac{tr[N_{k+1}]}{tr[M_{k+1}]} \tag{8.32}$$

which completes the proof. ■

8.3 Strong Tracking Event-Triggered Cubature Kalman Filter with Random one-step delay algorithm

In this section, we summarize the strong tracking event-triggered cubature Kalman filter in the presence of delay. In the previous sections, we use linearization to facilitate the fading factor derivation. Linearization of nonlinear systems add some errors which may lead to divergence in the tracking results. To overcome this problem, we derive the equivalent STF using cubature Kalman filter. Suppose that $\hat{P}^l_{k+1|k}$ is the predicted state error covariance matrix before introducing fading factor, then based on $\hat{P}^{xz}_{k+1|k} = \hat{P}_{k+1|k}B^T_{k+1}$, one can derive the following,

$$B_{k+1} = (\hat{P}^{xz^l}_{k+1|k})^T(\hat{P}^l_{k+1|k})^{-1}, \tag{8.33}$$

where $\hat{P}^{xz^l}_{k+1|k}$ is the cross-covariance matrix without fading factor. Now, we summarize STDECKF algorithm which uses the time update and measurement update steps to update the old states when it receives the new measurements.

Time Update

Step 1: First we factorize $\hat{P}^a{}_k = S^a_k(S^a_k)^T$, then we calculate the cubature points as follows,

$$X_{i,k} = \begin{bmatrix}(\xi^x_{i,k})^T & (\xi^\nu_{i,k})^T\end{bmatrix}^T = S^a_k\xi_i + \hat{x}^a{}_k, \tag{8.34}$$

where $i = 1, 2, ..., L$ and $L = 2(n+m)$ is the dimensionality of the augmented state $x_k{}^a$. n and m are the dimensionality of the states and measurement noise, respectively. $\xi^x_{i,k}$ shows the cubature points corresponding to the state and $\xi^\nu_{i,k}$ shows the cubature points corresponding to the measurement noise respectively.

Step 2: We propagate the cubature points as follows,

$$X^{*x}_{i,k+1|k} = f(\xi^x_{i,k}, u_k), \tag{8.35}$$

$$\Upsilon^{*x}_{i,k+1|k} = h(\xi^x_{i,k}, u_k), \tag{8.36}$$

where $i = 1, 2, ..., L$.

Step 3: We estimate the predicted states and predicted state error covariance as follows,

$$\hat{x}_{k+1|k} = \frac{1}{2L}\sum_{i=1}^{2L} X^{*x}_{i,k+1|k}, \tag{8.37}$$

$$\hat{P}^{l}_{k+1|k} = \frac{1}{2L}\sum_{i=1}^{2L} X^{*x}_{i,k+1|k}(X^{*x}_{i,k+1|k})^T - \hat{x}_{k+1|k}\hat{x}^T_{k+1|k} + Q_k, \tag{8.38}$$

Now it is time to calculate the fading factor as follows,

Calculate fading factor

Step 1: Factorize $\hat{P}^{l}_{k+1|k} = S^{l}_{k+1|k}S^{l^T}_{k+1|k}$, and calculate the cubature points as follows,

$$X^{l}_{i,k+1|k} = S^{l}_{k+1|k}\xi_i + \hat{x}_{k+1|k}, \tag{8.39}$$

where $i = 1, 2, ..., 2n$.

Step 2: We propagate the cubature points for $i = 1, 2, ..., 2n$ as follows,

$$Y^{l}_{i,k+1|k} = h(X^{l}_{i,k+1|k}, u_{k+1}). \tag{8.40}$$

Step 3: Now it is time to calculate $\hat{z}^{l}_{k+1|k}$, $\hat{P}^{zz,l}_{k+1|k}$, $\hat{z}^{l}_{k}$, $\hat{P}^{zz,l}_{k}$, $\hat{P}^{xz,l}_{k+1|k}$, and $\hat{P}^{xz,l}_{k+1,k}$ as follows,

$$\hat{z}^{l}_{k+1|k} = \frac{1}{2n}\sum_{i=1}^{2n} Y^{l}_{i,k+1|k}, \tag{8.41}$$

$$\hat{P}^{zz,l}_{k+1|k} = \frac{1}{2n}\sum_{i=1}^{2n} Y^{l}_{i,k+1|k}Y^{l^T}_{i,k+1|k} - \hat{z}^{l}_{k+1|k}\hat{z}^{l^T}_{k+1|k} + R_{k+1}, \tag{8.42}$$

$$\hat{z}^{l}_{k} = \frac{1}{2L}\sum_{i=1}^{2L}(\Upsilon^{*x}_{i,k+1|k} + \xi^{\nu}_{i,k}), \tag{8.43}$$

$$\hat{P}^{zz,l}_{k} = \frac{1}{2L}\sum_{i=1}^{2L}(\Upsilon^{*x}_{i,k+1|k} + \xi^{\nu}_{i,k})(\Upsilon^{*x}_{i,k+1|k} + \xi^{\nu}_{i,k|k})^T - \hat{z}^{l}_{k}(\hat{z}^{l}_{k})^T, \tag{8.44}$$

$$\hat{P}^{xz,l}_{k+1|k} = \frac{1}{2n}\sum_{i=1}^{2n} X^{l}_{i,k+1|k}Y^{l^T}_{i,k+1|k} - \hat{x}^{l}_{k+1|k}\hat{z}^{l^T}_{k+1|k}, \tag{8.45}$$

$$\hat{P}^{xz,l}_{k+1,k} = \frac{1}{2L}\sum_{i=1}^{2L} X^{*x}_{i,k+1|k}(\Upsilon^{*x}_{i,k+1|k} + \xi^{\nu}_{i,k})^T - \hat{x}^{l}_{k+1|k}\hat{z}^{l^T}_{k+1|k}. \tag{8.46}$$

Step 4: Calculate the measurement and measurement noise means and the covariances by the following equations,

$$\hat{\nu}^{l}{}_{k+1} = K^{\nu}_{k+1}\tilde{y}_{k+1|k} \tag{8.47}$$

$$K_{k+1}^{\nu,l} = P_{k+1|k}^{\nu y,l}(\overline{P}_{k+1|k}^{yy,l})^{-1} \tag{8.48}$$

$$\hat{P}_{k+1|k}^{\nu y,l} = (1-p_{k+1})(1+(1-\gamma_{k+1}))R_{k+1} \tag{8.49}$$

$$\hat{P}_{k+1}^{\nu\nu,l} = R_{k+1} - K_{k+1}^{\nu,l}\overline{P}_{k+1|k}^{yy,l}(K_{k+1}^{\nu,l})^T \tag{8.50}$$

$$\begin{aligned}\overline{P}_{k+1|k}^{yy,l} = (1-p_{k+1})\Big((1+b_1(1-\gamma_{k+1}))\hat{P}_{k+1|k}^{zz,l} + p_{k+1}(\hat{z}^l{}_{k+1|k} - \hat{z}^l{}_k)(\hat{z}^l{}_{k+1|k} - \hat{z}^l{}_k)^T \\ + (1+b_1^{-1})(1-\gamma_k)\delta\Big) + p_{k+1}\Big((1+b_2(1-\gamma_k))\hat{P}_k^{zz,l} + p_{k+1}(1-\gamma_k)(1+b_2^{-1})\delta\Big)\end{aligned} \tag{8.51}$$

Step 5: Calculate N_{k+1} and M_{k+1} to find the fading factor as follows,

$$\begin{aligned}N_{k+1} = {} & m_1\lambda_{k+1}V_{k+1}^0 - p_{k+1}(\hat{P}_{k+1|k}^{xz,l})^T(\hat{P}_{k+1|k}^l)^{-1}\hat{P}^{x\nu,l}{}_k - p_{k+1}((\hat{P}_{k+1|k^l}^{xz})^T(\hat{P}_{k+1|k}^l)^{-1})^T \\ & - m_2(1-p_{k+1})R_{k+1} - m_4p_{k+1}\hat{P}^{\nu\nu,l}{}_k - m_5(1-p_{k+1})(1-\gamma_{k+1})\delta - m_6p_{k+1}(1-\gamma_k)\delta \\ & - p_{k+1}(1-p_{k+1})(\hat{z}^l{}_k - \hat{z}^l{}_{k+1|k})(\hat{z}^l{}_k - \hat{z}^l_{k+1|k})^T - m_1(1-p_{k+1})(\hat{P}_{k+1|k}^{xz,l})^T(\hat{P}_{k+1|k}^l)^{-1} \\ & \times Q_k((\hat{P}_{k+1|k}^{xz,l})^T(\hat{P}_{k+1|k}^l)^{-1})^T\end{aligned} \tag{8.52}$$

$$\begin{aligned}M_{k+1} = {} & m_1\Lambda_{k+1}((1-p_{k+1})((\hat{P}_{k+1|k}^{zz,l}) - R_{k+1} - (\hat{P}_{k+1|k}^{xz,l})^T(\hat{P}_{k+1|k}^l)^{-1}Q_k(\hat{P}_{k+1|k}^l)^{-1}(\hat{P}_{k+1|k}^{xz,l}) \\ & + m_3p_{k+1}(\hat{P}_k^{zz,l} - (\hat{P}_{k|k-1}^{xz,l})^T(\hat{P}_{k|k-1}^l)^{-1}\hat{P}_k^{x\nu,l} - ((\hat{P}_{k|k-1}^{xz,l})^T(\hat{P}_{k|k-1}^l)^{-1}\hat{P}_k^{x\nu,l})^T - \hat{P}_k^{\nu\nu,l})\end{aligned} \tag{8.53}$$

Step 6: Calculate fading factor,

$$\Lambda_{k+1} = max\{1, \frac{tr[N_{k+1}]}{tr[M_{k+1}]}\} \tag{8.54}$$

Measurement Update

Step 1:Calculate the predicted state error covariance as follows,

$$\hat{P}_{k+1|k} = \frac{\Lambda_{k+1}}{2L}\sum_{i=1}^{2L} X_{i,k+1|k}^{*x}(X_{i,k+1|k}^{*x})^T - \Lambda_{k+1}\hat{x}_{k+1|k}\hat{x}_{k+1|k}^T + Q_k \tag{8.55}$$

Step 2: We repeat step 1 to step 4 of the calculating fading factor part again to derive $\hat{z}_{k+1|k}$, $\hat{P}_{k+1|k}^{zz}$, $\hat{z}_k$, $\hat{P}_k^{zz}$, $\hat{P}_{k+1|k}^{xz}$, $\hat{P}_{k+1,k}^{xz}$, $\hat{\nu}_{k+1}$, K_{k+1}^{ν}, $\hat{P}_{k+1|k}^{\nu y}$, and $\hat{P}_{k+1}^{\nu\nu}$.

Step 3: We derive the event-triggered cubature Kalman gain $K_{k+1} = S(T)^{-1}$, where

$$S = m_1(1-p_{k+1})(\hat{P}_{k+1|k}^{xz})^T(\hat{P}_{k+1|k})^{-1}\hat{P}_{k+1|k} + p_{k+1}\hat{P}_{k+1,k}^{xz}, \tag{8.56}$$

and,

$$\begin{aligned}T = {} & p_{k+1}(\hat{P}_{k|k-1}^{xz})^T(\hat{P}_{k|k-1})^{-1}\hat{P}^{x\nu}{}_k + p_{k+1}((\hat{P}_{k|k-1}^{xz})^T(\hat{P}_{k|k-1})^{-1}\hat{P}^{x\nu}{}_k)^T + m_1(1-p_{k+1}) \\ & \times(\hat{P}_{k+1|k}^{xz})^T(\hat{P}_{k+1|k})^{-1}\hat{P}_{k+1|k}((\hat{P}_{k+1|k}^{xz})^T(\hat{P}_{k+1|k})^{-1})^T + m_2(1-p_{k+1})R_{k+1} \\ & + m_3p_{k+1}(\hat{P}_{k|k-1}^{xz})^T(\hat{P}_{k+1|k})^{-1}\hat{P}_k((\hat{P}_{k|k-1}^{xz})^T(\hat{P}_{k|k-1})^{-1})^T + m_4p_{k+1}\hat{P}^{\nu\nu}{}_k \\ & + m_5(1-p_{k+1})(1-\gamma_{k+1})\delta + m_6p_{k+1}(1-\gamma_k)\delta + p_{k+1}(1-p_{k+1})(\hat{z}_k - \hat{z}_{k+1|k})(\hat{z}_k - \hat{z}_{k+1|k})^T\end{aligned} \tag{8.57}$$

Step 4: We estimate the updated state as follows,

$$\hat{x}_{k+1} = \hat{x}_{k+1|k} + K_{k+1}\lambda_{k+1}(\overline{y}_{k+1} - \hat{y}_{k+1|k}) \tag{8.58}$$

Step 5: The state error covariance is as follows,

$$\begin{aligned}
\overline{P}_{k+1} &= \Big(1 + a_1(1-\gamma_{k+1}) + a_5(1-\gamma_k)\Big)\Big(I - K_{k+1}(1-p_{k+1})(\hat{P}^{xz}_{k+1|k})^T(\hat{P}_{k+1|k})^{-1}\Big)\hat{P}_{k+1|k} \\
&\times \Big(I - K_{k+1}(1-p_{k+1})(\hat{P}^{xz}_{k+1|k})^T(\hat{P}_{k+1|k})^{-1}\Big)^T - p_{k+1}\Big(\hat{P}^{xz}_{k+1,k}K^T_{k+1} + K_{k+1}(\hat{P}^{xz}_{k+1,k})^T\Big) \\
&+ \Big(1 + a_2(1-\gamma_{k+1}) + a_6(1-\gamma_k)\Big)(1-p_{k+1})K_{k+1}R_{k+1}(K_{k+1})^T + \Big(1 + a_3(1-\gamma_{k+1}) \\
&+ a_7(1-\gamma_k)\Big)p_{k+1}\Big(K_{k+1}(\hat{P}^{xz}_{k|k-1})^T(\hat{P}_{k|k-1})^{-1}\hat{P}_k(K_{k+1}(\hat{P}^{xz}_{k|k-1})^T(\hat{P}_{k|k-1})^{-1})^T + \Big(1 \\
&+ a_4(1-\gamma_{k+1}) + a_8(1-\gamma_k)\Big)K_{k+1}\hat{P}^{\nu\nu}{}_k K^T_{k+1} + (1-p_{k+1})K_{k+1}(\hat{z}_k - \hat{z}_{k+1|k})(\hat{z}_k - \hat{z}_{k+1|k})^T \\
&\times K^T_{k+1}\Big) + (1 + a_1^{-1} + a_2^{-1} + a_3^{-1} + a_4^{-1})(1-p_{k+1})K_{k+1}(1-\gamma_{k+1})K_{k+1}\delta K^T_{k+1} \\
&+ p_{k+1}\Big((1 + a_5^{-1} + a_6^{-1} + a_7^{-1} + a_8^{-1})(1-\gamma_k)K_{k+1}\delta K^T_{k+1} + K_{k+1}\hat{P}^{xz^T}_{k|k-1}(\hat{P}_{k|k-1})^{-1}\hat{P}^{x\nu}_k \\
&\times K^T_{k+1} + K_{k+1}(\hat{P}^{xz^T}_{k|k-1}(\hat{P}_{k|k-1})^{-1}\hat{P}^{x\nu}{}_k)^T K^T_{k+1}\Big)
\end{aligned} \tag{8.59}$$

8.4 Simulation results

In this section the effectiveness of the proposed method is illustrated by simulation results. We consider the motion model of the UUV illustrated in *Chapter 7*, and we study the performance of the proposed STDECKF in the presence of one step randomly delayed measurement. The purpose of presenting this simulation result is to show the effectiveness of the proposed filter in the presence of sudden changes in the states compared to the previously proposed DECKF in [60, 61].

We use the same motion model of the UUV considered in *Chapter 7* [62],

$$\begin{bmatrix} x \\ y \\ z \\ \psi \\ u \\ v \\ w \\ r \end{bmatrix}_k = \begin{bmatrix} x + uTcos(\psi) - vTsin(\psi) \\ y + uTsin(\psi) + vTcos(\psi) \\ z + wT \\ \psi + rT \\ u \\ v \\ w \\ r \end{bmatrix}_{k-1} + \omega_{k-1}, \tag{8.60}$$

$$\boldsymbol{z_k} = H\boldsymbol{x_k} + \nu_k, \tag{8.61}$$

where x, y, z and ψ show position and heading of UUV, and u, v, w, and r show the linear velocity and angular velocity of UUV. ω shows the noise of the system which is white noise,

$\omega_k \sim N(0, Q)$, with zero mean and covariance $Q = \begin{bmatrix}0.1 & 0.1 & 0.1 & 0.1 & 0.1 & 0.1 & 0.1 & 0.1\end{bmatrix}$. H is the observation matrix which can be defined as follows,

$$H = \begin{bmatrix}0 & 0 & 1 & 0 & 0 & 0 & 0 & 0\\ 0 & 0 & 0 & 1 & 0 & 0 & 0 & 0\\ 0 & 0 & 0 & 0 & 1 & 0 & 0 & 0\\ 0 & 0 & 0 & 0 & 0 & 1 & 0 & 0\\ 0 & 0 & 0 & 0 & 0 & 0 & 1 & 0\end{bmatrix} \tag{8.62}$$

Recalling from *Chapter 7*, the initial values of x_0 and P_0 are considered as follows,

$$x_0 = \begin{bmatrix}2 & 3 & \pi/2 & \pi/3 & -1 & 3 & 1 & 1\end{bmatrix}$$

$$P_0 = \begin{bmatrix}0.01 & 0.01 & 0.01 & 0.01 & 0.1 & 0.1 & 0.1 & 0.1\end{bmatrix}$$

The initial state estimate $\hat{x}_0$ is chosen randomly from $N(x_0, P_0)$ in each run. We use the root mean square error (RMSE) to compare the performance of the proposed filters. The position RMSE is defined as follows,

$$RMSE_{(k)} = \sqrt{\frac{1}{N}\sum_{n=1}^{N}(x_k^n - \hat{x}_k^n)^2 + (y_k^n - \hat{y}_k^n)^2 + (z_k^n - \hat{z}_k{}^n)^2}$$

where, x_k^n, y_k^n, and z_k^n are the true, $\hat{x}_k^n$, $\hat{y}_k^n$, and $\hat{z}_k^n$ are the estimated states at the n-th Monte Carlo run, respectively. twi different scenarios to show the effectiveness of the proposed filter under different conditions, namely with different event-triggered mechanism threshold value and different delay probabilities.

In the first scenario, we compare the RMSE results of the proposed STDECKF with DECKF under different event-triggering threshold of 1 and 2. Note that the delay probability is the same for the both filters which are considered 10%. We make 20 independent Monte Carlo runs. As the Figure 8.1 shows, the proposed STDECKF has better performance in both conditions compared to the DECKF. To confirm the performance of the proposed filter under general condition, we repeat the simulation results for other scenario. In this scenario, we consider that the triggering threshold is kept constant during the simulation while we consider two different values for the delay probability. The simulation results demonstrate the performance improvement of the proposed filter.

8.5 Summary

A new nonlinear filter algorithm for the filtering problems of high dimensional nonlinear systems under the event-triggered protocol with one-step delay in measurement is proposed.

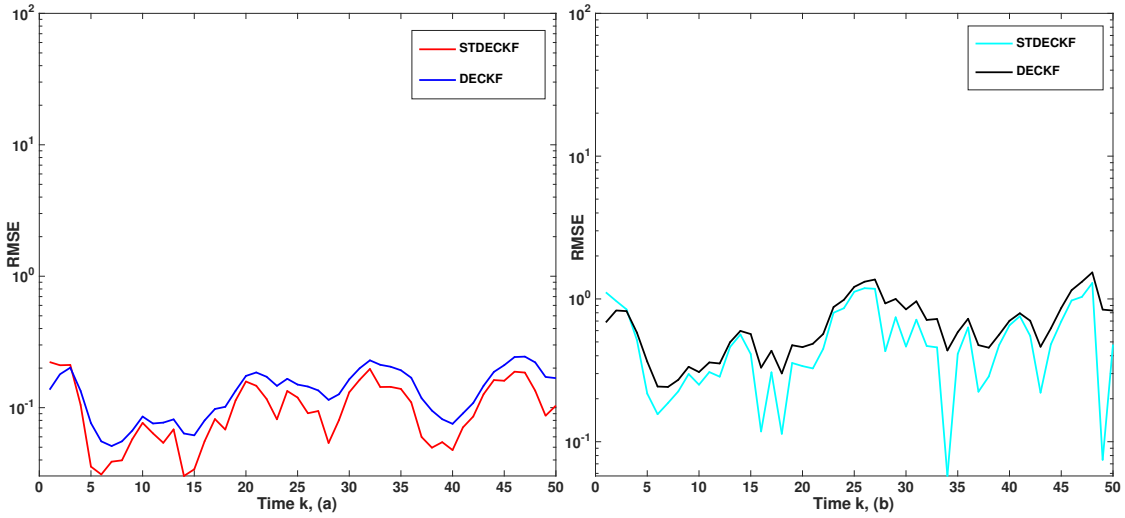

Figure 8.1: RMSE results of STDECKF and DECKF with different Event-Triggered Threshold (ETT) and constant Delay, (a) ETT=1, Delay =10%(b) ETT=2, Delay=10%

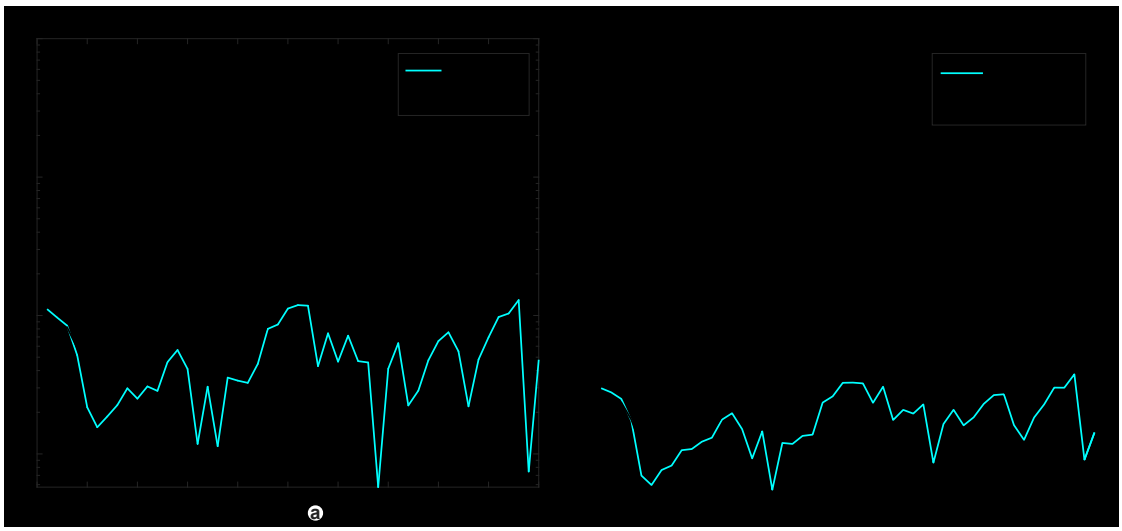

Figure 8.2: RMSE results of STDECKF and DECKF (a) Event-Triggered Threshold=2 and Delay=10% (b) Event-Triggered Threshold=2 and Delay=5%

We show when the communication channels are not perfect, the triggered measurements are transferred with delay and the state estimator can not be updated in realtime and the previous data affects on filtering process. In addition, when there are sudden changes in the states, the filter gain has a delay to be updated and the estimation results can not track the real states perfectly. So, we develop a new strong tracking CKF and we derive a fading factor to modify the error covariance matrix to reduce the measurement delay and sudden changes affects on the estimation results.

Simulation results show that the proposed STDECKF has better performance and less estimation error in the presence of different conditions compared to the previously proposed filter.

Chapter 9

Conclusions and Future Work

State estimation is currently an active area of research and a significant body of work has been already produced. For linear time invariant systems, Kalman filters constitute the gold standard and an essential tool used to estimate the system state while minimizing the variance of the estimation error. In general, however, the systems used in many applications are nonlinear and proper nonlinear filters should be developed for the estimation purposes.

In addition, in the classical estimation formulation, information from the sensors is directly available for processing. Over the past few years, however, systems and control have become reliant upon wireless communication networks to establish the interconnection of various system components in which the communication resources need to be carefully managed.

In this thesis, we investigate the development of the nonlinear event-based state estimator problem under different scenarios to solve the mentioned issues. The primary goal of this thesis is the reduction in data transmission between different components of the networked system while maintaining comparable performance under different condition. We consider a discrete-time nonlinear system with additive Gaussian noise, and look at the problem of sequentially estimating the state using Bayes's rule. In this context, the posterior density cannot be described by a finite number of statistics, and an approximation must be made. We develop cubature Kalman filters, which offer an attractive, numerically stable solution with low computational effort, to the nonlinear state estimation problem. The developed CKF assumes that the predictive density of the joint state-measurement random variable is Gaussian. In this way, the optimal Bayesian filter reduces to the problem of how to compute various multi-dimensional Gaussian weighted moment integrals whose integrands are all of the form nonlinear function$\times$Gaussian density which can be done efficiently using a cubature rule.

The outcomes of our research attempts are further summarized as follows:

- First, under a Gaussian assumption on the conditional distribution of the state in the presence of event-triggered mechanism, the event-based state estimator, discrete-time event-triggered cubature Kalman filter, for high dimensional nonlinear system with high nonlinearities is proposed. The proposed filter uses the "send on delta" event-triggered mechanism which reduces the number of feedback communication between sensors and the estimator. In addition, it reduces the measurement transmission between the sensors and the remote state estimator while it can ensure the estimation performance.

- Second, the effect of the packet dropout during the data transmission in the communication channels on the state estimation is investigated. We showed that if the packet dropout rate has an upper bound, the error covariance matrix would be bounded. The boundedness of the estimation error is also studied and it is shown that by properly choosing an event-triggered mechanism regarding to the packet dropout rate, one can achieve a bounded estimation error.

- Third, we assume that the sensor exchange the data via imperfect communication channels and the measurements are randomly delayed by one sampling time. We showed that the previous data affects the performance of the filter so we develop a new filtering algorithm to derive the filter gain which reduces the delay measurement affects on the filtering process and make the estimation error bounded.

- Fourth, we consider sudden changes in the states. Based on the "extended orthogonality principle", we derive the strong tracking filter and we adjusted the error covariance matrices in real time to have a better estimation performance. We showed that the upper bound of the estimation error would be affected by the sudden changes of the states and the packet dropout rate, so by properly adjusting the fading factor, and the event-triggered threshold we could have convergence in the estimation.

- Finally, we study the scenario in which the nonlinear system states have abrupt changes and the data is transferring through the communication channels with one-step randomly delay. So, the affect of the delayed measurements are considered in the designing of the new filter and the fading factor is introduced to reduce the affect of the delay measurements and sudden changes in the states on the performance of

the filter. The proposed filter reduces the estimation error while it needs less data communication.

The research results, provided in this thesis can be extended and pursued in the following areas:

- ***Event Triggered Square Root Cubature Kalman Filter:*** In each update cycle of the CKF, some operations such as matrix inversion, matrix square rooting may destroy the properties of the covariance matrix and the CKF may stop running. Square root Cubature Kalman filter has recently proposed to enhances the numerical stability, guarantees positive definiteness of the state covariance, and increases accuracy, which has high practicability. Providing an even-triggered square root CKF considering delay and packet dropouts in the communication channels which guarantee the boundedness of the estimation error can be an interesting area of research.

- ***Event-triggered CKF under cyber physical attack:*** As we mentioned before, recently there have been a growing interest towards cyber-physical systems (CPSs). CPSs are used in many applications such as autonomous vehicles, supply chains, power and transportation networks. Many of these applications are safety-critical which has triggered considerable attention to networked systems in the presence of attacks. Considering the effect of attack on the designing of the event-triggered CKF is an opening problem.

Bibliography

[1] "CPS Vision Statement: National Science Foundation," 2015. [Online]. Available: https://www.nitrd.gov/nitrdgroups/images/6/6a/Cyber/Physical/Systems/(CPS) /Vision/Statement.pdf

[2] B. D. O. Anderson and J. B. Moore, Optimal Filtering. Eaglewood Cliffs, NJ: Prentice-Hall, 1979.

[3] S. J. Julier, J. K. Ulhmann, and H. F. Durrant-Whyte, "A new method for nonlinear transformation of means and covariances in filters and estimators," *IEEE Trans On Autom. Control*, Vol. 45, No. 3, pp. 472-482, Mar. 2000.

[4] S. Kluge, K. Reif, and M. Brokate, "Stochastic stability of the extended Kalman filter with intermittent observations", *IEEE Trans On Autom. Control*, Vol. 55, No. 2, pp. 514-518, 2010.

[5] L. Li, D. Yu, H. Yang and C. Yan,"UKF for nonlinear systems with event-triggered data transmission and packet dropout", *3rd International Conference on Informative and Cybernetics for Computational Social Systems (ICCSS)*, pp. 37-42, Jinzhou, 2016.

[6] L. Li, Y. Xia, "UKF-based nonlinear filtering over sensor networks with wireless fading channel", *Information Sciences*, Vol. 316, pp. 132-147, 2015.

[7] S. Sarkka, Bayesian filtering and smoothing, Cambridge University Press, 2013.

[8] I. Arasaratnam, and S. Haykin, "Cubature Kalman Filters", *IEEE Trans. on Autom. Control*, Vol. 54, No. 6, pp. 1254-1269, 2009.

[9] D. Zhang, Z. Deng, B. Wang and M. Fu, "The application of Square-Root Cubature Kalman Filter in the SINS/CNS integrated navigation system", *Proc. Chinese Guidance, Navigation and Control Conference (CGNCC)*, pp. 2331-2335, Nanjing, 2016.

[10] M. T. Sabet, H. M. Daniali, A. Fathi, E. Alizadeh, "Identification of an Autonomous Underwater Vehicle Hydrodynamic Model Using the Extended, Cubature, and Transformed Unscented Kalman Filter", it IEEE Journal of Oceanic Engineering, No. 99, pp.1-11, 2017.

[11] G. R. Gopinath and S. P. Das,"Speed and position sensorless control of Interior Permanent Magnet Synchronous Motor using Square-root Cubature Kalman filter with joint parameter estimation", *IEEE Int. Conf. on Power Electronics*, Drives and Energy Systems (PEDES) , pp. 1-5, 2016.

[12] T. R. Wanasinghe, G. K. I. Mann, R. G. Gosine, "Stability analysis of the discrete-time cubature Kalman filter", *Proc. Conf. Dec. Control (CDC)* , pp. 5031 - 5036, Japan. 2015.

[13] B. Xua, P. Zhanga, H. Wenb, X. Wuc, "Stochastic stability and performance analysis of Cubature Kalman Filter", *Neurocomputing*, Vol. 186, pp.218-227, 2016.

[14] S. Li, Z. Li, J. Li, Q. Wang, Z. Song, Z. Chen, Y. Sheng, X. Liu, and Y. Liu, " Event-based Cubature Kalman Filter for Smart Grid Subject to Communication Constraint", *IFAC*, Vol. 50, pp. 49-54, 2017.

[15] D. Shi, L. Shi, T. Chen, "Event-Based State Estimation: A Stochastic Perspective", *Springer*, 2016.

[16] J. Hu, Z. Wang, H. Gao and L. K. Stergioulas, "Extended Kalman filtering with stochastic nonlinearities and multiple missing measurements", *Automatica*, voL 48, no. 9, pp. 2007-2015, 2012.

[17] G. Wang, J. Chen, J. Sun, "Stochastic stability of extended filtering for non-linear systems with measurement packet losses", *IET Control Theory*, Vol. 7, Iss. 17, pp. 2048-2055, 2013.

[18] Li L, Xia Y, "Stochastic stability of the unscented Kalman filter with intermittent observations", *Automatica* pp. 978-981,2012.

[19] B. Sinopoli, L. Schenato, M. Franceschetti, K. Poolla, M. I. Jordan, and S. S. Sastry, "Kalman Filtering With Intermittent Observations," *IEEE Trans on Autom. Control*, Vol. 49, No. 9, 2004.

[20] D. Shi, T. Chen, L. Shi, "An event-triggered approach to state estimation with multiple point and set-valued measurements," *Automatica*, Vol. 50, No. 6, pp. 1641-1648, 2014.

[21] K. P. B. Chandra, D.W. Gu, and I. Postlethwaite, "Cubature kalman filter based localization and mapping," *IFAC* , pp. 2121-2125, Sep 2011.

[22] I. Arasaratnam, S. Haykin, and T. R. Hurd, "Cubature kalman filtering for continuous-discrete systems: theory and simulations," *IEEE Transactions on Signal Processing*, vol. 58, no. 10, pp. 4977-4993, 2010.

[23] X. Liu, L. Li, Z. Li, T. Fernando and H. H. C. Iu,"Stochastic Stability Condition for the Extended Kalman Filter With Intermittent Observations," *IEEE Transactions on Circuits and Systems II: Express Briefs* , Vol. 64, No. 3, pp. 334-338, 2017.

[24] K. Reif , and R. Unbehauen, "Stochastic stability of the discrete-time extended Kalman filter", *IEEE Trans on Autom. Control*, Vol. 44, pp.714-728, 1999.

[25] W. Li, Y. Jia, and J. Du, "Event-triggered Kalman consensus filter over sensor networks," *IET Control Theory Appl.*, Vol. 10, No. 1, pp. 103-110, Jan. 2016.

[26] D.Shi,T.Chen, and L.Shi,"Event-based state estimation of linear dynamical systems: Communication rate analysis," *American Control Conference*, pp. 4665-4670, Jun. 2014.

[27] K. Astrom and B. Bernhardsson,"Comparison of periodic and event based sampling for first-order stochastic systems," *14th world congress of IFAC*, 1999.

[28] P. Tabuada, "Event-triggered real-time scheduling of stabilizing control task," *IEEE Trans. Autom. Control*, vol. 52, no. 9, pp. 1680-1685, 2007.

[29] W. Heemels, M. Donkers, and A. Teel, "Periodic event-triggered control for linear systems," *IEEE Trans. Autom. Control*, vol. 58, no. 4, pp. 847-861, 2013.

[30] D. Shi,1, T. Chen, L. Shi, "Event-triggered maximum likelihood state estimation," *Automatica*, 247-254, 2014.

[31] D. Han, J. Wu, S. Weerakkody, B.Sinopoli, L. Shi, "Stochastic Event-Triggered Sensor Schedule for Remote State Estimation," *IEEE transaction on Automatic control* , Vol.60, No. 10, Oct 2015.

[32] J. Sijs, M. Lazar, "Event Based State Estimation With Time Synchronous Updates," *IEEE transaction on Automatic control*, Vol.57, No. 10, Oct 2012.

[33] J. Sijs, B. Noack, U. Hanebeck, "Event-based state estimation with negative information". *In Proceedings of the 16th international conference on information fusion*, pp 2192-2199, 2013.

[34] M. Rabi, G. V. Moustakides, and J. S. Baras, "Adaptive sampling for linear state estimation," *SIAM Journal on Control and Optimization* , Vol. 50, No 2, pp. 672-702, 2012.

[35] L. Li, M. Lemmon and X. Wang, "Event-triggered state estimation in vector linear processes," *Proc. 2010 Amer. Control Conf*, pp. 2138-2143, Baltimore, MD, 2010.

[36] D. H. Zhou, Y. G. Xi, and Z. J. Zhang, "A suboptimal multiple fading extended Kalman Filter," *Chinese Journal of Automation*, Vol. 4, No. 2, pp. 145-152, 1992.

[37] Q.Liu, C. Huang and L. Peng"Distributed consensus strong tracking filter for wireless sensor networks with model mismatches," *International Journal of Distributed Sensor Networks*, Vol. 13, No. 11, 2017.

[38] H.Liu and W.Wu, "Strong tracking spherical simplex-radial cubature kalman filter for maneuvering target tracking," *Sensors*, Vol 17, 2017.

[39] Z.Li, W.Yang, D.Ding "Strong tracking cubature kalman filter for real-time orbit determination for impulse maneuver satellite," *Proceedings of the 36th Chinese Control Conference*, July 26-28, 2017, Dalian, China.

[40] M.Gao, H. Zhang, Y.Zhou, and B.Zhang, "Ground maneuvering target tracking based on the strong tracking and the cubature Kalman filter algorithms," *Journal of Electronic Imaging* Vol. 25, No.2, 2016

[41] H.Yang, H.Gao, and X. Liu, "Strong tracking filtering algorithm of randomly delayed measurements for nonlinear systems," *Hindawi Publishing Corporation Mathematical Problems in Engineering*, 2015.

[42] Z. Li, P. Pan, D. Gao, D. Zhao, "An improved unscented kalman filter based on STF for nonlinear systems," *2nd International Congress on Image and Signal Processing*, Tianjin, China, 2009.

[43] D.-J. Jwo and S.-Y. Lai, "Navigation integration using the fuzzy strong tracking unscented Kalman filter," *Journal of Navigation*, Vol. 62, No. 2, pp. 303-322, 2009.

[44] M. Boutayeb and D. Aubry, "A strong tracking extended Kalman observer for nonlinear discrete-time systems, *IEEE Transactions on Automatic Control*, Vol. 44,No. 8, pp. 1550-1556, 1999.

[45] Q. Ge,T. Shao, Ch. Wen, and R.Sun, "Analysis on Strong Tracking Filtering for Linear Dynamic Systems," *Hindawi Publishing Corporation Mathematical Problems in Engineering*, Volume 2015, Article ID 648125, 9 pages.

[46] H.Yang, H.Gao, and X. Liu, "Strong tracking filtering algorithm of randomly delayed measurements for nonlinear systems," *Hindawi Publishing Corporation Mathematical Problems in Engineering*, 2015.

[47] X.Wang, Y. Liang,Q. Pan, and C. Zhao, "Gaussian filter for nonlinear systems with one-step randomly delayed measurements," *Automatica*, vol. 49, no. 4, pp. 976-986, 2013.

[48] A. Hermoso-Carazo and J. Linares-Perez, "Extended and unscented filtering algorithms using one-step randomly delayed observations," Applied Mathematics and Computation, vol. 190, no. 2, pp. 1375-1393, 2007.

[49] D. H. Zhou and P. M. Frank, "Strong tracking filtering of nonlinear time-varying stochastic systems with coloured noise: application to parameter estimation and empirical robustness analysis", *International Journal of Control*, Vol. 65, No. 2, pp. 295-307, 1996.

[50] Z. Zhang and J. Zhang, "A strong tracking nonlinear robust filter for eye tracking", *Journal of Control Theory and Applications*, Vol. 8, No. 4, pp. 503-508, 2010.

[51] D.J. Jwo, C.F. Yang, C.H. Chuang, and T.-Y. Lee, "Performance enhancement for ultra tight GPS/INS integration using a fuzzy adaptive strong tracking unscented Kalman fiter", *Nonlinear Dynamics*, Vol. 73, No. 1-2, pp. 377-395, 2013.

[52] S. Kluge, K. Reif, and M. Brokate, "Stochastic Stability of the Extended Kalman Filter with Intermittent Observations," *IEEE Trans. Autom. Control*, Vol. 55, No. 2, pp. 514?518, 2010.

[53] D. Shi, T. Chen, L. Shi, "An event-triggered approach to state estimation with multiple point and set-valued measurements," *Automatica*, Vol. 50, No. 6, pp. 1641-1648, 2014.

[54] E. Ghahremani and I. Kamwa, "Online State Estimation of a Synchronous Generator Using Unscented Kalman Filter From Phasor Measurement Units, *IEEE Trans. on Energy Conversion*, Vol. 26, No. 4, December 2011.

[55] E. Ghahremani and I. Kamwa, "Dynamic State Estimation in Power System by Applying the Extended Kalman Filter With Unknown Inputs to Phasor Measurements, *IEEE trans. on Power systems*, Vol. 26, No. 4, November 2011.

[56] A. F. Taha, J. Qi, J. Wang, and J. H. Panchal, "Dynamic State Estimation under Cyber Attacks: A Comparative Study of Kalman Filters and Observers," arXiv preprint arXiv:1508.07252, 2015.

[57] J. Qi, K. Sun, J. Wang, and H. Liu, "Dynamic State Estimation for Multi-Machine Power System by Unscented Kalman Filter with Enhanced Numerical Stability," *IEEE Transactions on Smart Grid* , Vol. 9, No. 2, March 2018.

[58] J. Qi, A. F. Taha, J. Wang, "Comparing Kalman filters and observers for dynamic state estimation with model uncertainty and malicious Cyber attacks," arXiv:1605.01030v1 [cs.SY] 2 May 2016.

[59] H.Yang, H.Gao, and X. Liu, "Strong tracking filtering algorithm of randomly delayed measurements for nonlinear systems," *Hindawi Publishing Corporation Mathematical Problems in Engineering*, 2015.

[60] M. Kooshkbaghi, H. Marquez, "Event-Triggered Discrete-Time Cubature Kalman filter for Nonlinear Dynamic Systems with packet dropout," Accpeted for publication in *IEEE Transactions on Automatic Control*, Sep 2019.

[61] M. Kooshkbaghi, H. Marquez and W. Xu, "Event-Triggered Approach to Dynamic State Estimation of a Synchronous Machine Using Cubature Kalman Filter," *IEEE Transactions on Control Systems Technology*, DOI: 10.1109/TCST.2019.2923374.

[62] H. Wang, G. Fu, J. Li, Z. Yan, and X. Bian, "An Adaptive UKF Based SLAM Method for Unmanned Underwater Vehicle," *Mathematical Problems in Engineering*, vol. 2013, Article ID 605981, 12 pages, 2013.

[63] L. Li, D. Yu, H. Yang and C. Yan, "UKF for nonlinear systems with event-triggered data transmission and packet dropout," *3rd International Conference on Informative and Cybernetics for Computational Social Systems (ICCSS)*, pp. 37-42, Jinzhou, 2016.

[64] X. Meng, T. Chen, "Optimal sampling and performance comparison of periodic and event based impulse control", *IEEE Trans Autom. Control*, Vol.57, No.12, pp.3252-3259.

[65] K. E. Arzen, "A simple event-based PID controller," in Proc. of 14th IFAC World Congr, 1999

[66] H. Yu and P. Antsaklis, "Event-triggered real-time scheduling for stabilization of passive and output feedback passive systems," *Proc. Amer. Control Conf.*, pp. 1674-1679, June-July 2011.

[67] R. Postoyan, A. Anta, D. Nesic, and P. Tabuada, "A unifying Lyapunov-based framework for the event-triggered control of nonlinear systems," *Proc. IEEE Conf. Dec. Control and Eur. Control Conf.*, pp. 2559 - 2564, 2011.

[68] R. Postoyan, P. Tabuada, D. Nesic, and A. Anta, "A framework for the event-triggered stabilization of nonlinear systems," *IEEE Trans. Autom. Control,* vol. 60, no. 4, pp. 982-996, 2015.

[69] B. Wang, M. Fu, "Comparison of periodic and event-based sampling for linear state estimation," *Proc. IFAC world congress*, 2014.

[70] M. Rabi, G. Moustakides, and J. Baras, "Multiple sampling for estimation on a finite horizon," Proc. 45th IEEE CDC, pp 1351-1357, 2006.

[71] M. Rabi, G. Moustakides, and J. Baras, "Adaptive sampling for linear state estimation," *SIAM J Control Optim*, Vol.50, No.2, pp. 672-702, 2012.

[72] L. Li, M. Lemmon, "Performance and average sampling period of sub-optimal triggering event in event triggered state estimation," *Proc. 50th IEEE CDC and European Control Conf*, pp 1656-1661, 2011.

[73] D. Shi, T. Chen, and L. Shi, "Event-based state estimation of linear dynamical systems: communication rate analysis," *American control conference (ACC),* pp. 4665-4670, 2014.

[74] VH. Nguyen,YS. Suh, "Improving estimation performance in networked control systems applying the send-on-delta transmission method," *Sensors* Vol.7, pp. 2128-2138, 2007.

[75] S. Trimpe, R. D'Andrea, "An experimental demonstration of a distributed and event-based state estimation algorithm," *Proc. 18th IFAC*, pp. 8811-8818, Italy, 2011.

[76] S. Trimpe, R. D'Andrea, "Event-based state estimation with variance-based triggering," *IEEE Trans Autom Control,* Vol.59, No.12, pp. 3266-3281, 2014.

[77] J. Wu, Q. Jia, K. Johansson, L. Shi L, "Event-based sensor data scheduling: trade-off between communication rate and estimation quality," *IEEE Trans. Autom Control* Vol. 58, No.4, pp.1041-1046, 2013.

[78] D. Shi, T. Chen, L. Shi, "On set-valued Kalman filtering and its application to event-based state estimation," *IEEE Trans. Autom. Control* Vol.60, No.5, pp.1275-1290, 2015.

Appendices

Appendix A

Extended Kalman Filter

The EKF linearizes the nonlinear process and the measurement functions using the first-order Taylor series expansion. The discrete time EKF algorithm consists of two steps, Time update and measurement update,

Time Update

- Estimate the predicted state:

$$\hat{x}_{k+1|k} = f(\hat{x}_k, u_k)$$

- Estimate the predicted state error covariance:

$$\hat{P}_{k+1|k} = F_k \hat{P}_k F_k^T + Q_k$$

where $F_k = \frac{\partial f}{\partial x}|_{\hat{x}_k, u_k}$, and $H_k = \frac{\partial h}{\partial x}|_{\hat{x}_{k|k-1}}$ are the Jacobian matrices.

Measurement Update

- Compute the Kalman gain:

$$K_{k+1} = \hat{P}_{k+1|k} H_{k+1}^T (H_{k+1} \hat{P}_{k+1|k} H_{k+1} + R_{k+1})^{-1}$$

- Calculate the error covariance matrix:

$$\hat{P}_{k+1} = (I - K_{k+1} H_{k+1}) \hat{P}_{k+1|k}$$

- Compute the updated state estimation:

$$\hat{x}_{k+1} = \hat{x}_{k+1|k} + K_k [y_k - h(\hat{x}_{k+1|k})]$$

Appendix B

Unscented Kalman Filter

UKF has some important common properties shared with the CKF, such as using a set of deterministic weighted points to compute the means and the covariances. In UKF, unscented transformation (UT) was applied to propagate mean and covariance information by nonlinear transformation. UKF algorithm is as follows,

Time Update

- Calculate sigma point, χ_i, and the weight of the sigma points ϖ_i as follows,

$$\begin{aligned}
&\chi_{i,k} = \hat{x}_k \qquad i = 0 \\
&\chi_{i,k} = \hat{x}_k + (\sqrt{(n+k)\hat{P}_k})_i \qquad i = 1, ..., n \\
&\chi_{i,k} = \hat{x}_k - (\sqrt{(n+k)\hat{P}_k})_i \qquad i = 1, ..., 2n \\
&\varpi_0 = \frac{k}{n+k} \\
&\varpi_i = \frac{1}{2(n+k)} \\
&\varpi_{n+i} = \frac{1}{2(n+k)}
\end{aligned}$$

Note that k is a scaling parameter that determines the spread of the sigma points around the mean of the state $\hat{x}$ which is usually chosen as $k = 3 - n$ [8].

- Transform the sigma points using the nonlinear system equation,

$$\chi_{i,k+1|k} = f(\chi_{i,k}) \qquad i = 0, 1, ..., 2n$$

- Obtain the estimate of the predicted state,

$$\hat{x}_{k+1|k} = \sum_{i=0}^{2n} \varpi_i^m \chi_{i,k+1|k}$$

- Estimate the predicted error covariance matrix,

$$\hat{P}_{k+1|k} = \sum_{i=0}^{2n} \varpi_i^c (\chi_{i,k+1|k} - \hat{x}_{k+1|k})(\chi_{i,k+1|k} - \hat{x}_{k+1|k})^T + Q_k$$

- Propagate the sigma points,

$$y_{i,k+1|k} = h(\chi_{i,k+1|k}) \qquad = 0, 1, ..., 2n$$

- Calculate the predicted measurement,

$$\hat{y}_{k+1|k} = \sum_{i=0}^{2n} \varpi_i^m y_{i,k+1|k}$$

- Calculate the innovation covariance matrix

$$\hat{P}_{yy,k+1|k} = \sum_{i=0}^{2n} \varpi_i^c (y_{i,k+1|k} - \hat{y}_{k+1|k})(y_{i,k+1|k} - \hat{y}_{k+1|k})^T + R_{k+1}$$

- Calculate the cross covariance matrix

$$\hat{P}_{xy,k+1|k} = \sum_{i=0}^{2n} \varpi_i^c (\chi_{i,k+1|k} - \hat{x}_{k+1|k})(y_{i,k+1|k} - \hat{y}_{k+1|k})^T$$

- Calculate the Kalman gain, the updated state estimation and the updated state estimation error covariance matrix as follows,

$$K_{k+1} = \hat{P}_{xy,k+1|k} \hat{P}_{yy,k+1|k}^{-1}$$
$$\hat{x}_{k+1} = \hat{x}_{k+1|k} + K_k[y_k - h(\hat{x}_{k+1|k})]$$
$$\hat{P}_{k+1} = \hat{P}_{k+1|k} - K_{k+1} \hat{P}_{yy,k+1|k} K_{k+1}^T$$

Note that $\varpi_i^m = \varpi_i^c = \varpi$. As you can see in the algorithm mentioned above, when the system dimension increases (n > 3), however, UKF is highly susceptible to numerical errors. The weight of the centre sigma point becomes negative and the covariance matrix is not positive definite which causes the UKF to halt its operation. To overcome this problem, CKF uses a different set of deterministic weighted points which has numerical stability and is proper for high dimensional state space model [8].